Ulrich Borchers

Mechanism of tumor progression: Valuation of selective targets for the development of novel strategies in the therapy of solid tumors

Cuvillier Verlag Göttingen

Mechanism of tumor progression: Valuation of selective targets for the development of novel strategies in the therapy of solid tumors

Dissertation
zur Erlangung des Doktorgrades
der Mathematisch-Naturwissenschaftlichen Fakultäten
der Georg-August-Universität zu Göttingen

vorgelegt von
Ulrich Borchers
aus Hamburg

Göttingen 2000

Die Deutsche Bibliothek - CIP-Einheitsaufnahme

Borchers, Ulrich:
Mechanism of tumor progression: Valuation of selective targets for the development of novel strategies in the therapy of solid tumors / vorgelegt von Ulrich Borchers. -
1. Aufl. - Göttingen : Cuvillier, 2000
Zugl.: Göttingen, Univ., Diss., 2001
ISBN 3-89873-081-6

D 7

Referent:	Prof. Dr. Dr. h.c. L. F. Tietze
Korreferent:	Prof. Dr. A. Zeeck
Tag der mündlichen Prüfung:	31.01.2001

Nonnenstieg 8, 37075 Göttingen
Telefon: 0551-54724-0
Telefax: 0551-54724-21
www.cuvillier.de

1. Auflage, 2000
Gedruckt auf säurefreiem Papier

ISBN 3-89873-081-6

The work described in this dissertation has been carried out
under the guidance of Prof. Dr. Dr. h.c. L. F. Tietze
at the Institute of Organic Chemistry of the Georg-August-University in Göttingen
from February 1998 to December 2000.

I am sincerely grateful to Prof. Dr. Dr. h.c. L. F. Tietze
for the challenge topics, his constantly interest, guidance of this work and his
numerous suggestions and discussions.

Contents

1. Introduction 6

1.1. Regulation of EGF receptor activity by HK1-ceramide, a stable synthesized analogue of the ganglioside GM3-lactone. 7

1.2. A novel polyclonal antibody directed against the lactone form of ganglioside GM3: Analyses of its potential as tumor marker for melanomas. 9

1.3. Evaluation of the efficacy of novel synthetic drugs to inhibit tumor growth and progression of human pancreatic ductal adenocarcinoma. 11

1.3.1. Evaluation of the *seco*-CBI-derivative AF86.1 for its potential use in antibody directed enzyme prodrug therapy. 11

1.3.2. Evaluation of the antitumor and antimetastatic effect of different matrix metalloproteinase inhibitors on human pancreatic ductal adenocacinoma in the orthotopic SCID-mouse model. 17

1.3.2.1. Human pancreatic ductal adenocarcinoma. 17

1.3.2.2. Matrix metalloproteinases. 17

1.3.2.3. Matrix metalloproteinase-inhibitors. 18

1.3.2.4. The orthotopic SCID-mouse model. 20

2. Materials and Methods 22

2.1. Glycolipids. 22

2.2. Cell culture. 22

2.3. Analyses of EGF mediated tyrosine phosphorylation of EGF receptor in A431 cells. 23

2.4.. Determination of EGF-dependent mitogenesis. 25

2.5. Analyses of binding of the ^{125}I-EGF to cell surface receptor. 25

2.6. Animals. 26
2.7. Compounds. 27
2.8. Formulations and treatments. 27
2.9. Subcutaneous tumor implantation. 30
2.10. Orthotopic tumor implantation and tumor growth. 30
2.11. Immunohistochemistry. 31
2.12. Data analyses. 32

3. Results 34

3.1. Regulation of EGF receptor activity by HK1-ceramide, a stable synthesized analogue of the ganglioside GM3-lactone. 34
3.1.1. In situ effect of HK1-ceramide and HK2-ceramide on EGF-mediated tyrosine phosphorylation of EGF receptor in cultured intact A431 cells. 34
3.1.2. In situ effect of GM3 on EGF-mediated tyrosine phosphorylation of EGF receptor in cultured intact A431 cells in dependence of the pH. 38
3.1.3. Effect of HK1-ceramide on MAP kinase activity. 39
3.1.4. Effect of HK1-ceramide on specific binding activity of ^{125}I-EGF to cell surface receptor. 40
3.1.5. Effect of HK1-ceramide on EGF-dependent mitogenesis in KB cells. 41
3.2. A novel polyclonal antibody directed against the lactone form of ganglioside GM3: Analyses of its potential as tumor marker for melanomas. 42
3.3. Evaluation of the efficacy of novel synthetic drugs to inhibit tumor growth and progression of human pancreatic ductal adenocarcinoma. 47
3.3.1. The orthotopic SCID-mouse model 47
3.3.1.1. Growth characteristics of PancTu 1 cells after orthotopic implantation in SCID mice. 47

3.3.2. Evaluation of the *seco*-CBI-derivative AF86 for its potential use in antibody directed enzyme prodrug therapy. Preliminary results *in vivo* in SCID mice. 49
3.3.2.1. Acute Toxicity 49
3.3.2.1.1. Experimental Design 50
3.3.2.1.2. Tolerance to AF86.1 51
3.3.2.2.. First investigations of AF86.1 for its potential use in antibody-directed enzyme prodrug therapy. 52
3.3.2.2.1. Experimental Design 52
3.3.3. Evaluation of the antitumor and antimetastatic effect of the MMP inhibitor AG3340 on human pancreatic adenocarcinoma in the orthotopic SCID-mouse model. 55
3.3.3.1. Study design 55
3.3.3.2. Tolerance to AG3340 55
3.3.3.3. Effects of AG3340 on tumor growth and morphological properties 56
3.3.3.4. Effects of AG3340 on tumor invasion, disseminated tumor growth and metastasis 57
3.3.4. Evaluation of the antitumor and antimetastatic effect of the chemotherapeutic agent gemcitabine on human pancreatic adenocarcinoma in the orthotopic SCID-mouse model. 60
3.3.4.1. Study design. 60

3.3.4.2. Tolerance to gemcitabine. 60

3.3.4.3. Effects of gemcitabine on tumor growth, invasion, disseminated tumor growth and metastasis 61

3.3.5. Evaluation of the antitumor and antimetastatic effect of the MMP inhibitor Ro 28-2653 on human pancreatic adenocarcinoma in the orthotopic SCID-mouse model. 63

3.3.5.1. Study design 63

3.3.5.2. Tolerance to Ro28-2653. 64

3.3.5.3. Effects of Ro28-2653 on tumor invasion, disseminated tumor growth and metastasis. 64

3.3.6. Evaluation of the antitumor and antimetastatic effect of the combination therapy of the chemotherapeutic agent gemcitabine and the MMP inhibitor Ro 28-2653 on human pancreatic adenocarcinomas in the orthotopic SCID-mouse model. 67

3.3.6.1. Study design 67

3.3.6.2. Tolerance to Ro28-2653 and gemcitabine

3.3.6.3. Effects of Ro28-2653 and gemcitabine on tumor invasion, disseminated tumor growth and metastasis. 68

3.3.7. Evaluation of the effect of the combination therapy of the chemotherapeutic agent gemcitabine and the MMP inhibitor Ro 28-2653 on survival time of SCID mice with pancreatic tumors. 71

3.3.7.1. Study design 71

3.3.7.2. Tolerance to Ro28-2653 and gemcitabine. *72*

3.3.7.3. Effects of Ro28-2653 and gemcitabine on tumor invasion, disseminated tumor growth and metastasis. 72

4. Discussion 76

4.1. Regulation of EGF receptor activity by HK1-ceramide, a stable synthesized analogue of the ganglioside GM3-lactone. 76
4.2. A novel polyclonal antibody directed against the lactone form of ganglioside GM3: Analyses of its potential as tumor marker for melanomas. 79
4.3. Evaluation of the *seco*-CBI-derivative AF86.1 for its potential use in antibody directed enzyme prodrug therapy. 81
4.4. Evaluation of the antitumor and antimetastatic effect of different MMP inhibitors on human pancreatic adenocarcinomas in the orthotopic SCID-mouse model. 82

5. Summary 90

5.1. Regulation of EGF receptor activity by HK1-ceramide, a stable synthesized analogue of the ganglioside GM3-lactone. 90
5.2. A novel polyclonal antibody directed against the lactone form of ganglioside GM3: Analyses of its potential as tumor marker for melanomas. 91
5.3. Evaluation of the *seco*-CBI-derivative AF86.1 for its potential use in antibody directed enzyme prodrug therapy. 92
5.4. Evaluation of the antitumor and antimetastatic effect of different matrix metalloproteinase inhibitors on human pancreatic ductal adenocacinoma in the orthotopic SCID-mouse model. 92

6. References 94

7. Abbreviations and Acronymes 101

8. Acknowledgments 104

1 Introduction

Many cases of cancer can now be cured by surgery, radiation and chemotherapy. However this treatment has its limitations. Hope comes from new methods directed against single steps of tumorigenesis which will be even more effective. The available chemotherapeutic drugs often fail to cure patients because they kill many healthy cells und thus bring on serious side effects that limit the doses physicians can administer.

A simple, universal treatment that is effective for all cancers, is extremely unlikely to emerge anytime in the near future. But a large set of more specific and less toxic treatments is probably nearer at hand.

The conversion of normal cells into invasive cancers with metastatic potential is a process that involves several steps. These steps are manifested in distinguishable histological and temporal stages (normal tissue, hyperplasia with a high incidence of proliferating cells, dysplasia with the induction of angiogenesis before the emergence of frank tumors with metastatic potential). Analysis of the later stages of tumor progression has resulted in a multi-step theory of tumorigenesis on the basis of genetic changes involving activation of oncogenes, inactivation of tumor suppressor genes, and altered expression of tumor-associated molecules. Whereas cancer research has historically focussed on such intrinsic events, it has become evident that extrinsic factors – the local stromal microenvironment - also regulate critical parameters of tumorigenesis and evolve and undergo multi-step reconstruction paralleling neoplastic progression. Thus, the stroma, and its resident reactive host cells, constitutes a second important component of solid tumors.[1]

1.1. Regulation of EGF receptor activity by HK1-ceramide, a stable synthesized analogue of the ganglioside GM3-lactone

The involvement of gangliosides in tumor development and progression, e.g. processes of cell proliferation, migration and adhesion has been widely described.[2,3] In addition to proteins and lipids, carbohydrates - of which gangliosides constitute a large part - are essential elements of the cell surface. Gangliosides are neuraminic acid containing glycosphingolipids which are responsible for a variety of biological recognition processes. They are anchored in the lipid bilayer of the membrane by the ceramide portion with the carbohydrate moiety being exposed on the outside of the cell. The ganglioside pattern on the surface of tumor cells is distinguished from normal cells, for instance, the amount of GM3, GM2 and GD3 has been found to be increased on malignant melanomas. [4,5] It has been suggested that an equilibrium exists between the gangliosides and their lactones e.g. GM3 and its lactone **1** (Fig. 1) by reaction of the sialic acid moiety with a hydroxyl group of an adjacent sugar in the molecule. The ganglioside-lactones are thought to be formed to a higher extent on malignant cells probably due to a lower pH on these cells and may therefore play an important role as tumor associated antigens. [6]

Figure 1

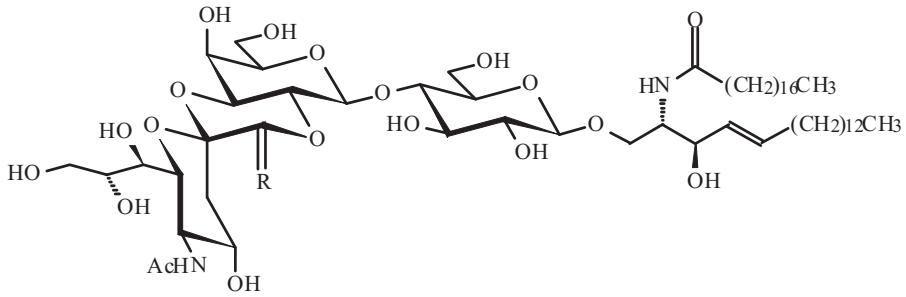

Structure of GM3-lactone and HK1-ceramide. GM3-lactone **1**: R = O. HK1-ceramid **2**: R = H_2

It has also been demonstrated that the GM3-lactone is more immunogenic in comparison to GM3. The anti-melanoma GM3 antibody, M2590, has shown a high affinity for GM3-lactone but a low affinity for GM3.[7] Ganglioside-lactones have become more of interest, particularly GM3-lactone, since it has been identified in mammary gland tumors and gastric tumors [8] and was found to bind to influenza virus hemagglutinin [9]. Furthermore, the gangliosides extracted from mullet milt were determined to be GM3, GM3 lactone, GM3 methylester, and 9-O-acetyl GM3.[10]

Recently, Tietze et al. succeeded in the preparation of the GM3-lactone analogue HK1-ceramide **2** (Fig. 1), which contains an ether moiety instead of the lactone functionality and is stable under physiological conditions.[11] To our knowledge HK1-ceramide **2** is the first and the only stable ganglioside-lactone-analogue so far synthesized. Therefore, HK1-ceramide seems to be a perfect tool to analyze the mode of action of the hypothetically fixed GM3-lactone or GM3-lactone-like conformation.

Ganglioside GM3 has been described to modulate cell growth through inhibition of EGF receptor associated tyrosine kinase.[12] Upon binding of EGF to the extracellular domain of the EGF receptor the tyrosine kinase is activated leading to the tyrosine phosphorylation of intracellular substrates such as Grb2, sos, ras, raf, MEK, ERK and ELK-1.[13] The effect of GM3 appears to be mediated by direct inhibition of EGF-receptor autophosphorylation and dimerization [12,14] and not by acting directly on the intracellular intermediates of EGF receptor signaling.[15]

The goal of this study was to determine if the lactone form of GM3 has a similar inhibitory effect on EGF induced cell growth and EGF-R tyrosine phosphorylation. In order to accomplish this, the influence of the stable ganglioside-lactone-analogue

HK-1 ceramide toward EGF receptor signaling and EGF mediated cell growth was examined and directly compared to the effects of GM3.

1.2. A novel polyclonal antibody directed against the lactone form of ganglioside GM3: Analyses of its potential as tumor marker for melanomas.

Melanoma is a tumor of the melanocytes, the melanin producing cells, distributed in the skin as well as in other organs. The prominent features of the melanocytes, in addition to their unique ability to synthesize melanin, is their motility in early life. Melanocytes express gangliosides, the qualitative pattern of which is somewhat characteristic of other extra-neural tissues. The quantity of the gangliosides is higher than that of other extra-neutral tissues. GM3 is the most predominant ganglioside. Other gangliosides of the melanocytes, which include GD3, GM2, GD1a, and GT1b, constitute less than 10 % of the total.[16]

The onset of the neoplastic transformation of melanocytes triggers the enzyme machinery associated with glycosylation, particularly that related to the addition of sialic acid (Sia) and N-acetyl galactosamine (Ga1Nac). Adding sialic acid to the preexisting sialic acid of GM3 results in the formation of GD3 [16] and GD3 accumulation is an important event associated with the growth and proliferation of melanoma.[17] Since the differences in the ganglioside profile of neoplastically transformed melanocytes correlates with the changes in the functional properties of the malignant cells, such as proliferation, migration, adhesion to basement membrane components, infiltration and metastasis,17,18 it was of interest to search for differences in the ganglioside pattern expressed in melanoma cells in comparison to naevus cells which comprise benign melanocyte tumors. Previous studies have

shown that it is possible to identify differences in protein antigen expression between benign and malignant melanocytes by searching for monoclonal antibodies which show differential reactivity with these cells *in situ.* [19,20] Mab MacG1 e.g. distinguishes between malignant melanoma and benign melanocytic nevi in tissue sections. Mab MacG1(IgG2a) was obtained following immunization with a mixture of gangliosides prepared from a melanoma lymph node metastasis. But in contrast to other antibodies directed to GM3, MacG1 does not stain the melanoma cells themeselves but rather granules associated with tumor infiltrating macrophages. *In vitro* studies suggest that the MacG1 epitope is generated during phagocytic degradation of ganglioside rich cellular debris. When tested with a panel of purified gangliosides, MacG1 showed a lack of reactivity with GM3-lactone. [21]

Melanoma-shed gangliosides have modulatory influence on both the humoral and cellular immune system in humans. Low concentrations are stimulatory, whereas increasing concentrations lead to a potent inhibition of all lymphocyte functions, this inhibition being reversible by removing the gangliosides from the extracellular medium. The shed gangliosides might thus be involved in the protection of tumor cells from immune killing.

The goal of this study was to investigate the expression pattern of gangliosides on melanoma cells applying the new polyclonal antibody against HK1[48]. It has been shown that this antibody show immunoreactivity with GM3 and its lactone form.

1.3. Evaluation of the efficacy of novel synthetic drugs to inhibit tumor growth and progression of human pancreatic ductal adenocarcinoma.

1.3.1. Evaluation of the *seco*-CBI-derivative AF86.1 for its potential use in antibody directed enzyme prodrug therapy

In the last decade scientists concentrated on developing a new, less cytotoxic strategy for the treatment of cancer by exploiting properties distinguishing neoplastic and normal cells. Monoclonal antibodies were used to carry enzymes at the tumor sites, in a two-step approach known as Antibody Directed Enzyme Prodrug Therapy (ADEPT). Several attempts have been made to generate an active drug from an inactive precursor, by the action of an enzyme present predominantly at the tumor site.[22]

Central to this strategy is the concept of a prodrug: a molecule which is not active itself, but which can be converted to a cytotoxic agent by enzymatic activation *in vivo*.[22] The criteria of a prodrug were set by Connors and Whisson [23,24,25] and are listed below:

a) The prodrug must be non-toxic, while its active derivates should be highly cytotoxic.
b) Tumors should contain the enzyme which activates the prodrug in considerably higher concentration than normal tissues.
c) The enzyme-prodrug system should be functional *in vivo*.
d) The active drug should not produce major toxicity to normal organs.

Since the use of a tumor-associated antibody as a carrier of a prodrug was not satisfactory, Philpott exploited the idea of using the antibodies to carry enzymes to the tumor sites.[26,27] This concept was further developed and described by Bagshawe [28,29] and Senter.[30,31] The interval between the two administrations of the antibody-enzyme-conjugate and the prodrug is optimized to achieve minimal systemic toxicity by accomplishing a satisfactory accumulation of the conjugate in the tumor and its clearance from blood and normal tissues. In addition, as the active drug diffuses throughout the tumor, it provides a bystander effect, killing antigen-negative cells.[22] The advantages of this treatment are 1) reduced toxicity:The systemic effect is minimized by optimizing the interval between the two steps. It is also possible to use enzymes not present in humans, to minimize the release of cytotoxic agent at sites other than the tumor, and 2) amplification: These systems can overcome the problem of low absolute uptake of the antibody by the tumor, because a single molecule of enzyme can activate more than one prodrug molecule.[32] It has also been shown that the drug generated at the surface of tumor cells is more effective than equivalent concentrations of free drug.[33]

Selection of a target antigen whose expression is restricted to cancer cells is very important. Heterogeneity of antigen expression in cancers of the same histologicaltype, occurring in different individuals, should also be examined.[22] Furthermore, it would be preferable to choose an antigen expressed by a wide range of tumors. Finally, the tumor heterogeneity could be circumvented with the application of a “cocktail” of conjugates constructed with the same enzyme and a variety of antibodies directed against different tumor-associated antigens.[34]

Several groups of antigens have been considered as potential ADEPT targets. These include oncogene products with an extracellular domain, such as c-myc[35]

or c-erbB-2 [36], overexpressed gene products, growth factor receptors and transmembrane adhesive molecules.[22]

in this approach a high affinity of the monoclonal antibody is essential, since it facilitates the binding of the antibodies in the periphery of tumor masses. The class of immunglobulin is not important, but their size should be taken into consideration:
IgM is usually avoided for ADEPT studies because of its low penetration, while IgG1 and IgG2 are more commonly used for systemic administration.[22] It is now recognized that whole antibodies penetrate tumors poorly.[37,38,39] Since smaller molecules penetrate tumors better, to increase further tumor penetration of the conjugate, antibody fragments rather than intact antibodies have been used: F(ab‘2), Fab, single chain antibodies and recombinant antigen-binding proteins. Unfortunately, the potential benefit of these molecules is hampered by the size of the enzyme used and the cost of their construction. (review). Another important point is that small sized molecules have a rapid blood clearance.[40] Although this is highly desirable after the localization of the conjugate at the tumor site, the rapid plasma clearance results in diminished absolute levels of tumor uptake and therefore a greater total amount of antibody-enzyme conjugate needed to be administered.[22]
A wide range of systems has been used for *in vitro* and *in vivo* trials of ADEPT, as demonstrated in Table 1.

Table 1 [22]: The antibody directed enzyme prodrug therapeutic systems (ADEPT) that have been tried for the treatment of cancer *in vitro* and *in vivo*:

Enzyme	Antibody	Antigen	Active drug
Carboxypeptidase G2	W14	human chorionic gonadotropin	benzoic acid
	A5B7	CEA	benzoicacid
Carboxypeptidase A	KS1/4	lung cancer-associated antigen	methotrexate
Alkaline phosphatase	L6	tumor-associated antigen	etoposide mitomycin c doxorubicin
Penicillin-V amidase	L6	lung cancer-associated antigen	doxorubicin melphalan
Penicillin-G amidase	L6	lung cancer-associated antigen	doxorubicin melphalan
Cytosine deaminase	L6	lung cancer-associated antigen	5-Fluoruracil
β-lactamase	L6	lung cancer-associated antigen	nitrogen mustard
β-glucoronidase	BW431	CEA	doxorubicin epirubicin
nitroreductase	BW431	CEA	CB1954
β-glucosidase	H17E2	hPLAP	cyanide

A new ADEPT system was developed by *L. F. Tietze*. The drug design was derived from the antibiotic CC-1065, which was isolated from *Streptomyces zelensis* cultures for the first time by the *Upjohn-Company* in 1978. At the present time CC1065 is one of the most potent anti-tumor agents.[41] Its cytotoxic effect is based on sequence specific alkylation of DNA by the addition of adenine-N3 to the cyclopropane unit.[42,43,44] But the antibiotic CC-1065 could not be used in clinical trials, because of its side effects. In preclinical investigations it showed a delayed lethal hepatotoxicity in mice.[45]

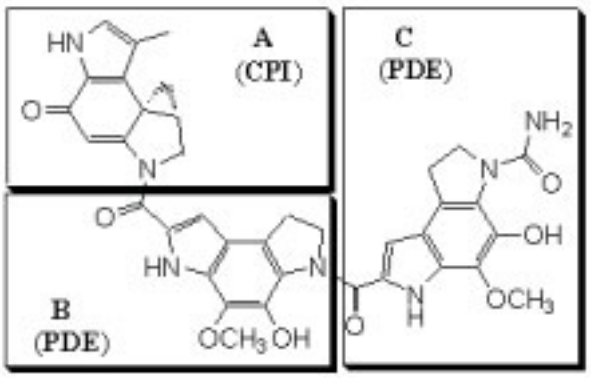

Figure 2: (+)-CC-1065

Recently, Tietze et al. succeeded in the preparation of a new *seco*-CBI-derivative,[46] which contains a tetrahydrobenzo[ƒ] chinolin as basic structure and a secondary chloride function as leaving group. The toxicity of this derivative can be reversed by glycosidation by (AF86.1).

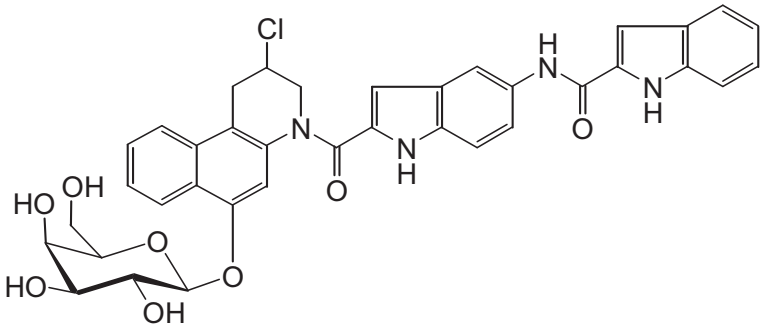

Figure 3: Seco-CBI-derivative AF86.1

A modified Human Tumor Colony Forming Ability – test (HTCFA-.test) with the lung carcinoma cell line A549 showed a particularly high selectivity between prodrug and activated drug (see Table 2) The activated prodrug was shown to be effective *in vitro.*

Table 2 : HTCFA – test with A549 cells , AF86.1 and galactosidase.[46]

SD_{50}	Enzyme : Galactosidase	Prodrug : AF86.1
0.2 nM	+	+
320 nM	-	+

In order to proof the principle of this new ADEPT-system including AF86.1 and an ephithelial membrane antigen antibody - β-D-galactosidase conjugate *in vivo* in the orthotopic SCID-mice model, preliminary investigations will be done to analyze at first the toxicity of AF86.1 in mice and secondly if AF86.1 is toxic by galactosidase *in vivo.*

1.3.2. Evaluation of the antitumor and antimetastatic effect of different matrix metalloproteinase inhibitors on human pancreatic ductal adenocacinoma in the orthotopic SCID-mouse model

1.3.2.1. Human pancreatic ductal adenocarcinoma

Despite improvements in therapeutic strategies including surgical techniques as well as adjuvant therapies, pancreatic ductal adenocarcinoma remains one of the leading causes of cancer death in industrialized countries. The majority of patients are found to have aggressive local invasion of adjacent structures and metastatic lesions and even with early surgical intervention there is no prospect for cure or even effective palliation because of almost inevitable local recurrence and/ or metastasis observed soon after surgery.[47]

1.3.2.2. Matrix metalloproteinases

Hope for novel therapies originates from new treatment strategies that attack specific steps of the metastatic cascade. Degradation of extracellular matrix barriers is a distinct step in the detachment of malignant cells in order to migrate through the tumor surrounding stroma to adjacent normal tissues, to invade blood vessels and lymphatics and to extravasate at distant sites. The major enzymes involved in these processes are matrix metalloproteinases (MMPs), mainly MMP-2 (Gelatinase A) and MMP-9 (Gelatinase B), which are able to degrade collagen type IV.[1] Individual

MMPs have been variously named, grouped and subdivided on the basis of their substrate specificities and either the presence or absence of specific functional protein domains. To date, 20 distinct vertebrate MMPs and 18 human homologues have been identified, as well as two non-vertebrate MMPs.[48] In pancreatic carcinoma tissue, like in other cancers[49] high transcript levels were reported for MMP-2, MMP-7, MMP-9 and MMP-11 and the membrane-associated activators MT1-MMP and MT2-MMP, as well as the tissue inhibitors of MMPs, TIMP-1 and TIMP-2.[50,51] MMP-2 expression and activity in pancreatic cancer appeared to be more abundant in stromal cells and strongly associated with the extent of the desmoplastic reaction and the invasive potential of pancreatic cancer cell lines.[52] MMPs have also been shown to be involved in the process of angiogenesis, mediating the remodeling and penetration of the extracellular matrix by new capillaries.[53] Therefore, specifically targeting MMPs should have the potential to inhibit both tumor growth and dissemination and should be a promising strategy in the therapy of this aggressive malignant disease.

1.3.2.3. Matrix metalloproteinase inhibitors.

As a result many pharmaceutical companies have designed novel drugs that variably block MMP activity. Many of the first synthetic inhibitors developed were designed to mimic part of the peptide sequence surrounding the point in the collagen molecule first cleaved by interstitial collagenase. This sequence allows the inhibitor to fit tightly within the active site of the MMP in a stereospecific manner.[54] The zinc atom in the MMP´s active site is then chelated through a zinc binding group, such as a hydroxamate, carboxylate, aminocarboxylate derivative.[55] Further development of synthetic MMPs, aided by x-ray cristallography data on the topography of the active

site, yielded a wider range of chemical structures. Several of these MMPs shown reasonable oral bioavailability and have since entered clinical trials.[55] A number of low molecular weight synthetic MMP inhibitors have been used in animal studies. The most widely studied is batimastat (also called BB-94, British Biotech Ltd, Oxford, United Kingdom), a MMP inhibitor with a broad spectrum, which delayed and inhibited tumor growth, angiogenesis and progression in several animal tumor models including pancreatic cancer, however without eradicating tumors.[56,57,58,59,60,61,62]

Phase II clinical studies with the orally applicable broad spectrum MMP inhibitor marimastat, alone or in combination with cytotoxic agents, have shown encouraging results with improved survival in patients with advanced pancreatic ductal carcinoma.[63] To reduce the side effects which have been obseved in these studies, e.g. arthralgies, it would be desirable to specifically inhibit gelatinases, the major enymes involved in tumor progression. To this end, several low molecular weight noncytotoxic non-peptide MMP inhibitors have been synthesized, which utilize differences in the active site to improve selectivity for MMP-2 (gelatinase A) over MMP-1 (collagenase-1). One of them, AG3340, has one of the lowest K_is for MMP-2 and MMP-9 (50 - 150 pM) and for MMP-3 (30 pM), MMP-13 and MT1-MMP (300 pM).[64,65] When given orally and intraperitoneally, this compound has shown antitumor activity in several mainly subcutaneously implanted cancers, [66,67] an antimetastatic effect in the Lewis lung murine cancer model [64] and is currently in clinical trials as a treatment for lung and prostate carcinoma. [65, 68] Another promising novel MMP inhibitor is Ro28-2653 (Roche). High specificity for the target enzymes (MMP-2, -9 and MT-MMP) differentiates Ro28-2653 from AG3340 and Bay 12-9566. AG3340 has shown also inhibitory activity for MMP-1 (Prinomastatarticel) which might be

responsible for the observed side effect (splenomegalie). Bay 12-9566 displays high specificity for MMP-2 but moderate specificity for MMP-9 and MT-MMP.

Notably, the Bayer Corporation recently announced that is was halting their clinical trial of BAY 12-9566 as “patients who took the drug experienced greater progression of cancer than half who took placebo”. These results are somewhat surprising and contrary to Bayer´s preclinical data, which confirmed that the drug inhibited tumor activity in rodents. A body of data over the past few years indicates, however, that proteinases and proteinase inhibitors may, under specific circumstances, either favor or block tumor progression.[1]

1.3.2.4. The orthotopic SCID-mouse model

Many *in vivo* models studying the preclinical efficacy of novel therapeutic agents for pancreatic carcinoma have been described. The subcutaneous growth of tumors lacks many of the features found in patients with pancreatic ductal carcinoma, including invasive and metastatic behaviour [69], whereas the transplantations of a suspension of various tumor cell lines or solid tumor fragments of histologically intact pancreatic cancer into the corresponding organ of nude mice have shown a higher uptake rate and the development of local and distal dissemination.[70,71,72,73,74,75] The more immunocompromised SCID mouse has been considered to be a suitable host for human tumor transplantation experiments by showing in some cases a higher rate of tumor take and metastases.[76] Crossing SCID mice with transgenic mice which develop primary pancreatic adenocarcinoma resulted in faster growing tumors and a distribution of metastases similar to that recorded in patients with pancreatic cancer.[77]

An orthotopic model of human pancreatic ductal adenocarcinoma in SCID mice was established using the human pancreatic ductal adenocarcinoma cell line PancTu 1 to evaluate the effect of novel antimetastatic strategies.

2. Materials and Methods

2.1. Glycolipids.

HK1-ceramide, HK2-ceramide [11] and GM3 [78] were synthesized in the Department of Organic Chemistry of Göttingen, Germany. All glycolipids were dissolved in DMSO/ H_2O (stock solution: 2.32 mM). Human EGF was kindly provided by W.E. Schmidt, University of Bochum, Germany and recombinant human (3-[125-I]iodotyrosyl) EGF was purchased from Amersham (Braunschweig, Germany).

2.2. Cell culture.

Ovarial epidermoid carcinoma A431 cells and human oral epidermoid carcinoma KB cells

Ovarial epidermoid carcinoma A431 cells [79] and human oral epidermoid carcinoma KB cells were purchased from DSMZ Braunschweig, Germany. A431 cells contain an unusually high content of the EGF receptor at the cell surface, and only a very small quantity of EGF is required to stimulate A431 cell growth and to affect the receptor kinase activity.[80] KB cells have been characterized by the presence of a moderate concentration of a high-affinity EGF receptor and a EGF-dependent mitogenesis.[81] All cells were grown in Dulbecco`s modified Eagle`s medium (DMEM) supplemented with penicillin (50 IU/ ml), streptomycin (50 μg/ ml), L-glutamine (2 mM) (Gibco BRL, Eggenstein, Germany) and 10 % heat inactivated fetal calf serum (FCS) (PAN, Aidenbach, Germany) at 37 °C in a humified atmosphere of 5 % CO_2.

The human bronchial carcinoma cell line A549

The human bronchial carcinoma cell line A549 was purchased from DSMZ Braunschweig, Germany. Cells were grown in DMEM supplemented with 10 % FCS , 44 mM $NaHCO_3$, and 4 mM glutamine at 37 °C in a humified atmosphere of 7.5 % CO_2.

PancTu 1 cell line

The human pancreatic ductal adenocarcinoma cell line PancTu 1 (Dr. M. v. Bülow, Mainz, Germany) was obtained from Prof. Dr. H. Kalthoff, Department of Surgery, University of Kiel, Germany.[82] Cells were maintained in complete medium consisting of RPMI 1640 with penicillin (50 IU/ ml), streptomycin (50 μg/ ml), L-glutamine (2 mM) (Gibco BRL, Eggenstein, Germany) and 10 % heat inactivated fetal calf serum (PAN, Aidenbach, Germany) at 37° C in a humidified atmosphere of 5 % CO_2. For implantation, cells were harvested by brief trypsination (0.25 % trypsin and 1 mM ethylendiaminetetraacetic) (Gibco) from semiconfluent culture dishes, washed several times with medium and placed in phosphate buffered saline (PBS) shortly before implantation. The cells were free of mycoplasma. Viabilty of the cells tested by trypan blue exclusion was > 95 %.

2.3. Analyses of EGF mediated tyrosine phosphorylation of EGF receptor in A431 cells.

Cells were seeded in 24-well plates in DMEM/ 10% FCS and grown to 80 % confluency. Then, the medium was replaced by DMEM without FCS and cells

Were incubated for 24 h. Aliquots of solutions containing different quantities of HK1-ceramide, HK2-ceramide and GM3 were added to each well as indicated and incubated for 3 h at 37 °C. Cells were stimulated with EGF (50 ng/ ml). 30 min prior to lysis. After washing the cells three times with cold PBS, the monolayers were solubilized by the addition of 125 µl lysis buffer containing 1% NP40, 0.25% Na-deoxycholate, 50 mM Tris-HCl (pH 7.4), 150 mM NaCl, 1 mM EGTA, 1 mM PMSF,1 µg/ ml aprotinin, leupeptin, and pepstatin A, 1 mM NaF and 1 mM Na-orthovanadate. The cellular lysates were centrifuged 10 min at 4 °C and 21000 x g and aliquots of the supernatants were subjected to SDS-PAGE. Lysates were adjusted to contain equal amounts of protein, using the BCA Protein assay (Pierce, Rockford, Illinois). Proteins were transferred to nitrocellulose membrane (Amersham Life Sciences Inc., Arlington Heights, IL) and immunoblotted with antibodies, the monoclonal antiphosphotyrosine antibody (IgG 2bk, 100µg/ ml, Paesel + Lorei, Duisburg, Germany), diluted 1: 1000, or the polyclonal anti-EGFR antibody (Santa Cruz Biotechnology Inc., Heidelberg, Germany), diluted 1 : 1000 or for investigating MAP kinase activity, the monoclonal anti-p erk antibody, detecting tyrosine phosphorylated erk 1 and erk2, diluted 1: 1000 (IgG_{2a}, 200 µg/ ml, Santa Cruz Biotechnology Inc) in 50 mM G-NET (Tris-HCl (pH 7.5), 150 mM NaCl, 5 mM EDTA, 0.25 % gelatin) overnight at 4 °C. Western blots were developed using horseradish peroxidase-coupled secondary goat-anti-mouse antibody (Biorad, München, Germany), diluted 1:20000 in 50 mM G-NET for 1 h at room temperature, and enhanced chemiluminescence (Amersham). For reprobing the membrane was stripped in 70 mM Tris (pH 6.8), 2% SDS, 0.1% β-mercaptoethanol at 55 °C for 30 min.

2.4. Determination of EGF-dependent mitogenesis.

This experiment was performed with KB cells, since mitogenic stimulation by EGF can be clearly observed in a wider range of EGF concentrations in KB cells in comparison to the results obtained in A431 cells, stimulated by EGF.[81] To measure cell growth, the KB cells (1.2 x 10^3 cells) were seeded in 96-well plates (Nunc, GmbH & C0. Kg, Wiesbaden, Germany) and cultivated in DMEM medium containing 5% FCS for 24 h. Then the medium was replaced with FCS free medium and the cells were incubated for 24 h with different quantities of gangliosides as indicated. 1 ng/ ml EGF in the presence of 100 μg/ ml BSA was added to each well and the cells were cultered for 18 h. To analyze cell proliferation the colorimetric BrdU immunoassay (Roche Diagnostics, Penzberg, Germany) was used, which is based on the measurement of BrdU incorporation during DNA synthesis. These experiments were done in triplicates.

2.5. Analyses of binding of the ^{125}I-EGF to cell surface receptor

The specific binding capacity and affinity of ^{125}I-EGF to the EGF receptor were measured in KB cells, grown in 48-well plates (Falcon) in the presence or absence of different quantities of HK1-ceramide for 24 h in DMEM without FCS. Cells were washed, and ^{125}I-EGF with a specific activity of 2.8×10^5 cpm/ ng was added to each well and incubated at 4 °C for 2 h. Nonspecific binding of EGF was determined by preincubation of a 500 – 1000 fold excess of cold EGF in four separate wells with different quantities of ^{125}I-EGF (0.25, 0.5, 1, 3.5, 10, 15 and 20 ng/ ml ^{125}I-EGF). Cells were washed and incubated with 1 N NaOH at 25 °C for 1 h and the radioactivity associated with the cell monolayers was counted with a γ counter (Wallac LKB1282

CompuGamma). The background value was substracted. The effect of HK1-ceramide on the specific binding of ^{125}I-EGF is presented by the method of Scatchard.[83]

2.6. Animals.

SCID mice of both sexes, strain C.B-17/ Ztm-*scid*, 10 - 12 weeks old, were used to ensure a tolerable size of the pancreatic tissue for tumor cell implantation. Leaky SCID mice were detected by measuring serum immunoglobulin (Ig) levels by an enzyme linked immunosorbent assay (ELISA) for Ig. Leaky mice with more than 10 μg/ ml of Ig were excluded from the experiment.[84] All animals were maintained in a sterile environment in special cages with filter hoods and in a scantainer (Scanbur, Koge, Denmark) on daily 12 h light/ 12 h dark cycles. Cages, bedding and water were all autoclaved and the food gamma irradiated. All manipulations were conducted under aseptic conditions in a laminar flow hood. All experiments were conducted according to German regulations for animal experimentations and approved by the administration of Lower Saxony, Germany (Bezirksregierung Braunschweig, Nr. 509.42502/01-28.98).

2.7. Compounds.

Table 3: Specification of compounds

Name	Mol. Weight	Supplier (ordering number)
AF86.1	697.14	Institute f. Organic Chemistry Göttingen
0.9 % NaCl		Braun Melsungen, Germany
Gemcitabine HCL	299.66	Lilly, Germany
Dimethylacetamid (DMA)		Merck, no. 8.03235.1000
Polyethylenglycol (PEG400)		Merck, no. 8.17003.1000
Ro 28-2653	485	Roche
Natrium-Carboxymethylcellulose		Roche
AG3340	432.5	Institute f. Organic Chemistry Göttingen

2.7. Formulations and treatments.

AF86.1 (Acute toxicity)

The acute toxicity of *seco*-CBI derivative AF 86.1 was evaluated by administration to young male and female SCID-mice using DMSO/ 0.9% saline solution (1:200) as vehicle. Each animal received either a single dose (group 2), or three doses (group 3), or five doses (group 4), respectively one dose containing 20 μg/kg daily. Control animals (group 1) received five i.p. doses, vehicle solution, equivalent to the volume of test solution administered. The application volume was 5 ml/ kg body weight. After treatment application all animals were observed for 14 days for mortality and signs of toxicity. One animal (group 5) received a single dose of 2000 μg/ kg for investigating long-time toxicity (4 month).All organs e.g. liver, spleen, kidneys, lung, stomach, mesentery, brain were excised and fixed in formalin. Further histological examinations were performed. Before sacrification blood samples were taken from each mouse by retrobulbar puncture and

hematological and clinical parameters were analysed.

AF86.1

On day 28 after subcutaneous tumor implantation AF86.1, 25 μg/ kg, using DMSO/ 0.9% saline solution (1:200) as vehicle, were applied to the mice, i.p. After 1 h, 5μl (≈ 90 units) oft he enzyme β-D-galactosidase (Sigma, G2513, 250-600 units per mg protein) were administered directly into the subcutaneous tumors. The animals were sacified on day 30.

AG3340

AG3340, 3(S)-2,2-dimethyl-4-[4-pyridin-4-yloxy)-benzenesulfonyl]-thimorpholine-3-carboxylic acid hydroxyamide (M_r 432.5) was synthesized as previously described.[85] An aqueous suspension was prepared fresh every day by homogenizing and sonicating AG3340 in 0.5 % methylcellulose (Sigma, Deisenhofen, Germany). Animals were injected with either 100 mg/ kg AG3340 or 0.5 % methylcellulose alone as vehicle control, intraperitoneal (i.p.), every 12 h. Compounds or vehicle were applied at a volume of 10 ml/ kg. The treatment was started on day 8 after orthotopic implantation and given until sacrifice on day 29.

Gemcitabine HCL

The compound is formulated as a lyophilized product containing an equivalent of gemcitabine. Gemcitabine was reconstituted by adding 0.9 % sodium chloride solution fresh every day.

Animals received either 0.9, 2.2, 6.6 mg/ kg gemcitabine or 0.9 % NaCl alone as vehicle control, intraperitoneal (i.p.), every 48 h. Tumor bearing randomized animals were used for each experiment. The treatment was started on day 8 after

orthotopic implantation and given until sacrifice. Compounds or vehicle were applied at a volume of 4 ml/ kg.

Ro28-2653 (single treatment)

One volume of dimethylacetamide (DMA) was mixed with 9 volumes of 50 % polyethylenglycole (PEG) 400 in aqua bidest. Ro28-2653 was dissolved at a concentration of 4.5 mg/ ml (eventually warmed at 35 - 40 °C) in DMA/ PEG400 fresh every day, followed by sonication,.

Animals were treated with either 45.0, 22.5, 11.0 mg/ kg Ro 28-2653 or DMA/ PEG400 alone as vehicle control, orally, every 24 h. Tumor bearing randomized animals were used for each experiment The treatment was started on day 8 after implantation and given until sacrifice (Figure1). Compounds or vehicle were applied at a volume of 10 ml/ kg.

Ro28-2653 and Gemcitabine HCL (Combination study)

Ro28-2653 (containing 50 % Eudragit) was dissolved at a concentration of 9 mg/ ml (eventually warmed at 35-40 °C) in Natrium-Carboxymethylcellulose (CMC). Gemcitabine was formulated as described earlier.

Animals were treated with either 45.0 mg/ kg Ro 28-2653 or CMC alone as vehicle control, p.o., every 24 h in combination with 2.2 mg/kg Gemcitabine or 0.9 % NaCl as vehicle control, i.p. every 48 h. One group received no treatment. The treatment was started on day 7 after implantation and given until sacrifice. Ro28-2653 or vehicle were applied at a volume of 10 ml/ kg, gemcitabine or vehicle at a volume of 4ml/ kg.

Ro28-2653 and Gemcitabine HCL (Combination study and survival)

Animals were treated with either 45.0 mg/ kg Ro 28-2653 or Natrium-Carboxymethylcellulose (CMC) alone as vehicle control, p.o., every 24 h. in combination with 2.2 mg/ kg gemcitabine or 0.9 % NaCl as vehicle control, i.p. every 48 h. The treatment was started on day 7 (group 1-4) or on day 21 (group 5) after implantation and given for 24 days. Animals were inspected daily. Tumor invasion caused complications such as high weight loss, rough hair and apathetic behavior and sacrifation was performed immediately. Days of survival were counted.

2.9. Subcutaneous tumor implantation

For subcutaneous tumor implantation (s.c.) 1 x·10^6 A549 or Panc Tu1 tumor cells, in a volume of 100 µl PBS were injected slowly, into the flank of SCID mice. For this procedure no anesthesia were performed. The sizes of subcutaneous tumors were recorded twice weekly using linear calipers. The tumors were excised and analyzed by histologigal examination. Five sections of each tumor were stained with H&E.

2.10. Orthotopic tumor implantation and tumor growth

General anesthesia was performed by i. p. application using ketamine (100 mg/ kg) and xylazine (20 mg/ kg). A median laparotomy was performed, the peritoneum opened and the pancreas exposed by applying gentle traction at the stomach. Tumor cells, 1 x 10^6 in a volume of 15 µl PBS were injected with an insulin syringe, 29 gauge × $^1/_2$ (Becton Dickinson, Heidelberg, Germany) into the proximal part of the pancreas through the serosa into the pancreatic tissue. The cells were implanted so as to visibly infiltrate the pancreatic tissue. The pancreas was then returned to the

abdominal cavity and the incision was closed in two layers using a 4-0 Vicryl suture (Ethicon, Norderstedt, Germany). All animals tolerated the procedure well. After implantation, mice were inspected twice a week for body weight loss and tumor formation in the peritoneal cavity (abdominal distension).

The animals‘ general condition (defined in terms of the condition of the coat and nutrition, and behaviour) after a defined number of days dependent on the treatment schedule (see results) was assessed before the animals were sacrified by cervical dislocation. Autopsies were performed and the abdomen and thoracic cavity were examined systematically. All findings, complications, grade of invasion into the surrounding tissue and the size, numbers and location of metastases were recorded. The length, width and height of pancreatic tumors were measured and the volumes were calculated according to the formula 0.5 x length x width x height. The pancreatic tumor mass including the attached organs, metastases, and different organs were excised, placed in phosphate - buffered 4 % formalin for 16 hours at room temperature and embedded in paraffin. 2.5 μm tissue sections were obtained, stained with hematoxylin and eosin (H & E) or Masson Goldner and were reviewed for routine microscopic examinations.

Macroscopic metastases were defined by their visibility as white nodules, but were verified by histological examination. Microscopic metastasis was only histologically detected. Necrotic areas in the tumors were estimated on histological sections and defined as proportion of the total area of tumor tissue.

2.11. . Immunohistochemistry

HK1-staining

For immunohistochemistry, 2.5 μm sections from formalin-fixed and paraffin-embedded tissues, were mounted on slides, deparaffinized in xylene and rehydrated

in ethanol/ water dilutions. For HK1- staining the slides were pretreated by boiling them in a microwave oven five times for 5 min in citrate buffer (pH 6.0) for antigen retrieval. Endogenous peroxidases were inactivated by 3 % hydrogen peroxide for 10 min. Tris buffered 10 % swine serum solution (Dako, Hamburg, Germany) was then added to block nonspecific protein binding and slides were incubated with the rabbit polyclonal antibody anti-HK1[48] for 90 min (1:800) followed by exposure to the secondary antibody, biotinylated swine anti rabbit (Dako 1:200) for 60 min. Sections were then incubated with avidin-peroxidase solution (Dako), stained with aminoethylcarbazole (AEC substrate solution, Sigma), rinsed in water and finally counterstained with hematoxylin.

Ki67-staining

For immunohistochemistry, 2.5 μm sections from formalin-fixed and paraffin-embedded tissues, were mounted on slides, deparaffinized in xylene and rehydrated in ethanol/ water dilutions. The slides for Ki67 staining were pretreated by boiling in a microwave oven five times for 5 min in citrate buffer (pH 6.0) for antigen retrieval. Endogenous peroxidases were inactivated by 3 % hydrogen peroxide for 10 min. Tris buffered 10 % rabbit serum solution (Dako, Hamburg, Germany) was then added to block nonspecific protein binding and slides were incubated with the monoclonal antibody mouse anti-human Ki67 (Dianova, Hamburg, Germany) for 60 min (2 μg/ ml) followed by exposure to the secondary antibody, biotinylated rabbit anti mouse *F(ab')$_2$*-fragment (Dako16.8 μg/ ml) for 30 min. Sections were then incubated with avidin-peroxidase solution (Dako), stained with aminoethylcarbazole (AEC substrate solution, Sigma), rinsed in water and finally counterstained with hematoxylin. The average number of Ki67 positive nuclei was counted in three most cellular fields in

the tumors containing subjectively the highest density of mitotic figures and was defined as a proportion of total nuclei stained with H & E in the same areas.[86]

Cytokeratin-staining

Before incubating the monoclonal antibody mouse anti-human cytokeratin (Immunotech, Hamburg, Germany) at a dilution of 1:2 for 2 h, the slides were pretreated in a Tris buffer-solution with 0.1 % trypsin, 0.1 % calciumchloride for 10 min at 37° C followed by preincubation with Tris buffered 10 % rabbit serum solution. Detection of primary antibody was performed using the alkaline phosphatase antialkaline phosphatase, APAAP method (Dako, 2.5 μg/ ml) with rabbit anti-mouse secondary antibody (Dako, 87.5 μg/ ml) and development with Newfuchsin (Sigma) for 30 min. Counterstaining was done with hematoxylin. For searching micrometastases portion of the lung and liver were sliced into 25 serial sections where only each fifth section was analyzed by histological examination.

2.12. Data analyses

Statistical analyses of data were performed using unpaired Student`s t-test with two-tailed comparison taking into account the degree of freedom according to Satterthwaite.[87]

Differences of $p < 0.05$ were considered to be significantly different.

3. Results

3.1. Regulation of EGF receptor activity by HK1-ceramide, a stable synthesized analogue of the ganglioside GM3-lactone

The goal of this study was to determine whether the lactone form of GM3 has a similar inhibitory effect on EGF-R tyrosine phosphorylation and EGF induced cell growth. In order to accomplish this, the influence of the stable ganglioside-lactone-analogue

HK1 ceramide toward EGF receptor signaling and EGF mediated cell growth were examined.

3.1.1. *In situ* effect of HK1-ceramide and HK2-ceramide on EGF-mediated tyrosine phosphorylation of EGF receptor in cultured intact A431 cells.

Human epidermoid carcinoma cells, A431 cells contain high numbers of EGF receptors (2×10^6) [80] and the tyrosine kinase is activated upon binding of EGF to the extracellular portion of the receptor as demonstrated by Western-blot analysis immunoblotted with an anti-phosphotyrosine antibody (Figure 4A, lane 5).

The phosphorylated band observed at 170 kD is consistent with the single polypeptide chain of the EGF-R (Figure 4B) and the smaller band at 116 kD most likely represents a protein downstream of the signal transduction pathway. The 170 kD band is already apparent even without ligand stimulation (lane 7). In order to analyze the effect of GM3-lactone on EGF-R phosphorylation, A431 cells were incubated with different concentrations of HK1-ceramide for 2h and stimulated (+) or not (-) with 50 ng/ ml EGF for 30 min. All gangliosides investigated were dissolved in DMSO, resulting in a final DMSO concentration of 0.86 % in each well. Addition of

Figure 4

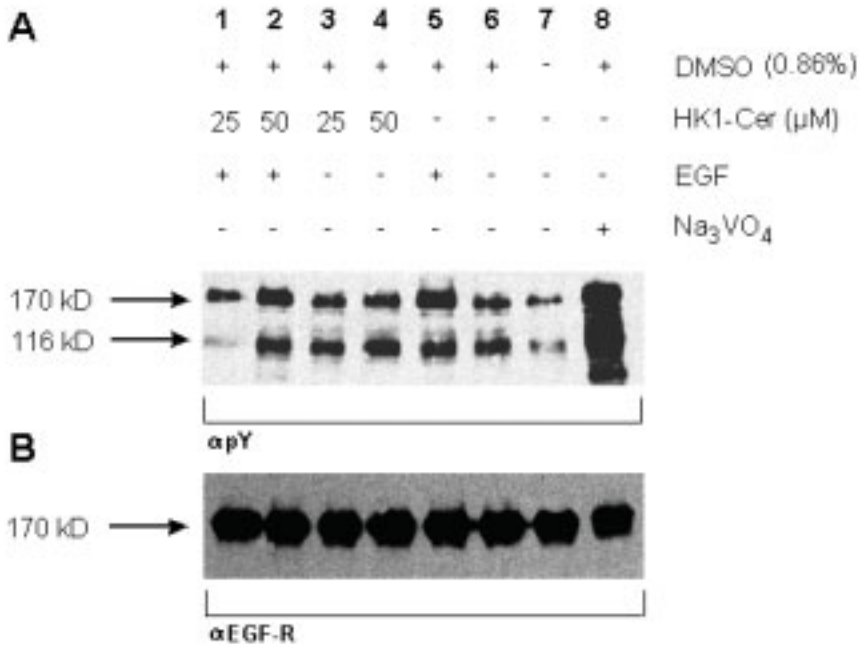

(A) Effect of HK1-ceramide on EGF-dependent tyrosine phosphorylation in A431 cells. A431-cells were incubated with 50 ng/ ml of EGF for 30 min at 37 °C prior to lysis in the presence or absence of different quantities of HK1-ceramide or DMSO as control, added for 3 h. Phosphotyrosine was detected by Western blotting of total lysates using a monoclonal anti-phosphotyrosine antibody (α-PY). The arrows indicate the location of the EGF receptor (170 kD) and proteins downstream of the signal transduction pathway (116 kD). Molecular weight standards are shown in kD. Each lane represents phosphorylation pattern of total lysates of A431 cells in the presence or absence of 50 ng/ml EGF incubated with different quantities of HK1-ceramide. DMSO was used as control. *Lane 1*, 7.5 nmol HK1-ceramide, 50 ng/ml EGF; *lane 2*, 15 nmol HK1-ceramide, EGF; *lane 3*, 7.5 nmol HK1-ceramide, no EGF; *lane 4*, 15 nmol HK1-ceramide, no EGF; *lane 5*, no HK1-ceramide, 50 ng/ml EGF; *lane 6*, no HK1-ceramide, no EGF; *lane 7*, no HK1-ceramide, no EGF, no DMSO; *lane 8*, no HK1-ceramide, no EGF, 9 µg/ ml orthovanadate.

(B) Detection of the expression of equal amounts of EGF-R (170 kD) in each total lysate by reblotting the membrane with the EGF-R specific antibody. Similar results were obtained in seven separate experiments.

DMSO and orthovanadate (Na_3VO_4) (lane 8), an inhibitor of tyrosine specific phosphatases, were used as controls. In the presence of DMSO alone, a slight increase of EGF-R autophosphorylation was observed (lane 6). Addition of EGF resulted in an enhanced tyrosine-phosphorylation especially of the 170 kD band, representing the EGF receptor (lane 5). The EGF-stimulated tyrosine-phosphorylation is reduced by HK1-ceramide (lane 1) in a small range of influence c_{effect}= (25.0 ± 1.5) μM (up to 100 % inhibition of EGF-R phosphorylation). Additionally an inhibition of phosphorylation by HK1-ceramide was detected in other bands in response to EGF. In particular, the phosphorylation of the 116 kD protein was reduced in HK1-ceramide treated cells in comparison to controls suggesting that downstream targets of the EGF-R were also affected by HK1-ceramide. Concentrations of HK1-ceramide ranging from 0 - 20 μM and from 30 - 100 μM showed no significant inhibitory effect on EGF-R phosphorylation (Figure 4A, lane 2, Figure 5, Table 4). The inhibitory effect of 25 μM HK1-ceramide in a small range of concentration on EGF-R autophosphorylation was only observed in the presence of EGF (Figure 4A, lane 3, 4). Similar results were obtained in seven separate experiments.

Reblotting of the nitrocellulose membranes with a specific EGF receptor antibody showed that equal amounts of receptor were expressed in each assay (Figure 4B). The β-isomere, HK2-ceramide in concentrations in the range of 20 - 100 μM had no effect on phosphorylation of the EGF receptor nor of proteins downstream of the signal transduction pathway (data not shown).

Figure 5:

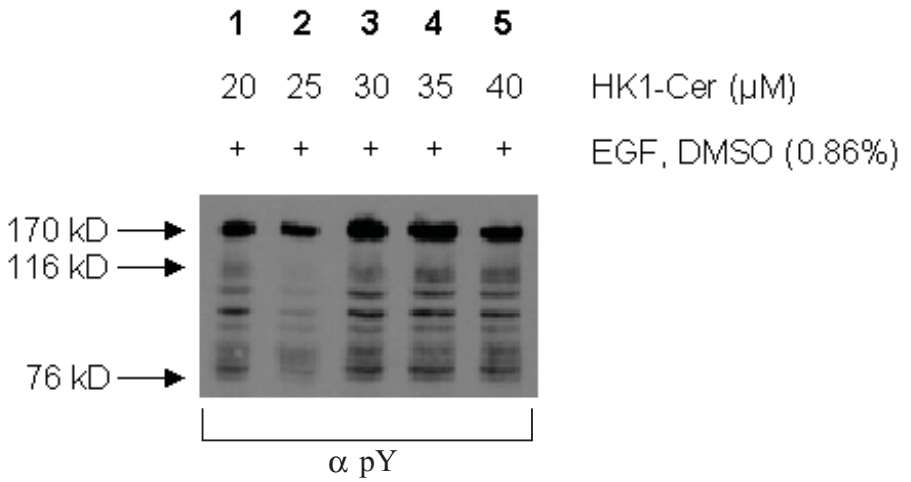

Effect of increasing amounts of HK1-ceramide on EGF-dependent tyrosine phosphorylation in A431 cells. Different concentrations of HK1-ceramide (ranging from 6 – 12 nmol) or DMSO as control were added to A431-cells for 3 h and each well was incubated with 50 ng/ ml of EGF 30 min at 37 °C prior to lysis. The amount of tyrosine phosphorylation of total lysates was analyzed by Western blotting with anti-phosphotyrosine antibody (α-PY). *Lane 1*, 6 nmol HK1-ceramide; 50 ng/ ml EGF; *lane 2*, 7.5 nmol HK1-ceramide, 50 ng/ ml EGF; *lane 3*, 9 nmol HK1-ceramide, 50 ng/ ml EGF; *lane 4*, 10.5 nmol HK1-ceramide, 50 ng/ ml EGF; *lane 5*, 12 nmol HK1-ceramide, 50 ng/ ml EGF. The arrow indicates the location of the EGF receptor (170 kD).

Table 4

Cell-line	Ganglioside added	Concentration nmol/300 µl	50 ng of EGF	Inhibition of tyrosine phosphorylation - fold stimulation of receptor -[a]	Per cent inhibition[a]
A431	No addition	-	-	1.0	-
	No addition	-	+	3.8	-
	HK1-Cer	0.0 - 7.0	+	3.8	0 %
	HK1-Cer	7.0 - 8.0	+	1.0	≤ 100 %
	HK1-Cer	8.0 - 30.0	+	3.8	0 %
	HK2-Cer	0.0 - 30.0	+	3.8	0 %
	GM3	0.0 - 30.0	+	3.8	0 %
	GM3	60.0	+	2.1	60 %

[a] Mean of three determinations

3.1.2. *In situ* effect of GM3 on EGF-mediated tyrosine phosphorylation of EGF receptor in cultured intact A431 cells in dependence of the pH.

Moderate inhibition of EGF-R tyrosine phosphorylation was observed in the presence of 200 μM GM3 at physiological pH values (60 % inhibition, Fig. 6, Table 4), whereas no inhibition was observed in the presence of 0 - 100 μM GM3 (Table 4, data not shown). In order to analyze whether the inhibitory effect of high concentrations of GM3 on EGF receptor phosphorylation might be due to a lactonization of GM3, we determined EGF dependent receptor tyrosine phosphorylation in A431 cells in the presence of 200 μM GM3 and low pH values. Decreasing pH values resulted in enhanced EGF-independent tyrosine-phosphorylation of the receptor (Fig. 6A, lane 1-5). In contrast, upon EGF stimulation a reduced tyrosine-phosphoylation of the receptor could be observed at low pH values (Fig. 6B, lane 1-5). Addition of 200 μM GM3 showed no inhibitory effect on EGF receptor activity at different pH values (Fig. 6C, lane 1-5).

Figure 6:

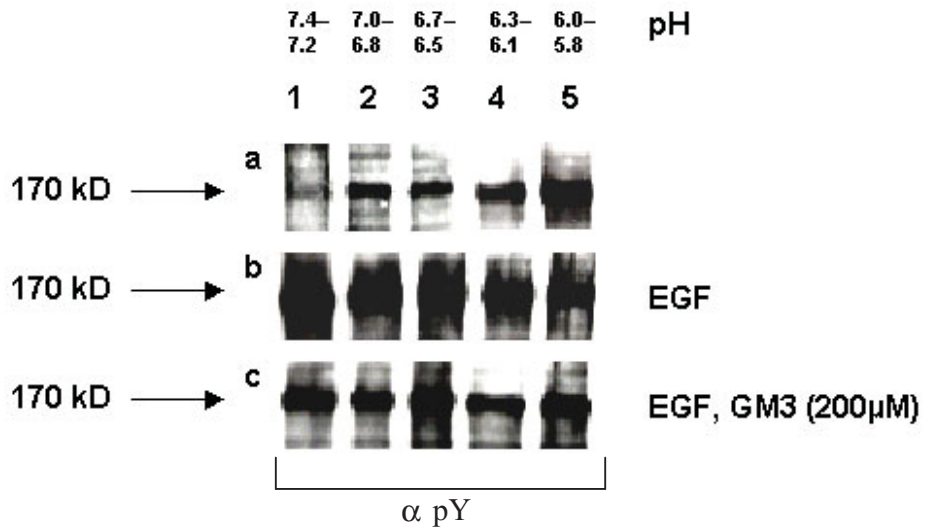

EGF-dependent phosphorylation of EGF-receptor in A431 cells in the presence of 200 μM GM3 at physiological and decreased pH. EGF-Receptor tyrosine phosphorylation was measured by Western blotting of total cellular lysates with anti-phosphotyrosine antibody (α-PY). *(a)* No treatment, *(b)* 50 nmol/ ml EGF, *(c)* 50 nmol/ ml EGF, 200 μM GM3. The arrow indicates the location of the EGF receptor (170 kD).

3.1.3. Effect of HK1-ceramide on MAP kinase activity.

For analyzing the effects of HK-1 ceramide on MAP kinase activity A431-cells were incubated with 50 ng/ ml of EGF for 30 min at 37 °C prior to lysis in the presence or absence of of 25 μM HK1-ceramide or DMSO as control, added for 3 h. A phosphotyrosine blot was performed and reblotted with pERK antibody that recognizes tyrosine phosphorylated erk1 and erk2. The effect of HK1-ceramide on MAP kinase activities is shown in Figure 7. Map kinases are activated after EGF stimulation in intact cells (Figure 7, lane 2). HK1-ceramide, at a concentration of 25 μM, inhibited EGF dependent MAP kinase erk1 activity almost completely (lane 1):
The phosphorylation of the 44 kD protein (erk1) was markedly reduced in HK1-ceramide treated cells in comparison to controls (lane 3).

Figure 7:

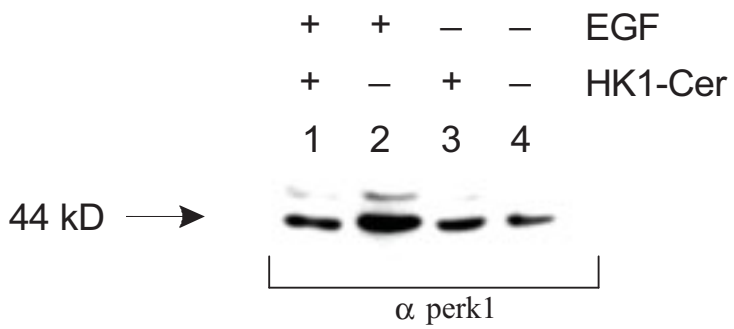

Effect of HK1-ceramide on MAP kinase activity in A431 cells. An antiphosphotyrosine blot of total lysates of A431 was re-blotted with anti pERK antibody which reacts with both tyrosine-phosphorylated erk 1 and erk2. *Lane 1,* 7.5 nmol HK1-ceramide, 50 ng/ ml EGF, DMSO; *Lane 2*, no HK1-ceramide, 50 ng/ ml EGF, DMSO; *Lane 3*, 7.5 nmol HK1-ceramide, no EGF, DMSO; *Lane 4*, no HK1-ceramide, no EGF, DMSO. The arrow indicates the location of perk1 (44 kD).

Effect of HK1-ceramide on specific binding activity of ^{125}I-EGF to cell surface receptor.

To determine if the change in tyrosine phosphorylation of the EGF-R observed after HK1-ceramide incubation was due to an alteration of EGF-R binding characteristics, competition binding experiments were performed with HK1-ceramide treated and control cells. The binding activities of ^{125}I-EGF on the cell surface of KB cells grown in normal culture media and in media to which different amounts of HK1-ceramide (6 μM, 11 μM, 25 μM and 56 μM) were added are shown in Figure 8. No difference were observed in the binding activities obtained from HK1-ceramide treated cells compared to controls.

Figure 8.

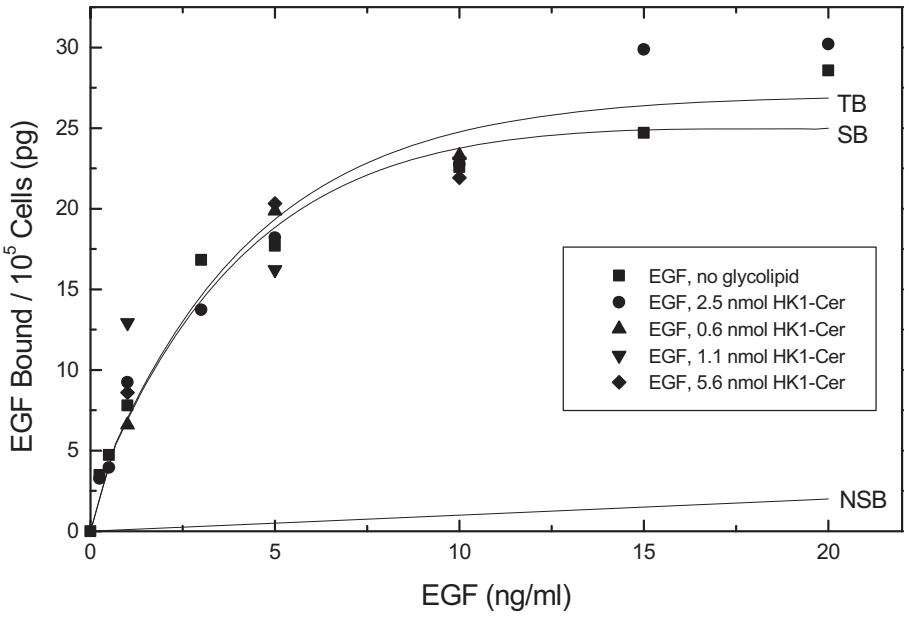

Effects of the presence or absence of different quantities of HK1-ceramide (2.5 nmol, 0.6 nmol, 1.1 nmol and 5.6 nmol HK1-ceramide) on the specific binding capacity and affinity of ^{125}I-EGF to the EGF receptor in A431 cells. The cell monolayers were washed, and ^{125}I-EGF with a specific activity of 2.8×10^5 cpm/ ng was added to each well and incubated at 4 °C for 2 h. Nonspecific binding of EGF was determined by preincubation of a 500 – 1000 fold excess of cold EGF in four separate wells with different quantities of ^{125}I-EGF (0.25, 0.5, 1, 3.5, 10, 15 and 20 ng/ ml ^{125}I-EGF). The cells were washed and incubated with 1 N NaOH at 25 °C for 1 h and the radioactivity associated with the cell monolayers was counted with a γ counter. The effect of HK1-ceramide on the specific binding of ^{125}I-EGF is presented by the method of Scatchard

TB Total Binding; SB Specific Binding; NSB Non Specific Binding ; **1** ^{125} **I-**EGF, no glycolipid; **2** ^{125} **I-**EGF, 2.5 nmol HK1-ceramide; **3** ^{125} **I-**EGF, 0.6 nmol HK1-ceramide; **4** ^{125} **I-**EGF, 1.1 nmol HK1-ceramide; **5** ^{125} **I-**EGF, 5.6 nmol HK1-ceramide. Total volume of reaction mixture was 100 µl.

3.1.3. Effect of HK1-ceramide on EGF-dependent mitogenesis in KB cells.

Since high concentrations of EGF inhibit the growth of A431 cells [80], we used the epidermoid carcinoma KB cells for analyzing the effect of HK1-ceramide on EGF-dependent mitogenesis. The growth of KB cells was clearly inhibited in the presence of different concentrations of HK1-ceramide (6 µM, 17 µM and 25 µM) in a dose dependent manner (Table 5).

Table 5

HK1-Ceramide[a]	1 ng/ ml EGF	OD (450 nm)	EGF dependent inhibition
-	-	0.140	-
-	+	0.473	-
0.6 nmol	+	0.265	62 (± 8) %
1.7 nmol	+	0.204	81 (± 4) %
2.5 nmol	+	0.185	86 (± 1) %

[a] Total volume of reaction was 100 µl. Cells were seeded at day 0, 1.2×10^3 cells/ well (Falcon 96- well plate).The value is the arithmetic mean of five determinations.

3.2. A novel polyclonal antibody directed against the lactone form of ganglioside GM3: Analyses of its potential as tumor marker for melanomas.

As demonstrated in figures 9, 10, 12 - 14 and 16 the expression pattern of GM3 and probably GM3-lactone on different types of malignant melanoma (SSM, LMM, ALM using the polyclonal antibody HK1) are very similar to each other with only slight degree of variation. Melanoma cells within these lesions express GM3-lactone or GM3 at the dermal-epidermal junction as well as within atypical nests of the upper dermis. Lower dermal parts of the tumor show either a very weak staining or a complete loss of expression (Fig. 12). In dysplastic melanocytic nevi only melanocytes that have aggregated in the epidermal compartment show a positive staining. The intradermal lying nests of melanocytes are negative (Fig. 15). As shown on Fig. 11 atypical nests of malignant melanoma cells within a congenital melanocytic nevus prove a strong positivity, whereas the surrounding melanocytic cells are negative for HK1 staining. Melanophages are characterized by the cytoplasm-rich cells, packed with strong staining granules. The melanocytes in the basal layer of normal skin do not show any expression of gangliosides detected by the HK1-antibody.

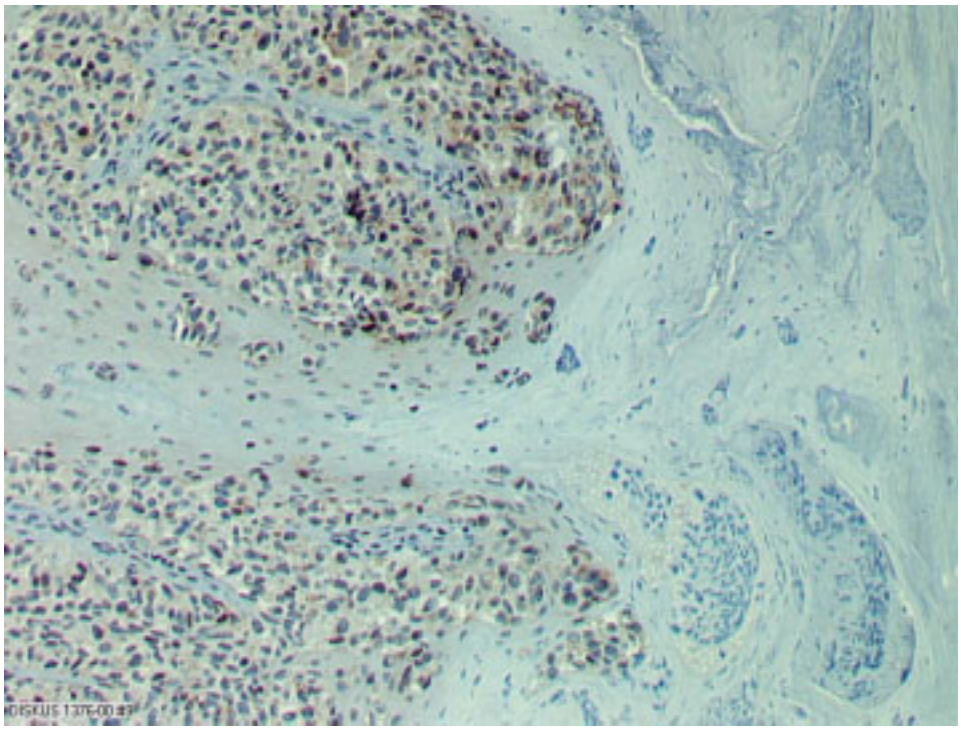

Figure 9: Acral lentiginous melanoma (ALM)

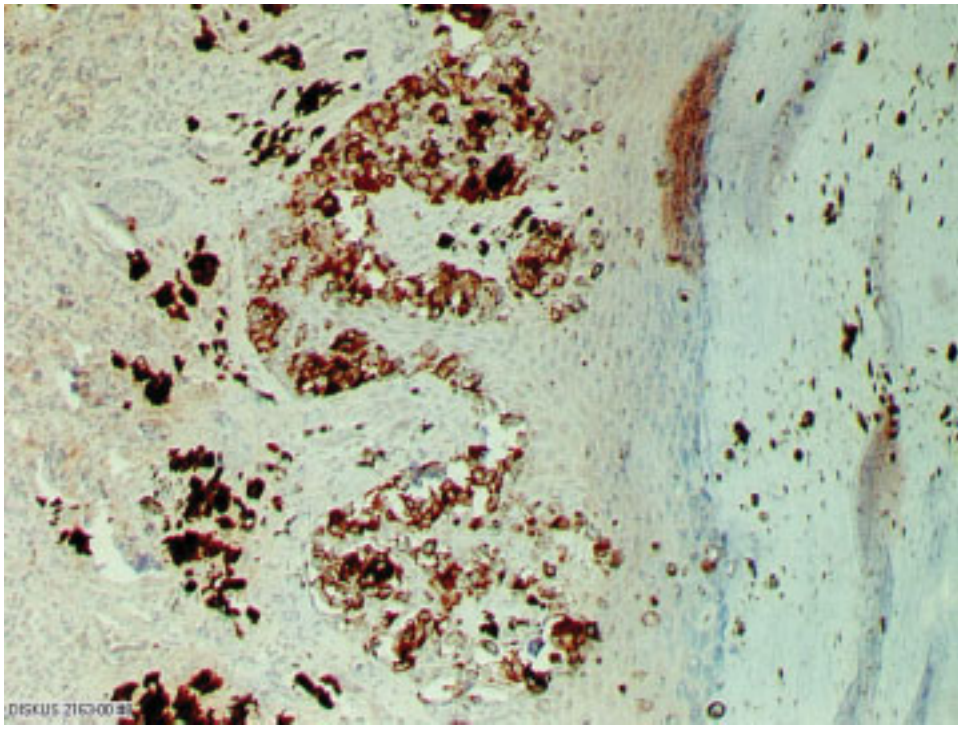

Figure 10: Acral lentiginous melanoma (ALM)

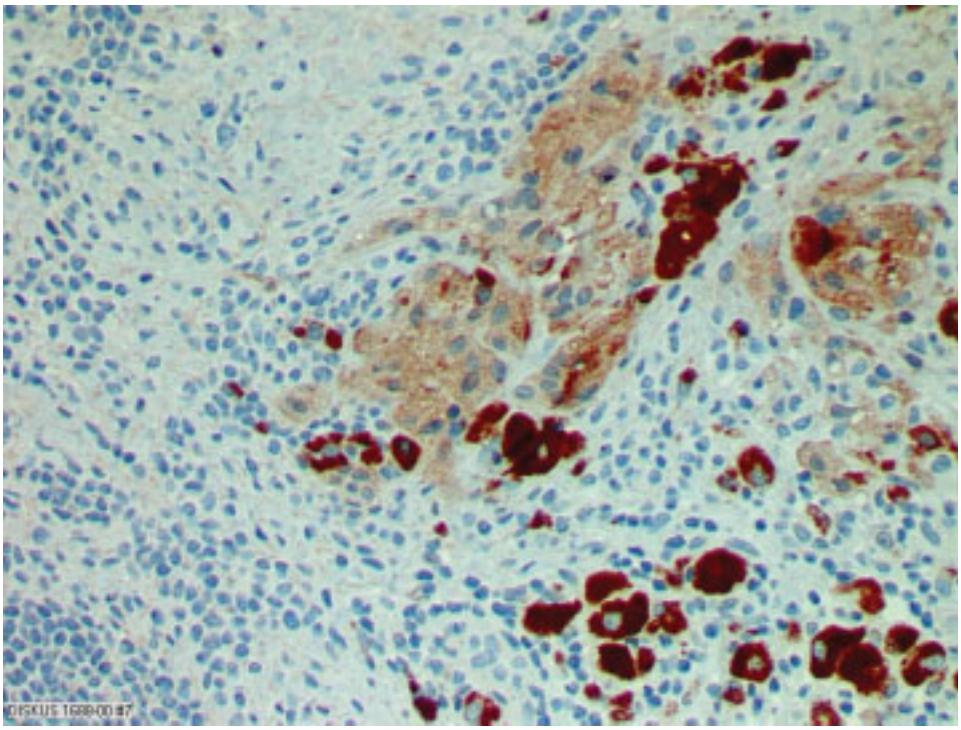

Figure 11: Malignant melanoma arising in congenital melanocytic nevus.

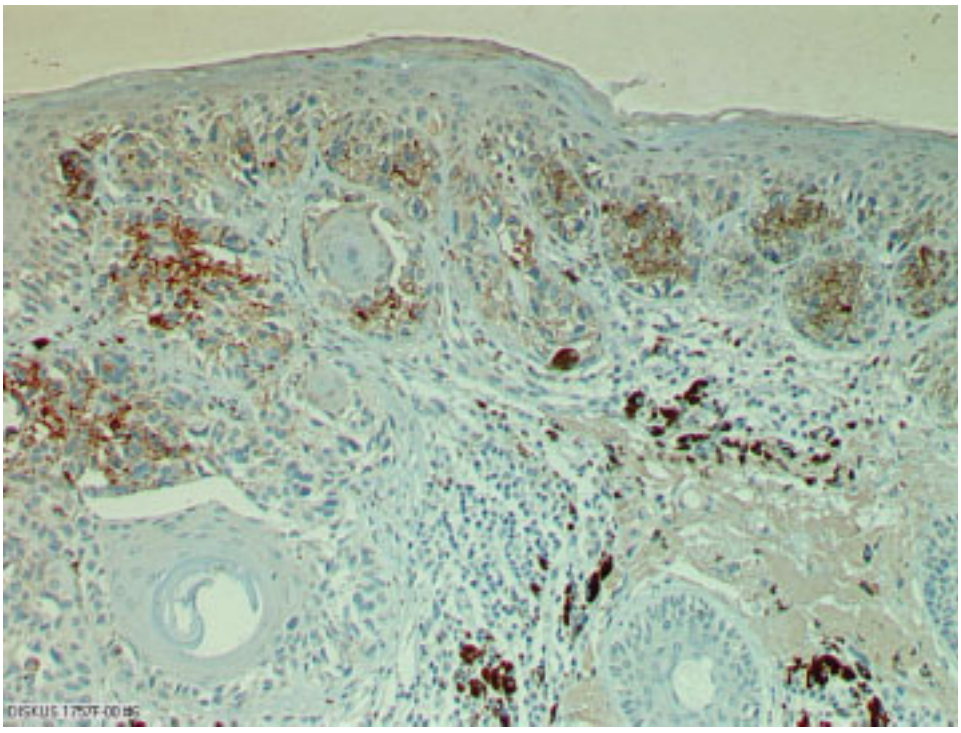

Figure 12: Lentigo maligna melanoma (LMM)

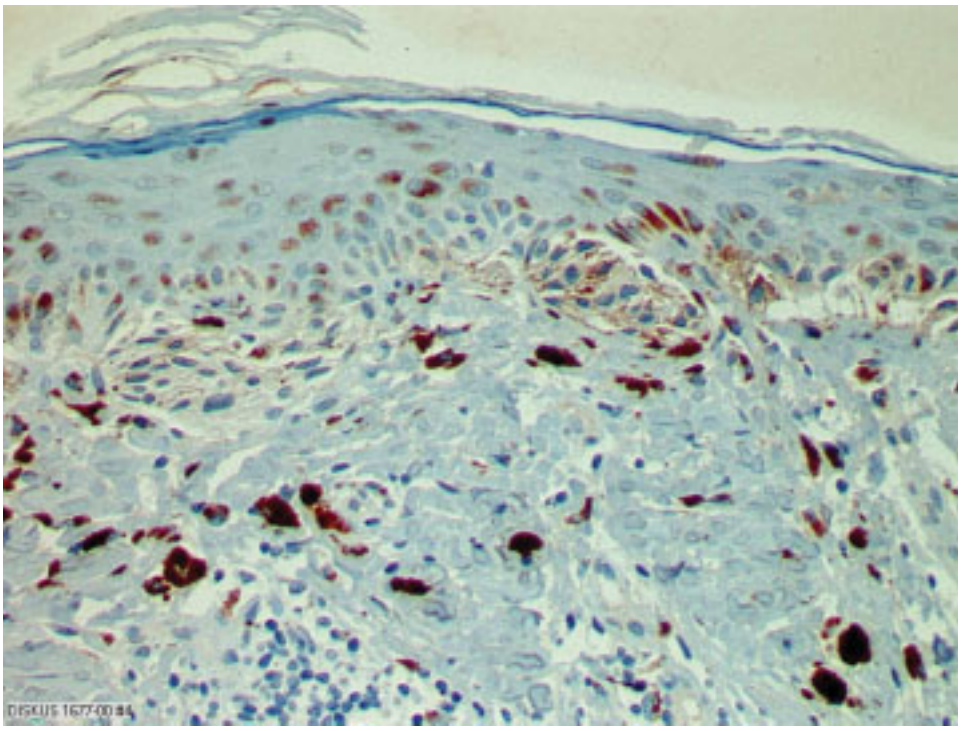

Figure 13: Superficial spreading malignant melanoma (SSM) with partial regression.

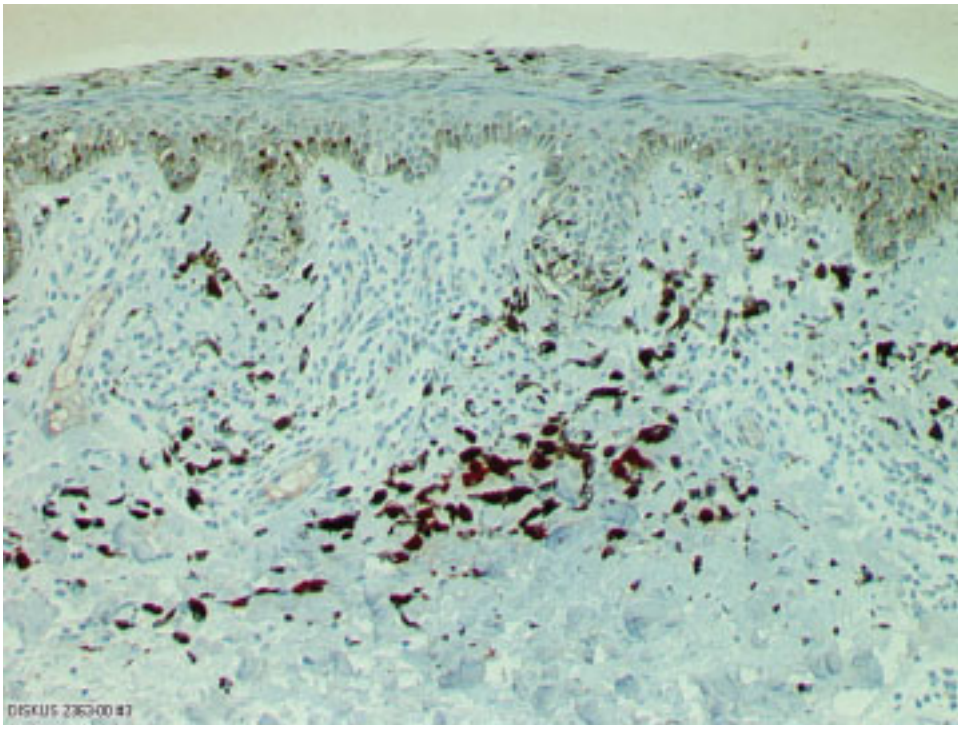

Figure 14: Malignant melanoma in situ

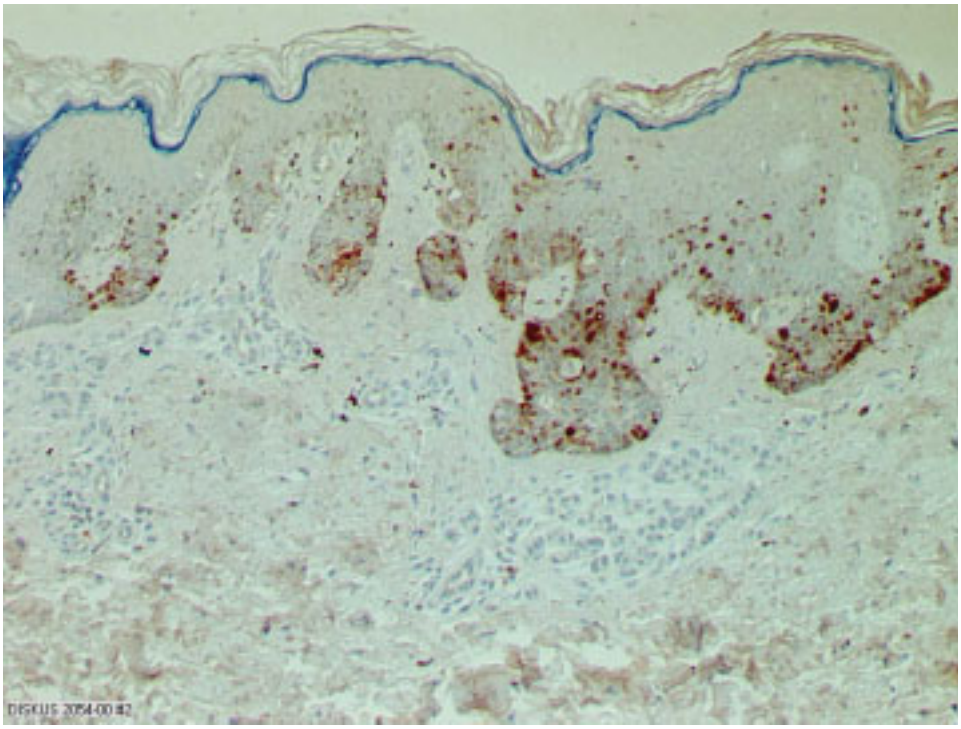

Figure 15: Compound dysplastic nevus.

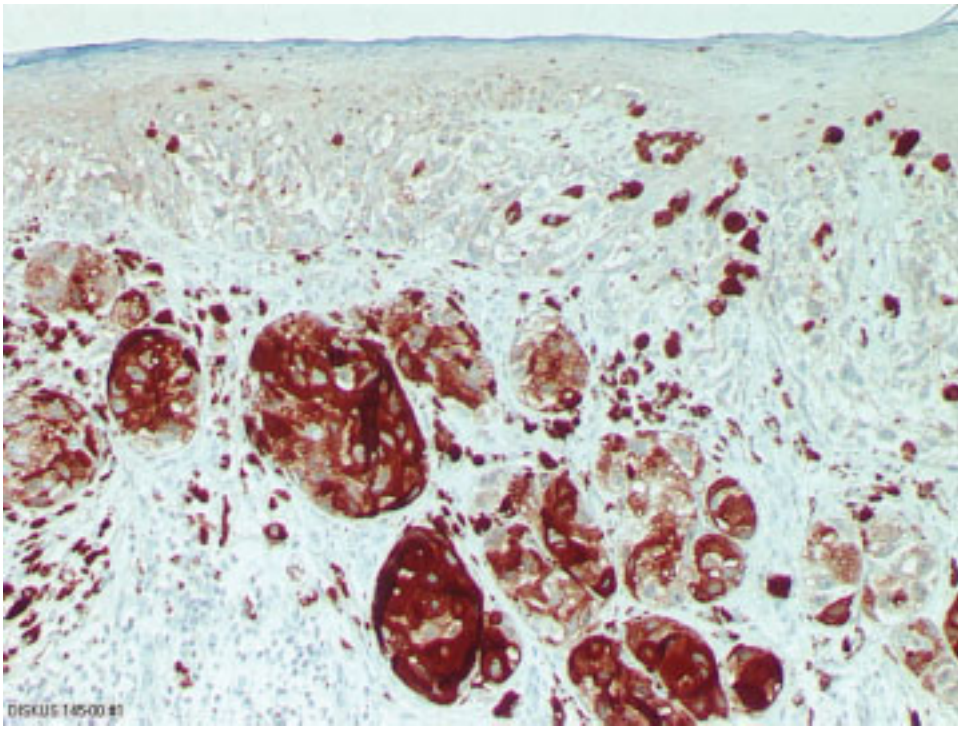

Figure 16: Superficial spreading malignant melanoma (SSM).

3.3. Evaluation of the efficacy of novel synthetic drugs to inhibit tumor growth and progression of human pancreatic ductal adenocarcinoma

3.3.1. The orthotopic SCID-mouse model

3.3.1.1. Growth characteristics of human PancTu 1 after orthotopic implantation in SCID mice

Orthotopic implantation of human PancTu 1 cells in controls, treated with vehicle only, resulted in locally invasive tumors (Figure 17A) that compares well to the situation in human. Histologically, the PancTu 1 cells formed poorly differentiated ductal adenocarcinomas in all controls, with a high mitotic rate and scarce stromal reaction (Figure 17G). The tumors showed invasion into neighbouring organs, such as liver and porta hepatis (Figure 17A, 17B, 17I), duodenum, stomach (Figure 17B, 17K) and, occassionally, spleen (Table 10) and infiltrated the normal pancreatic tissue (Figure 17G). Small clusters of tumor cells were observed in the lymphatic vessels and in lymph nodes surrounding the pancreas. Massive growth into the surrounding organs resulted in obstruction of the stomach (Figure 17B) causing gross body weight loss. In addition, there were peritoneal nodules in the mesentery (Figure 17C), diaphragm, pelvis and attached to the kidneys, spleen and reproductive organs or at the site of the surgical incision (Table 11). Hematogenous metastases were detected in the lung (Figure 17J) and mediastinum.

Figure 17

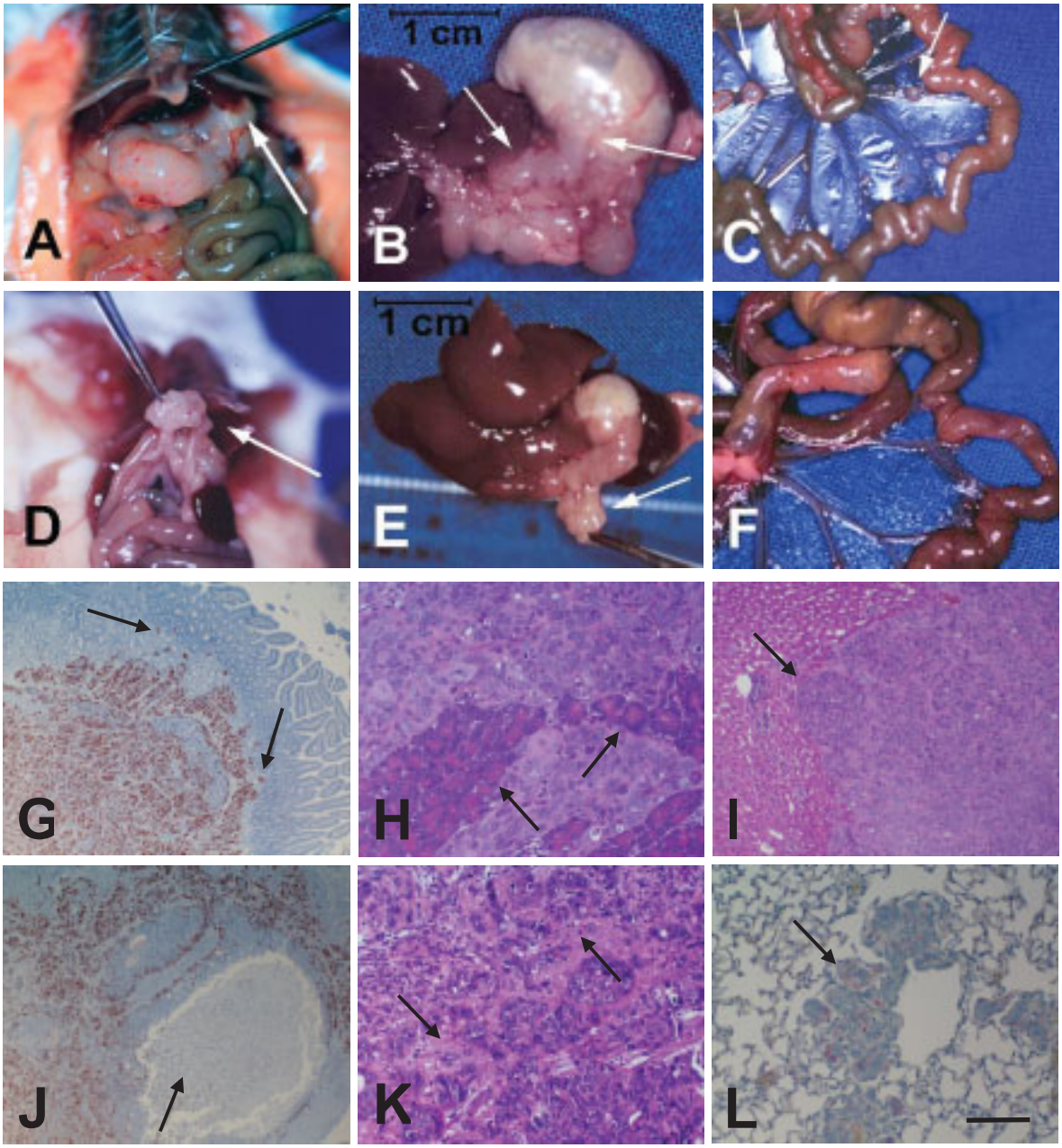

Macroscopy: (A) Pancreatic tumor in a control mouse invading into the liver (arrow). (B) Pancreatic tumor in a control mouse invading into the liver (arrow) and the stomach (arrow) resulting in stomach obstruction. (C) Multiple metastases in the mesentery of a control mouse (arrows). (D) Pancreatic tumor of a AG3340 treated mouse (arrow). (E) Pancreatic tumor of a AG3340 treated mouse, which shows small tumor volume and lacks invasive growth (arrow). (F) Mesentery of a AG3340 treated mouse lacking metastases.

Histological characteristics: (G) Immunostaining for Ki67 shows a highly proliferating tumor and marked tumor invasion (arrows) into the stomach mucosa of a control mouse. (H) Pancreatic tumor tissue in a control mouse showing a poorly differentiated ductal adenocarcinoma with little desmoplastic reaction and invasion of acinar tissue, H & E (arrows). (I) Pancreatic tumor in a control mouse invading the liver, H & E (arrow). (J) Immunostaining for Ki67 of a pancreatic tumor of a AG3340 treated mouse. Area of necrosis (arrow). Tumor cells surrounding the necrotic area and small tumor nodules with absent Ki67 expression. (K) Pancreatic tumor tissue in a AG3340 treated mouse shows a moderately differentiated ductal adenocarcinoma, H & E (compare with H). There are many apoptotic cells and an almost cell free stroma(arrows).
(L) Immunostaining for cytokeratin labels micrometastases (arrow) in the lung of an untreated mouse (arrow). The length of the bar in L represents 100 μm in H, K and L, and 200 μm in I, and 500 μm in G and J.

3.3.2. Evaluation of the *seco*-CBI-derivative AF86.1 for its potential use in antibody directed enzyme prodrug therapy. Preliminary results *in vivo* in SCID mice.

In order to proof the principle of this new ADEPT-system including AF86.1 and an ephithelial membrane antigen antibody - β-D-galactosidase conjugate *in vivo* in the orthotopic SCID-mice model, preliminary investigations have been done to analyze at first the toxicity of AF86.1 in mice and secondly if AF86.1 is toxic by galactosidase *in vivo.*

3.3.2.1. Acute Toxicity

The acute toxicity of AF86.1 was studied in SCID-mice, using the interperitoneal route of administration. The schedule of timings and treatments are illustrated in figure 18, and experimental groups and doses are summarized in table 6

3.3.2.1.1. Experimental Design

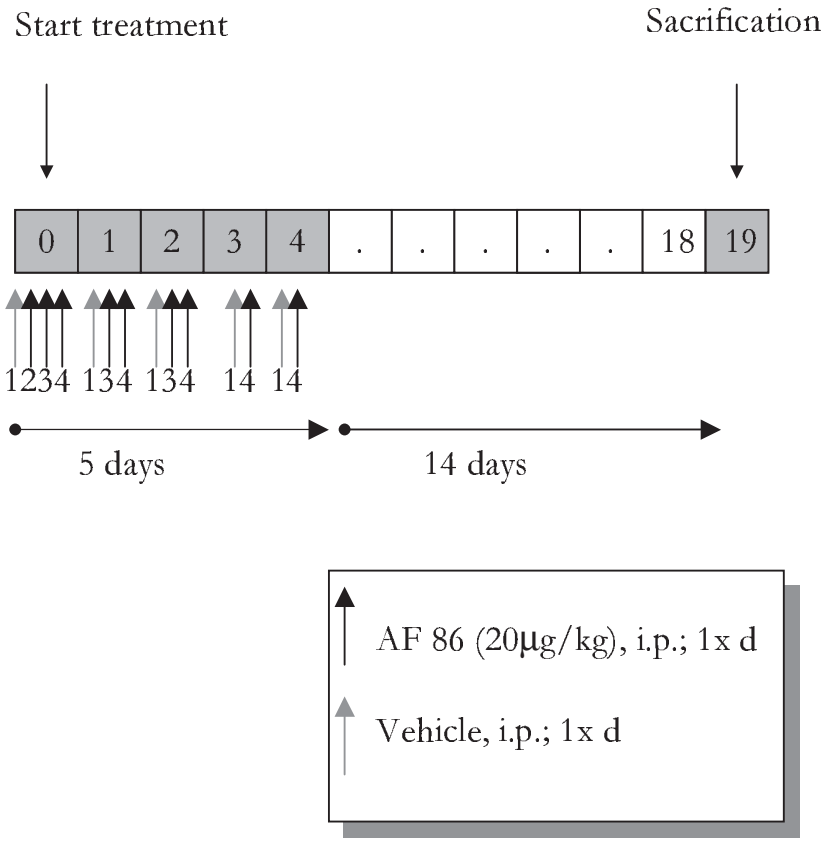

Figure 18: Experimental design for the analyses of acute toxicity of AF86.1 in SCID mice

Table 6:

Group	n	Vehicle	Dose [µg/kg]	Doses/ Day	Mode	Volume [ml/kg]	No. of Doses	Cumulative Dose [g/kg]
1	3	DMSO/0.9%saline solution (1:200)	-	x1	i.p.	5	5	-
2	3	DMSO/0.9%saline solution (1:200)	20	x1	i.p.	5	1	20
3	3	DMSO/0.9%saline solution (1:200)	20	x1	i.p.	5	3	60
4	3	DMSO/0.9%saline solution (1:200)	20	x1	i.p.	5	5	100
5	1	DMSO/0.9%saline solution (1:2)	2000	x1	i.p.	5	1	2000

3.3.2.1.2. Tolerance to AF86.1.

All animals tolerated the treatment well without any complications like body weight loss or apathetic behaviour. In all organs examined (e.g. lung, liver, spleen, kidneys) no macroscopical or microscopical changes could be detected by histological examination All hematological and clinical parameters were equal to the one obtained from control animals.

In summary AF86.1 shows no acute toxicity in SCID mice.

3.3.2.2. First investigations of AF86.1 for its potential use in antibody-directed enzyme prodrug therapy.

3.3.2.2.1. Experimental Design

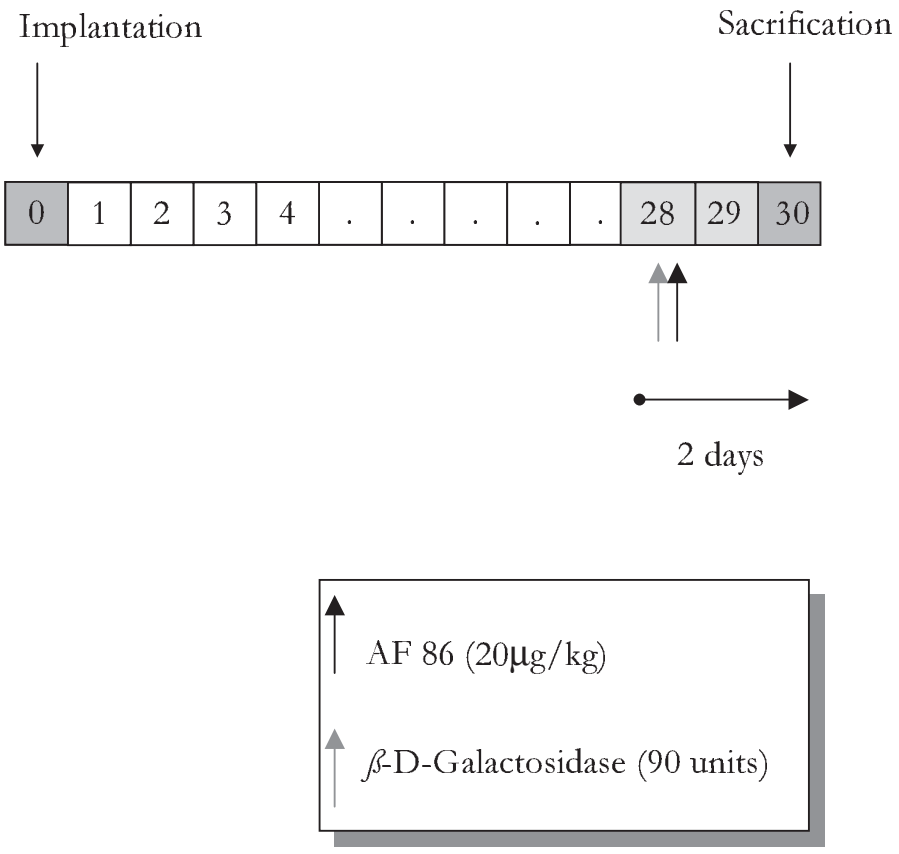

Figure 19: Experimental design for toxicity of AF86.1 after glycosidation by β-D-galactosidase *in vivo* in SCID-mice

Table 7

Group	n	Vehicle	Compound	Dose	Mode	Numbe rs of Doses	Cell line	Application volume [ml /kg]
1	3	DMSO/0.9% saline solution (1:200) 0.9%saline solution	AF86.1 Enzyme	25[µg/kg] 5 µl	i.p. intra-tumor al	1 1	A549 (s.c.)	5
2	1	DMSO/ 0.9% saline solution (1:200) 0.9%saline solution	- enzyme	25[µg/kg] 5 µl	i.p. intra-tumor al	1 1	A549 (s.c.)	5
3	2	DMSO/0.9% saline solution (1:200) 0.9%saline solution	AF86 enzyme	25[µg/kg] 5 µl	i.p. intra-tumor al	1 1	PancTU1 (s.c.)	5
4	2	DMSO/0.9% saline solution (1:200) 0.9%s aline solution	- enzyme	25[µg/kg] 5 µl	i.p. intra-tumor al	1 1	PancTU1 (s.c.)	5

The study was designed to evaluate the potency of AF86.1 to inhibit tumor growth of subcutaneous tumors (A549 and Panc Tu1) *in vivo* n All animals showed subcutaneous tumors with tumor volumes up to 0.75 cm^3 on day 28 after implantation. The pancreatic tumors showed only minor necrosis or tumor volume reduction compared to controls after treatment of AF86.1 and β-D-galactosidase (Figure 19, Table 7). In contrast the A549 lung tumors displayed marked necrosis in response to treatment (Figure 20) compared to control. KI67-staining demonstrated

that > 80 % of the tumor cells stopped to proliferate after one single dose of AF86.1and β-D-galactosidase.

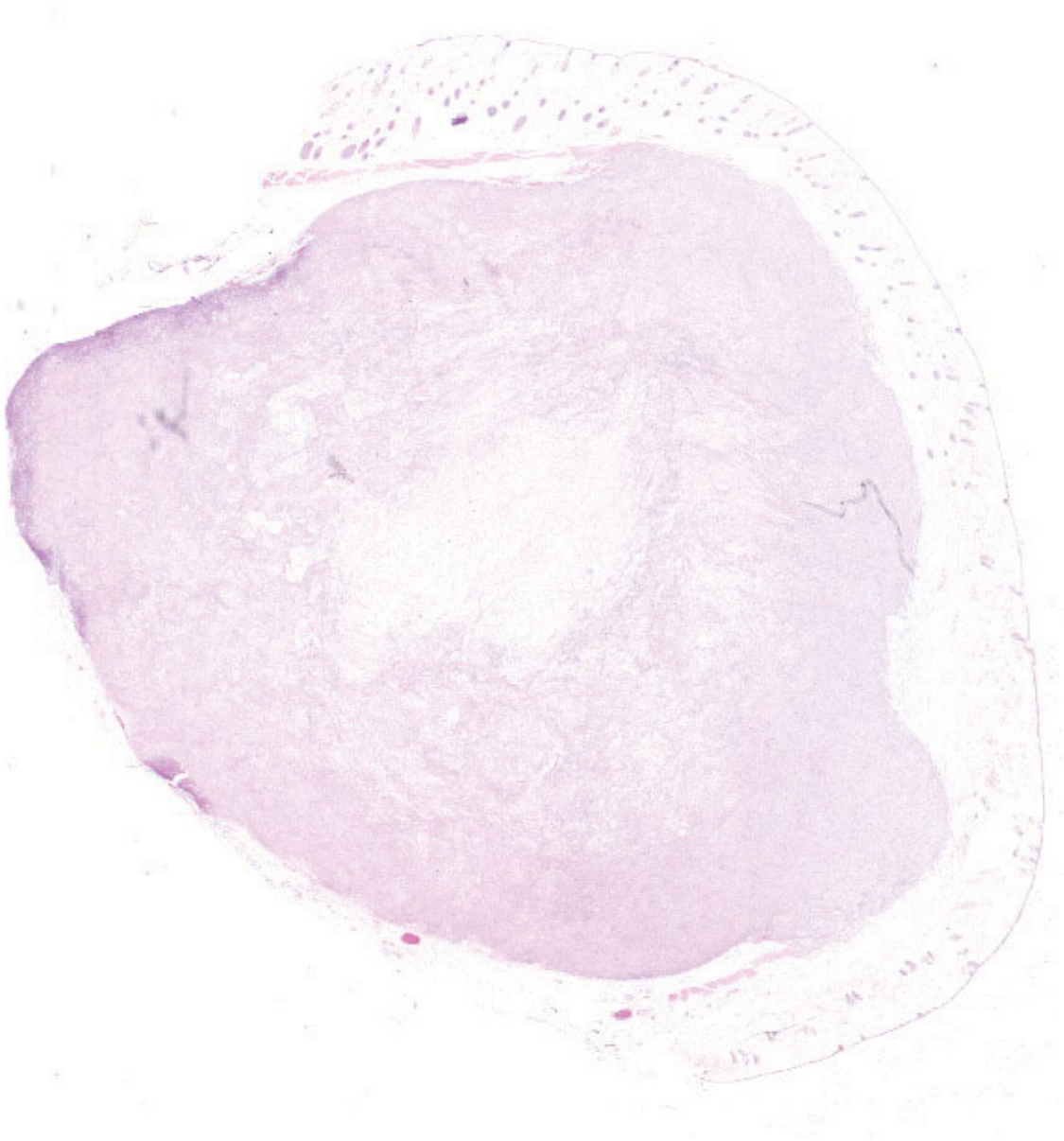

Figure 20 : H & E staining of a s.c. lung tumor (A549 cells) after treatment with AF86.1 and β-D-galactosidase

3.3.3. Evaluation of the ant-tumor and anti-metastatic effect of the MMP inhibitor AG3340 on human pancreatic adenocarcinoma in the orthotopic SCID-mouse model.

3.3.3.1 Study design.

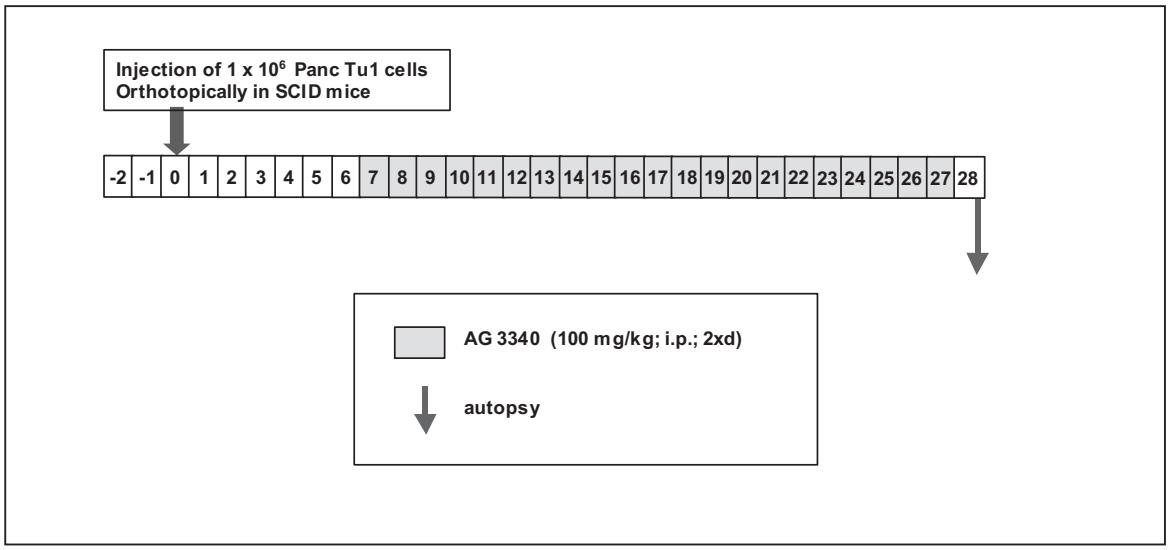

Figure 21: Schedule

Table 8

Group	Animals / group	Treatment	Dose [mg/kg]	Mode of application (applications per day)	Days/periods of treatment	Number of applications	Cumulative dose [mg]
1	8	Vehicle 0.5% MC	-	i.p. (2x)	d7-d27	42	-
2	8	AG 3340	100	i.p. (2x)	d7-d27	42	4200

3.3.3.2. Tolerance to AG3340.

Treatment with AG3340, intraperitoneally twice daily for 21 days was started one week after implantation of the PancTu 1 cells into the pancreatic head (Figure 21,

Table 8). AG3340 was well tolerated in all animals. The general condition of the animals recorded and scored at the day of sacrifice was similar in control mice

receiving only the vehicle. Control animals lost ΔW_m = -14 (± 12) % body weight, AG3340 treated mice ΔW_m = -7 (± 5) %. Tumor invasion caused complications such as weight loss, rough hair and apathetic behavior in the control animals. All AG3340 treated animals had a splenomegaly because of a granulomatous reaction consisting of aggregates of monocytic cells representing macrophages. Some of these cells formed giant cells.

3.3.3.3. Effects of AG3340 on tumor growth and morphological properties.

Primary tumor volumes in AG3340 treated mice were significantly decreased to 19.0 (± 7.7) % of control tumor volumes ($p < 0.01$) (Table 9, Figure 17D, Figure 22). To assess tumor cell proliferation Ki67 positive nuclei were counted in areas containing the highest density of mitotic figures (Figure 17K, 17L). The percentage of Ki67 positive nuclei was 70 (± 11) % in the AG3340 group versus 87 (± 5) % in the control group ($p < 0.1$).

The carcinomatous tissue in all AG3340-treated animals appeared to be better differentiated than that in controls, showing better developed glandular structures. In addition, all tumors of AG3340 treated animals displayed more stromal tissue and less normal pancreatic tissue than the tumors of controls (Figure 17H). Tumor cells were ocassionally observed in the lymphatic and blood vessels within the tumors. Larger tumor nodules displaying central necrosis were observed in 75 % of AG3340 treated mice (Figure 17L). No expression of the proliferation marker Ki67 was observed in tumor cells surrounding the necrotic areas and in regions with beginning

necrosis (Figure 17L). Necrosis amounted to 34 (± 6) % of the tumor area in histological sections. In controls only two tumors - although having significantly greater sizes – showed small areas of necrosis amounting to 6 (± 4) % of tumor tissue. The estimation of tumor volumes in the AG3340 treated mice by caliper measurement underestimated the actual percent inhibition of growth by AG3340 because both viable and necrotic tumor areas were included.

Table 9: Effects of AG3340 on tumor growth

		AG3340 n = 8	**Vehicle control n = 8**
Tumor take rate	Primary tumor	100 %	100 %
Volume	Primary tumor	V_m=59 (± 24) mm^3	V_m=311 (± 186) mm^3
Necrosis	Primary tumor	75 %	25 %
Body weight		W_m=93 (± 5)%	W_m=86 (± 12)%

V_m: Mean of primary tumor volumes and standard deviation

W_m: Mean of body weight and standard deviation in % of body weight at transplantation

3.3.3.4. Effects of AG3340 on tumor invasion, disseminated tumor growth and metastasis.

In control mice, the pancreatic tumors invaded into the stomach (Figure 17B, 17K), duodenum, liver, along the porta hepatis (Figure 17A, 17B, 17I) and ocassionally into the spleen. In three of these mice tumor invasion of the stomach resulted in stomach obstruction that led to rapid weight loss and malnutrition (Table 10). In 5/ 8 AG3340 treated mice, there was no tumor invasion into the neighbouring organs (Figure 17D,

17E). The other three showed only microscopic tumor invasion (Table 10). Also, the peritoneal tumors which developed at the site of surgical incision were much smaller in AG3340 treated animals than in controls (Table 11).

All control mice showed a similar spread and distribution of metastases (Table 11), mainly in the mesentery (Figure 17C), diaphragm and pelvis. The administration of AG3340 significantly reduced or even abolished these metastases especially in the mesentery (Figure 17F). In six control mice, 3 - 20 metastases (2 - 18 mm^3 in size) were found in the mesentery, whereas in four AG3340 treated mouse, only 1 – 2 metastases of smaller sizes were detected (< 2 mm^3, in two mice only by histological examination, Table 11). Microscopic metastases were detected in lung and mediastinum in five control mice (Figure 17J). In AG3340 treated animals only one micrometastasis was found in the lung of the same animal that also showed tumor invasion and had a peritoneal tumor at the site of surgical incision.

Table 10: Effects of AG3340 on tumor invasion

	AG3340 **n = 8**	**Vehicle control** **n = 8**
Invasion		
Duodenum	25 %	63 %
Stomach	38 %[1]	88 %
Liver	38 %[1]	88 %
Spleen	0 %	38 %
Not invasive	63 %	0 %
Complications		
Stomach obstruction	0 %	38 %

The percentages of animals showing invasive growth are listed

[1]Minor or microscopic invasion, verified by histological examination

Table 11: Effects of AG3340 on tumor spread

	AG3340	**Vehicle control**
	n = 8	**n = 8**
Metastases		
Lung/ Mediastinum	13 %[1]	63 %[1]
Kidneys/ Adrenal gland (capsule)	0 %	25 %
Spleen (serosa), gastrosplenic ligament	25 %	25 %
Mesentery < 3 metastases (< 2 mm^3)	50 %[2]	0 %
Mesentery 3 - 20 metastases (2-18 mm^3)	0 %	75 %
Ligament of the uterus/ testis (serosa), seminal vesicles	0 %	38 %
Diaphragm	0 %	63 %
Pelvis	0 %	63 %
Site of surgical incision		
Small > 1 mm^3	25 %	0 %
< 10 mm^3	50 %	0 %
Medium < 50 mm^3	25 %	38 %
Large 80 - 280 mm^3	0 %	63 %

The percentages of animals showing invasive growth are listed

[1]Only detected by histological examination
[2]In two mice micrometastases were only detected by histological examination

Figure 22: Primary tumor volumes of AG3340 treated group and controles

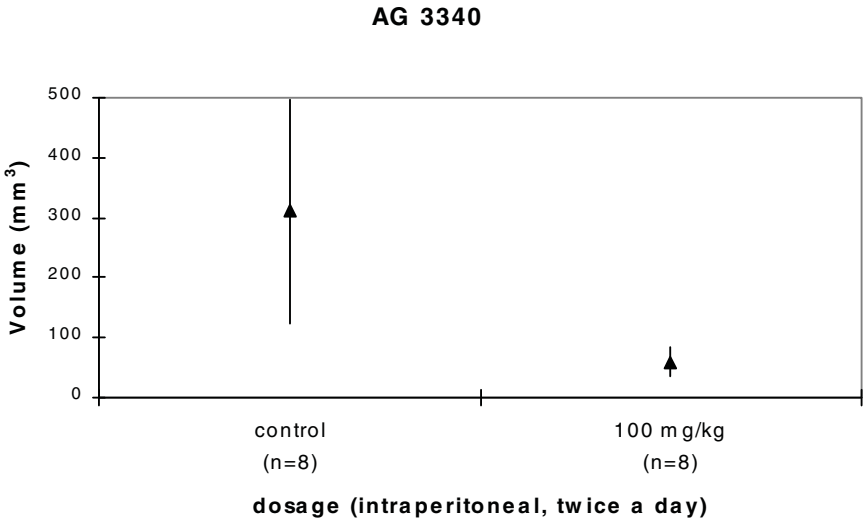

3.3.4. Evaluation of the antitumor and antimetastatic effect of the chemotherapeutic agent gemcitabine on human pancreatic adenocarcinoma in the orthotopic SCID-mouse model.

3.3.4.1. Study design.

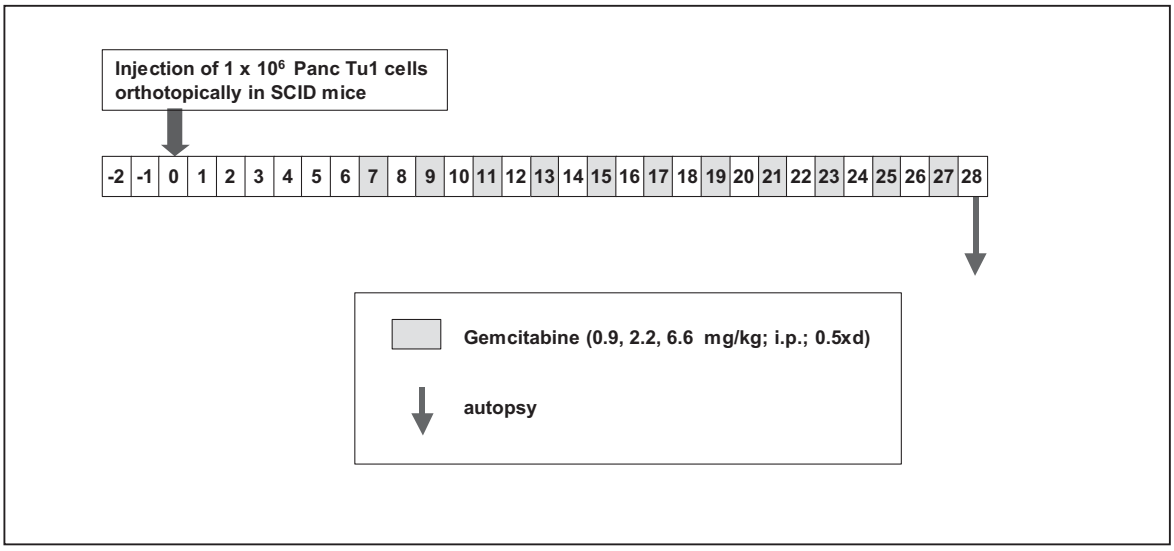

Figure 23: Schedule

Table 12

Group	Animals/ group	Treatment	Dose [mg/kg]	Mode of application (applications per day)	Days/periods of treatment	Number of applications	Cumulative dose [mg]
1	5	Vehicle 0.9% NaCl	-	i.p. (0.5x)	d7-d27	11	-
2	5	Gemcitabine	0.9	i.p. (0.5x)	d7-d27	11	10
3	6	Gemcitabine	2.2	i.p. (0.5x)	d7-d27	11	24
4	5	Gemcitabine	6.6	i.p. (0.5x)	d7-d27	11	73

3.3.4.2. Tolerance to gemcitabine.

Treatment with gemcitabine, intraperitoneally every second day for 21 days was started one week after implantation of the PancTu 1 cells into the pancreatic head (Figure 23, Table 12). Gemcitabine was well tolerated in most animals. 3/5 mice

treated with 6.6 mg/kg b.w. gemcitabine showed a splenomegalie. The general condition of the animals recorded and scored at the day of sacrifice was similar in control mice receiving only the vehicle. Only control animals lost ΔW_m = -2 (± 1) % body weight. Tumor invasion caused complications such as weight loss, rough hair and apathetic behavior in the control animals.

3.3.4.3. Effects of gemcitabine on tumor growth, invasion, disseminated tumor growth and metastasis.

Primary tumor volumes in gemcitabine treated mice were significantly decreased in a dose dependant manner up to 2.4 (± 0.8)% of control tumor volumes ($p < 0.01$) (Table 13, Figure 24). The estimation of tumor volumes in the gemcitabine treated mice by caliper measurement underestimated the actual percent inhibition of growth by gemcitabine because both viable and necrotic tumor areas were included. All primary tumors of gemcitabine treated mice were not invasive and showed essentially no metastasis and disseminated tumor growth. Only one mouse developed a liver metastasis on the serosa.

Table 13 : Effect of gemcitabine on tumor growth, invasion and tumor spread

		Vehicle	Gemcitabine 0.9 mg/kg bw	Gemcitabine 2.2 mg/kg bw	Gemcitabine 6.6 mg/kg bw
Tumor take rate	Primary tumor	5/5	5/5	6/6	5/5
	Volume	V_m=245 (± 56) mm^3	V_m=66 (± 27) mm^3	V_m=15 (± 7) mm^3	V_m=6 (± 2) mm^3
Body weight		Δm=-2 (± 1)%	Δm=-1(±2)%	Δm=1 (± 4) %	Δm=1 (± 3) %
Necrosis		1/5	3/5	4/6	3/5
Complications	Gall bladder obstruction	1/5	0/5	0/6	0/5
	Splenomegalie	0/5	0/5	0/6	3/5
Invasion	Duodenum	2/5	0/5	0/6	0/5
	Stomach	3/5	0/5	0/6	0/5
	Liver	1/5	0/5	0/6	0/5
	Spleen	0/5	0/5	0/6	0/5
	Not invasive	1/5	5/5	6/6	5/5
Metastases	Lung/ Mediastinum	2/5	0/5	0/6	0/5
	Liver on serosa	2/5	0/5	1/6	0/5
	Liver hilus	0/5	0/5	0/6	0/5
	Liver parenchym	0/5	0/5	0/6	0/5
	Kidneys/ Adrenal gland (capsule)	0/5	0/5	0/6	0/5
	Spleen (serosa), gastrosplenic ligament	0/5	0/5	0/6	0/5
	Mesentery < 3 metastases (< 2 mm^3)	4/5	0/5	0/6	0/5
	Mesentery 3 - 20 metastases (2-18 mm^3)	0/5	0/5	0/6	0/5
	Ligament of the uterus/ testis (serosa), seminal vesicles	0/5	0/5	0/6	0/5
	Diaphragm	0/5	0/5	0/6	0/5
	Pelvis	0/5	0/5	0/6	0/5
	Retroperitoneum	1/5	0/5	0/6	0/5
Site of surgical incision	Small >1mm^3 < 10 mm^3	2/5	1/5	0/6	0/5
	Medium < 50 mm^3	0/5	0/5	0/6	0/5
	Large 80 - 280 mm^3	1/5	0/5	0/6	0/5
	Disseminated growth	0/5	0/5	0/6	0/5

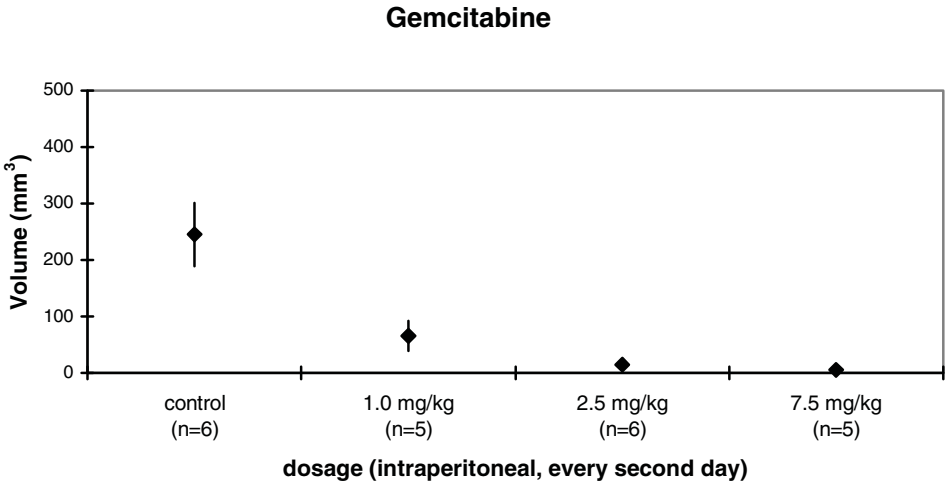

Figure 24: : Primary tumor volumes of gemcitabine groups and controles.

3.3.5. Evaluation of the antitumor and antimetastatic effect of the MMP inhibitor Ro 28-2653 on human pancreatic adenocarcinoma in the orthotopic SCID-mouse model.

3.3.5.1. Study design.

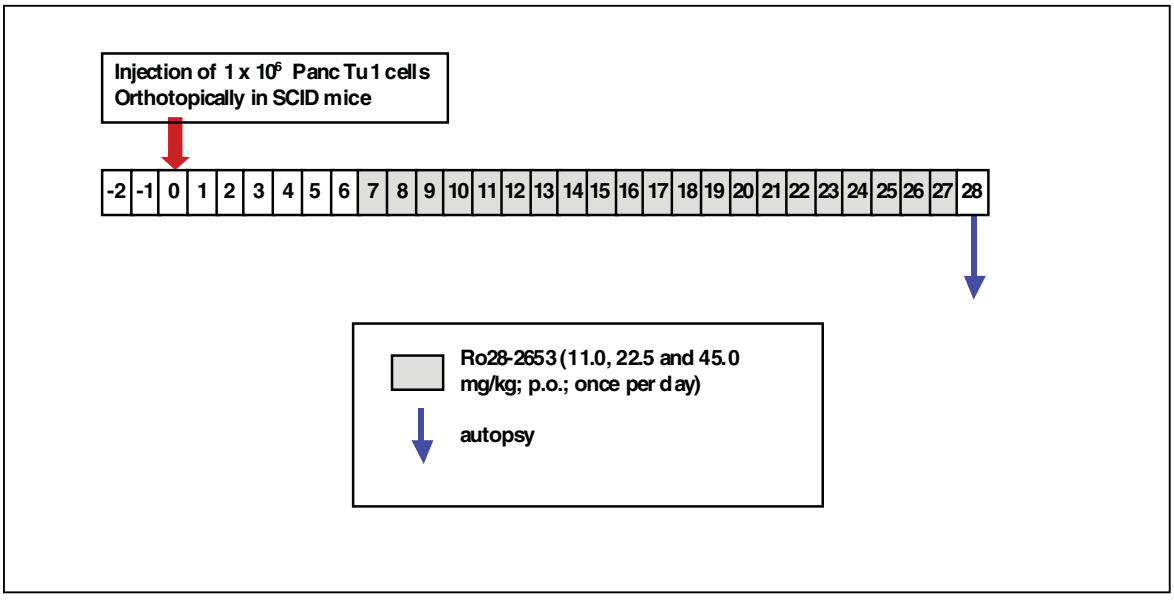

Figure 25 Schedule

Table 14

Group	Animals / group	Treatment	Dose [mg/kg]	Mode of application (applications per day)	Days/periods of treatment	Number of applications	Cumulative dose [mg]
1	9	Ro 28-2653 , DMA+PEG400	45.0	p.o. (1x)	d7-d27	21	945
2	4	Ro 28-2653 , DMA+PEG400	22.5	p.o. (1x)	d7-d27	21	473
3	4	Ro 28-2653 , DMA+PEG400	11.0	p.o. (1x)	d7-d27	21	231
4	9	DMA+PEG400	-	p.o. (1x)	d7-d27	21	-

3.3.5.2. Tolerance to Ro28-2653.

Treatment with Ro28-2653, p.o, once daily for 21 days was started one week after implantation of the PancTu 1 cells into the pancreatic head (Figure 25, Table 14). Ro28-2653 was well tolerated in all animals. The general condition of the animals recorded and scored at the day of sacrifice was similar in control mice receiving only the vehicle. Control animals lost ΔW_m = -8 (± 9) % body weight, Ro28-2653 treated mice lost dose dependant ΔW_m = -2 (± 7) % minimum (see Table 15). All animals tolerated the treatment well, as demonstrated by body weight, see table 15.

3.3.5.3. Effects of Ro28-2653 on tumor invasion, disseminated Tumor growth and metastasis.

Primary tumor volumes in Ro28-2653 treated mice were significantly decreased in a dose dependant manner up to 33 (± 11)% of control tumor volumes ($p < 0.01$) (Table 15, Figure 26). Necrosis was not found in all tumors. Tumor invasion into the neighbouring organs was observed in all groups in a dose dependant manner. In

group 1 (45 mg/ kg b.w. Ro28-2653) 6/9 primary tumors were free of invasion, in group 4 (controles) only 2/9.

The dose dependant effects of different concentrations of Ro28-2653 on disseminated tumor growth and metastasis were measured (see Table15). All control mice showed a similar spread and distribution of metastases, mainly in the mesentery, diaphragm and pelvis. The administration of different Ro28-2653 concentrations significantly reduced or even abolished these metastases especially in the mesentery. In seven control mice, 3 - 20 metastases (2 - 18 mm^3 in size) were found in the mesentery, whereas in two Ro28-2653 (45 mg(kg bw) treated mouse, only 1 – 2 metastases of smaller sizes were detected (< 2 mm^3). Microscopic metastases were detected in lung and mediastinum in four control mice. Only in Ro28-2653 (45 mg/kg bw) treated animals three micrometastasis were found in the lung of the same animals that also showed tumor invasion and had a peritoneal tumor at the site of surgical incision.

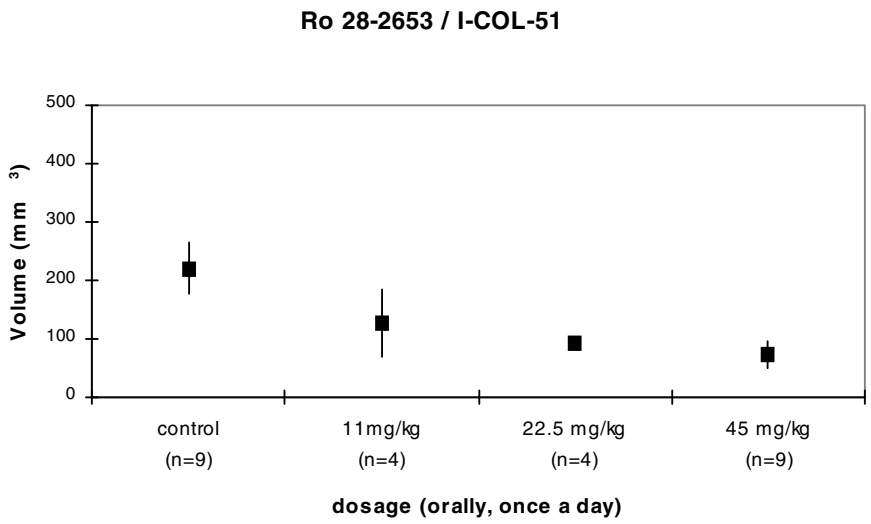

Figure 26: : Primary tumor volumes of Ro28-2653 treated animals and controles

Table 15 : Effects of Ro28-2653 on tumor growth, invasion and spread

		+ Ro28-2653 45 mg/kg bw	**+ Ro28-2653 22.5 mg/kg bw**	**+ Ro28-2653 11 mg/kg bw**	**Vehicle**
Tumor take rate	Primary tumor	9/9	4/4	4/4	9/9
	Volume	V_m=74 (± 24) mm^3	V_m=91 (± 9) mm^3	V_m=127 (± 56) mm^3	V_m=221 (± 45) mm^3
Body weight		Δm=-2 (± 7) %	Δm=-1 (± 5) %	Δm=-8 (± 11) %	Δm=-8 (± 9) %
Necrosis		0/9	0/4	0/4	0/9
Complications	Gall bladder obstruction	0/9	0/4	1/4	4/9
	Stomach obstruction	0/9	0/4	0/4	2/9
Invasion	Duodenum	3[1]/9	¼	2/4	6/9
	Stomach	1/9	¼	3/4	7/9
	Liver	2[2]/9	¼	2/4	6/9
	Spleen	0/9	0/4	1/4	0/9
	Not invasive	6/9	2/4	1/4	2/9
Metastases	Lung/ Mediastinum	3/9	0/4	0/4	4/9
	Liver on serosa	1/9	0/4	0/4	3/9
	Liver hilus	0/9	0/4	1/4	3/9
	Liver parenchym	0/9	¼	0/4	1/9
	Kidneys/ Adrenal gland (capsule)	0/9	0/4	0/4	1/9
	Spleen (serosa), gastrosplenic ligament	1/9	0/4	0/4	2/9
	Mesentery < 3 metastases (< 2 mm^3)	2/9	0/4	1/4	1/9
	Mesentery 3 - 20 metastases (2-18 mm^3)	0/9	¼	2/4	7/9
	Ligament of the uterus/ testis (serosa), seminal vesicles	1/9	0/4	1/4	0/9
	Diaphragm	2/9	2/4	0/4	5/9
	Pelvis	0/9	0/4	0/4	3/9
	Retroperitoneum	0/9	0/4	1/4	2/9
Site of surgical incision	Small > 1 mm^3 < 10 mm^3	2/9	¼	1/4	1/9
	Medium < 50 mm^3	4/9	¼	0/4	1/9
	Large 80 - 280 mm^3	2/9	2/4	3/4	7/9
	Disseminated growth	1/9	¼	1/4	4/9

[1] In 2/3 of animals only detected by histological examination.
[2] In 2/2 of animals only detected by histological examination.

3.3.6. Evaluation of the antitumor and antimetastatic effect of the combination therapy of the chemotherapeutic agent gemcitabine and the MMP inhibitor Ro 28-2653 on human pancreaticadenocarcinomas in the orthotopic SCID-mouse model.

3.3.6.1. Study design.

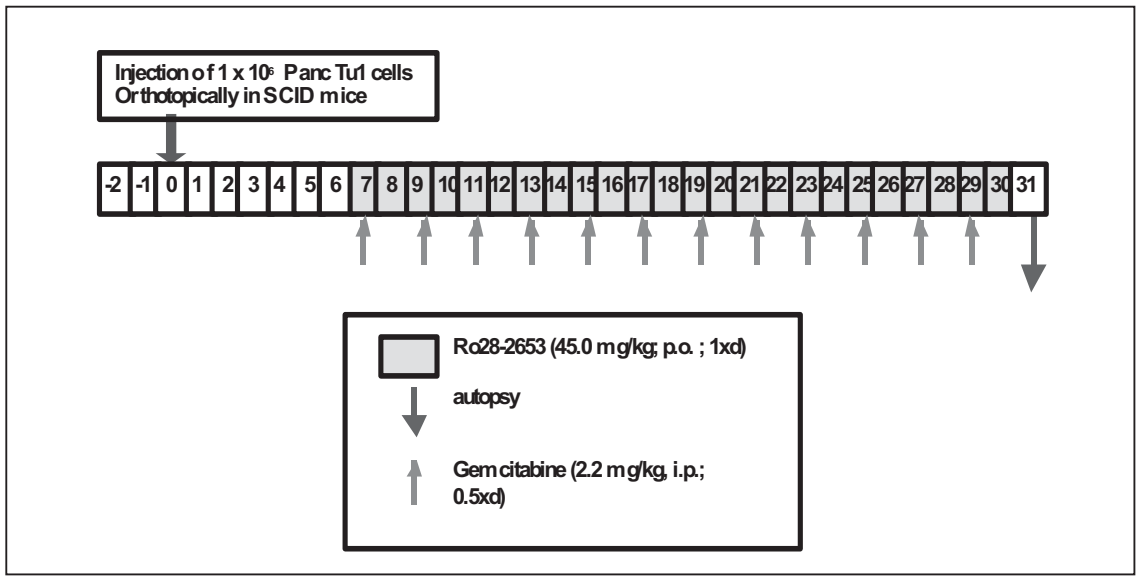

Figure 27

Table 16

Group	Animals/ group	Vehicle	Treatment	Dose [mg/kg]	Mode of application (applications per day)	Days/periods of treatment	Number of applications	Cumulative dose [mg/kg]
1	9	-	-	-	-	-	-	-
2	10	0.9 % NaCl CMC	- -	- -	i.p.(x 0.5) p.o. (x1)	d7-d30 d7-d30	12 24	- -
3	13	0.9 % NaCl CMC	Gemcitabine -	2.2 -	i.p.(x 0.5) p.o. (x1)	d7-d30 d7-d30	12 24	26.4 -
4	13	0.9 % NaCl CMC	- Ro 28-2653	- 45.0	i.p.(x 0.5) p.o. (x1)	d7-d30 d7-d30	12 24	- 1080
5	13	0.9 % NaCl CMC	Gemcitabine Ro 28-2653	2.2 45.0	i.p.(x 0.5) p.o. (x1)	d7-d30 d7-d30	12 24	26.4 1080

3.3.6.2. Tolerance to Ro28-2653 and gemcitabine.

Treatment with Ro28-2653, p.o. once daily for 24 days in combination with gemcitabine, intraperitoneally every second day for 24 days was started one week after implantation of the PancTu 1 cells into the pancreatic head (Figure 27, Table 16). Both, Ro28-2653 and gemcitabine alone and in combination were well tolerated in all animals. The general condition of the animals recorded and scored at the day of sacrifice was similar in control mice.

Control animals (no treatment) lost ΔW_m = -10 (± 5) % body weight and control animals (vehicle 1+2) ΔW_m = -11 (± 7) %, respectively. Whereas the treated animalss had only a weak body weight loss (see table 17). Tumor invasion caused complications such as weight loss, rough hair and apathetic behavior in both control groups.

3.3.6.3. Effects of Ro28-2653 and gemcitabine on tumor invasion, disseminated tumor growth and metastasis.

The effects of Ro28-2653 and gemcitabine on tumor invasion disseminated tumor growth and metastasis were added up in the combination group. Primary tumor volumes decreased in combination treatment

up to 6 (± 1)% compared to vehicle control tumor volumes ($p < 0.01$) (Table 17). Primary tumors showed necrosis in 7% of Ro28-2653-treated mice, in 31 % of gemcitabine treated mice and in 69 % of animals treated with Ro28-2653 and gemcitabine in combination.

The estimation of tumor volumes in the gemcitabine and gemcitabine/ Ro28-2653 treated mice by caliper measurement underestimated the actual percent inhibition of

growth by gemcitabine and combination because both viable and necrotic tumor areas were included. All primary tumors of gemcitabine and in combination treated mice were not invasive and showed only in site of surgical incision small metastasis (1/13, 2/13, respectively). In latter groups disseminated tumor growth was not found.

54 % of Ro28-2653 treated mice only were free of invasion and metastasis (Table 18,19).

Table 17: Effects of Ro28-2653 and gemcitabine on tumor growth

		No treatment n=9	**Vehicle 1 + 2** n=10	**Gemcitabine + Vehicle 2** n=13	**Ro28-2653 + Vehicle 1** n=13	**Gemcitabine + Ro28-2653** n=13
Tumor take rate	Primary tumor	9/9	10/10	13/13	13/13	13/13
Volume	Primary tumor	Vm=(293±79)mm3	Vm=(333±87)mm3	Vm=(51±14)mm3	Vm=(112±46)mm3	Vm=(20±4)mm3
Necrosis	Primary tumor	0/9	0/10	4/13	1/13	9/13
Body weight		m=(-10 ±5)%	m=(-11 ±7)%	m=(-2 ±5)%	m=(-5 ±4)%	m=(-1 ±4)%

V : Mean of primary tumor volumes and standard deviation
m: Mean of body weight and standard deviation in % of body weight at transplantation

Table 18 : Effects of Ro28-2653 and gemcitabine on tumor invasion

	No treatment n=9	**Vehicle 1 + 2** n=10	**Gemcitabine + Vehicle 2** n=13	**Ro28-2653 + Vehicle 1** n=13	**Gemcitabine + Ro28-2653** n=13
Invasion					
Duodenum	8/9	10/10	0/13	5/13	0/13
Stomach	7/9	10/10	0/13	4/13	0/13
Liver	6/9	6/10	0/13	1/13	0/13
Spleen	1/9	3/10	0/13	0/13	0/13
Not invasive	1/9	0/10	13/13	7/13	13/13
Complications					
Stomach obstruction	2/9	0/10	0/13	0/13	0/13

Table 19 : Effects of Ro28-2653 and gemcitabine on tumor spread

	No treatment n=9	**Vehicle 1 + 2** n=10	**Gemcitabine + Vehicle 2** n=13	**Ro28-2653 + Vehicle 1** n=13	**Gemcitabine + Ro28-2653** n=13
Metastasis					
Lung/ Mediastinum	7/9	4/10	0/13	2/13	0/13
Liver	2/9	2/10	1/13	1/13	0/13
Liver in parenchyme	3/9	3/10	1/13	3/13	0/13
Liver on serosa	1/9	1/10	1/13	2/13	0/13
Liverpforte	1/9	2/13	0/13	4/13	0/13
Kidneys/Adrenal gland (capsule)	4/9	3/10	0/13	1/13	0/13
Spleen (serosa), gastrosplenic ligament	3/9	3/10	0/13	0/13	0/13
Lymphknoten in Mesentery	2/9	2/10	0/13	2/13	0/13
Mesentery < 3 metastasis(2 mm3)	1/9	0/10	0/13	0/13	0/13
Mesentery 3-20 metastasis(1-18 mm3)	7/9	7/10	0/13	5/13	0/13
Ligament of the uterus / testis (serosa), seminal vesicles	5/9	3/10	0/13	0/13	0/13
Diaphragm	3/9	5/10	0/13	3/13	0/13
Pelvis	1/9	3/10	0/13	0/13	0/13
Site of surgical incision					
Small < 10 mm3	0/9	1/10	2/13	2/13	1/13
Medium < 50 mm3	0/9	1/10	1/13	3/13	0/13
Large 80-280 mm3	8/9	8/10	0/13	6/13	0/13

3.3.7. Evaluation of the effect of the combination therapy of the chemotherapeutic agent gemcitabine and the MMP inhibitor Ro 28-2653 on survival time of SCID mice with pancreatic tumors.

3.3.7.1. Study design

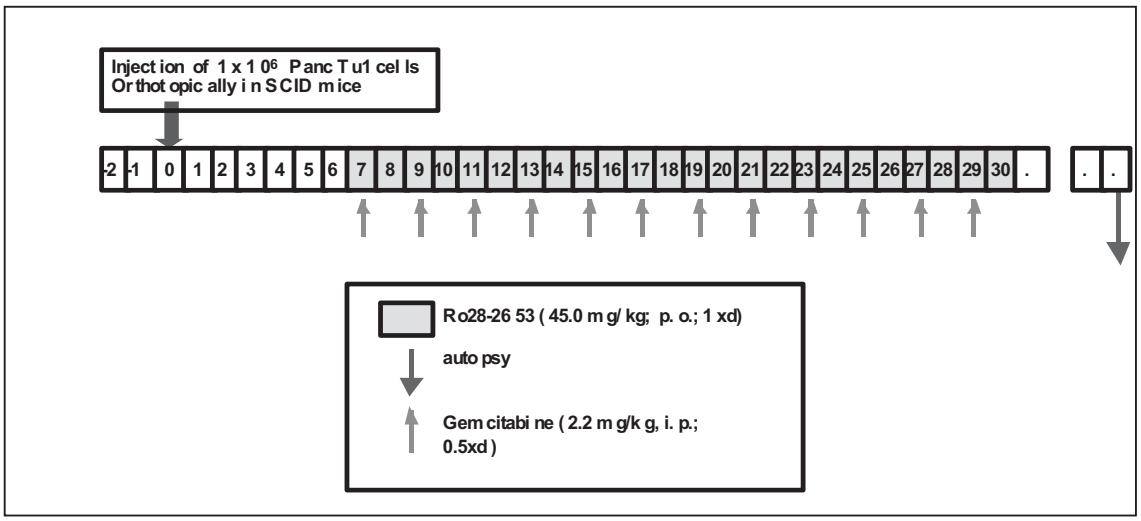

Figure 28 *: Schedule for groups 1-4, early begin of therapy.*

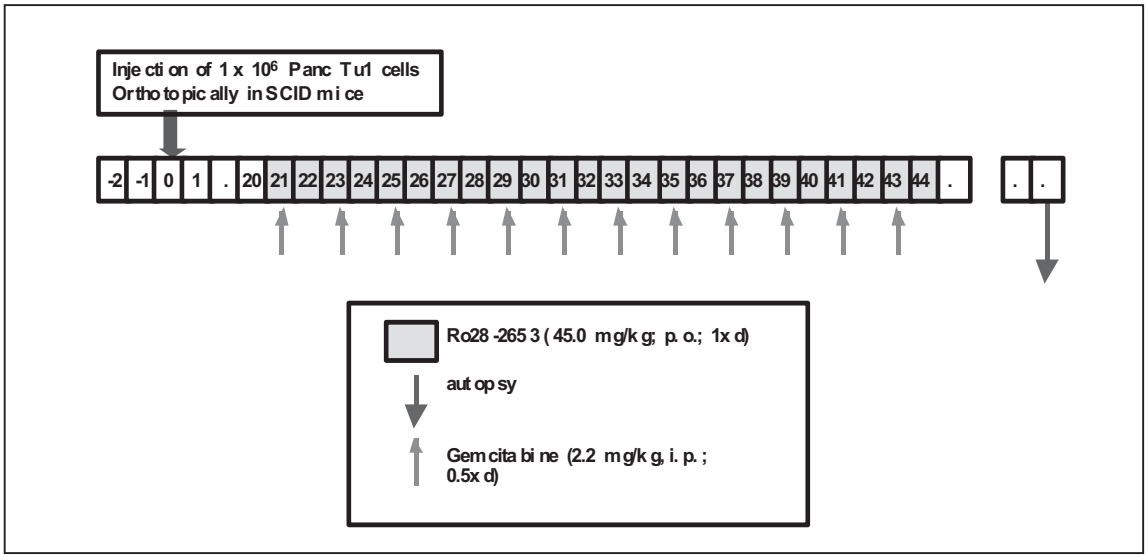

Figure 29 *: Schedule for group 5, late begin of therapy.*

Table 20

Group	Animals/ group	Vehicle	Treatment	Dose [mg/kg]	Mode of application (applications per day)	Days/periods of treatment	Number of applications	Cumulatie dose [mg/kg]
1(A)	10	0.9 % NaCl CMC	- -	- -	i.p.(x 0.5) p.o. (x1)	d7-d29 d7-d30	12 24	- -
2(B)	10	0.9 % NaCl CMC	Gemcitabine -	2.2 -	i.p.(x 0.5) p.o. (x1)	d7-d29 d7-d30	12 24	26.4 -
3©	10	0.9 % NaCl CMC	- Ro 28-2653	- 45.0	i.p.(x 0.5) p.o. (x1)	d7-d29 d7-d30	12 24	- 1080
4(D)	10	0.9 % NaCl CMC	Gemcitabine Ro 28-2653	2.2 45.0	i.p.(x 0.5) p.o. (x1)	d7-d29 d7-d30	12 24	26.4 1080
5(E)	11	0.9 % NaCl CMC	Gemcitabine Ro 28-2653	2.2 45.0	i.p.(x 0.5) p.o. (x1)	d21-d43 d21-d44	12 24	26.4 1080

3.3.7.2. Tolerability

Treatment with Ro28-2653, p.o. once daily for 24 days in combination with gemcitabine, intraperitoneally every second day for 24 days was started one week (groups 1-4) or three weeks (group 5) after implantation of the PancTu 1 cells into the pancreatic head (see Figure 28, 29, Table 20). Both, Ro28-2653 and gemcitabine alone and in combination were well tolerated in all animals, consistent with the data of the previous study (see chapter 3.3.6.2.) Sacrification was performed when the animals‘ general condition decreased (defined in terms of the condition of the coat and nutrition, and behaviour. Complications like stomach obstruction were observed in 69 % of all animals (Table 22). Lost of body weight was recorded in the range of –13 and –17 % (Table 21).

3.3.7.4. Effects of Ro28-2653 and gemcitabine on tumor invasion, disseminated tumor growth and metastasis.

The effects of different Ro28-2653 and gemcitabine alone and the combination of Ro28-2653 and gemcitabine on tumor growth, invasion, disseminated tumor growth and metastasis were analyzed (see Table 21-23). Furthermore, the days of survival after tumor implantation were determined (Table 24, Figure30). All animals showed

invasion, disseminated tumor growth with lung metastases, invasion (Table 24). This demonstarated that the primary tumors in the pancreas and metastases started or continued to grow after therapy was stopped: Animals treated with gemcitabine and Ro28-2653 (group 4) survived 84 ± 6 days. That means 53 days after end of therapy. Vehicle controles survived 51 ± 8 days after tumor implantation. Gemcitabine alone (group 2) was more effective (77±10 days) than Ro28-2653 alone (64±12 days Late begin of therapy represents the clinical situationmore closely. Three weeks after implantation the pancreatic tumors showed already signs of tumor. Treated mice with combination (group 5) survived 69 ± 4 days after tumor implantation.

Table 21: Effects of Ro28-2653 and Gemcitabine on tumor growth

		Vehicle 1 + 2 n=10	**Gemcitabine + Vehicle 2** n=10	**Ro28-2653 + Vehicle 1** n=10	**Ro28-2653 + Gemcitabine** *(1)* n=10	**Ro28-2653 + Gemcitabine** *(2)* n=11
Tumor take rate	Primary tumor	10/10	10/10	10/10	10/10	11/11
Volume	Primary tumor	Vm=668 (± 170)mm^3	Vm=718 (±204)mm^3	Vm=783 (± 462)mm^3	Vm=847 (± 258)mm^3	Vm=560 (± 360)mm^3
Body weight		m=-17 (± 6)%	m=-17 (± 3)%	m=-20 (± 5)%	m=-13 (± 4)%	m=-16 (± 6)%

V : Mean of primary tumor volumes and standard deviation
m: Mean of body weight and standard deviation in % of body weight at transplantation
(2): Late begin of therapy

Table 22: Effects of Ro28-2653 and Gemcitabine on tumor invasion

	Vehicle 1 + 2 n=10	**Gemcitabine + Vehicle 2** n=10	**Ro28-2653 + Vehicle 1** n=10	**Ro28-2653 + Gemcitabine** *(1)* n=10	**Ro28-2653 + Gemcitabine** *(2)* n=11
Invasion					
Duodenum	9/10	10/10	9/10	9/10	11/11
Stomach	10/10	10/10	9/10	10/10	10/11
Liver	7/10	8/10	3/10	3/10	5/11
Spleen	3/10	1/10	1/10	1/10	1/11
Not invasive	0/10	0/10	0/10	0/10	0/11
Complications					
Stomach obstruction	6/10	9/10	6/10	6/10	8/11

Table 23: Effects of Ro28-2653 and Gemcitabine on tumor spread

	Vehicle 1 + 2 n=10	**Gemcitabine + Vehicle 2** n=10	**Ro28-2653 + Vehicle 1** n=10	**Ro28-2653 + Gemcitabine** *(1)* n=10	**Ro28-2653 + Gemcitabine** *(2)* n=11
Metastasis					
Kidneys/Adrenal gland (capsule)	4/10	0/10	3/10	1/10	4/11
Spleen (serosa), gastrosplenic ligament	8/10	5/10	5/10	2/10	5/11
Mesentery ≤ 3 metastasis(2 mm^3)	1/10	5/10	0/10	6/10	3/11
Mesentery 4-20 metastasis(1-18 mm^3)	8/10	2/10	8/10	1/10	3/11
Ligament of the uterus / testis (serosa), seminal vesicles	4/10	0/10	2/10	1/10	3/11
Diaphragm	9/10	7/10	4/10	6/10	6/11
Pelvis	6/10	3/10	4/10	3/10	5/11
Site of surgical incision					
Small < 10 mm^3	0/10	0/10	0/10	0/10	0/11
Medium < 50 mm^3	0/10	1/10	1/10	1/10	1/11
Large 80-280 mm^3	9/10	6/10	7/10	4/10	10/11

Table 24: Days of survival after tumor implantation

	Vehicle 1 + 2 n=10	**Gemcitabine + Vehicle 2** n=10	**Ro28-2653 + Vehicle 1** n=10	**Ro28-2653 + Gemcitabine** *(1)* n=10	**Ro28-2653 + Gemcitabine** *(2)* n=11
MEAN OF DAYS	51± 8	77± 10	64± 12	84± 6	69± 4

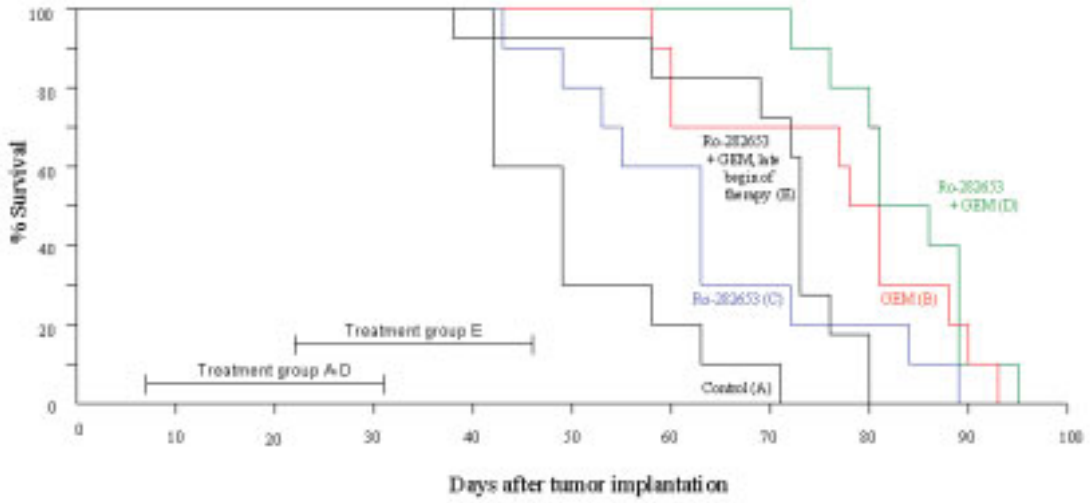

Figure 30: Survival curves of all groups beginning at day 0 of tumor implantation and continuing up to 95 days until all mice were dead or sacrified. Treatment mice with combination therapy survived longer than mice receiving other therapies or control vehicle.

4. Discussion

4.1. Regulation of EGF receptor activity by HK1-ceramide, a stable synthesized analogue of the ganglioside GM3-lactone.

Gangliosides have been described as modulators of cell growth. One of them, GM3 has been found to affect cell growth presumably by inhibiting EGF receptor phosphorylation. Changes in the structure, synthesis and cell surface exposure of gangliosides have been described to be associated with tumor progression. For example, the lactone form of ganglioside GM3 are thought to be formed to a higher extent on malignant cells probably due to a lower pH on these cells. There is some evidences that lactones of gangliosides may even play an important role as tumor associated antigens.[6] The murine monoclonal antibody M2590 was found to have much higher affinity with GM3 lactone than with GM3. It was suggested, therefore, that the real melanoma associated immunogen is GM3 lactone, or a derivative having a tertiary structure similar to that of GM3 lactone. However, the detailed mechanism of how the GM3-lactone or its lactone-like conformation is generated by the high density of GM3 is not known[88]. Extensive immunization with GM3 lactone in C57/BL6 mice resulted in greatly enhanced tumor-promoting effect; in contrast, weak immunization with GM3 lactone resulted in clear reduction of melanoma deposits in lung[89]

The aim of this study was to determine whether GM3 lactone has, in similarity to GM3, an inhibitory effect on EGF dependent tyrosine phosphorylation and therefore on modulation of cell growth. Since the GM3-lactone is not stable in aqueous solution we use an ether analogon **2**(figure 31)[11] which is stable and should have a similar conformation as the lactone.

Figure 31

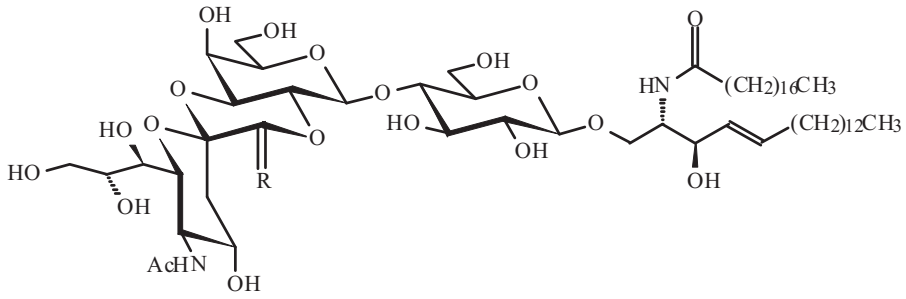

Structure of GM3-lactone and HK1-ceramide. GM3-lactone **1**: R = O. HK1-ceramid **2**: R = H_2

Therefore the cyclic ether as a substitute for the lactone form of GM3 **1** was examined on EGF receptor signaling and mitogenesis in the human ovarial epidermoid carcinoma A431 cell line and human oral epidermoid carcinoma KB cell line. Here, it could be demonstrated that the GM3 lactone analogue HK1-ceramide, in a concentration of 25 μM inhibited ligand dependent activation of EGF receptor in A431 cells compared to control cells without affecting EGF receptor content in the cells. In addition, the tyrosine phosphorylation of EGF receptor substrates was reduced, particularly of proteins with an apparent molecular weight of 116 kD. The inhibitory effect of HK1-ceramide on EGF receptor activation is only observed in a small range of concentration. In contrast to HK1-ceramide, GM3 showed an inhibitory effect on EGF-receptor phosphorylation at much higher concentrations in the range of 100 μM to 500 μM, in a dose-dependent manner. The concentrations of GM3 used in this study are consistent with the concentrations previously reported to inhibit EGF-receptor phosphorylation[10,12,90] In A431 cells, tyrosine phosphorylation of the EGF receptor was found to be specifically inhibited by exogenous addition of GM3 but not by other gangliosides or neutral glycolipids.[12] These results indicate that an inhibition of the EGF-dependent tyrosine phosphorylation of the EGF-receptor by HK1-

ceramide is achieved at low concentration of 25 μM, whereas GM3 showed a similar effect at a much higher concentration of 500 μM [10] (20 fold). The underlying mechanisms why HK1-ceramide is only effective in a small range of concentration are not understood. Hence, to analyze whether the inhibitory effect of EGF receptor phosphorylation in response to high concentration of GM3 might be due to in part lactonization of GM3, high concentrations of GM3 were incubated at pH values < 7, since lactonisation should be catalysed in an acider medium. Lower pH values (pH 7.0-5.8), GM3 had no variable inhibitory effect on EGF dependent receptor phosphorylation and one might speculate that a lactonization of GM3 is not responsible for the inhibitory effect of GM3 on receptor activation observed in A431 cells. Consistently, HK1-ceramide at a concentration of 25 μM is able to inhibit EGF dependent activity of the MAP kinase erk1 almost completly. Autophosphorylated tyrosine residues on the EGF receptor bind to SH2 domains containing specific molecules and are often themselves phosphorylated by the receptor, thus initiating the signaling cascade. The inhibition of MAP kinase activation by GM3 has been shown to be not complete.[15] In similarity to GM3, HK1-ceramide seems to have no influence to the binding of EGF to the cell surface receptor.[12] This result support the hypothesis that HK1-ceramide acts by the same mechanism as GM3. Growth of KB cells was clearly inhibited by HK1-ceramide in a dose dependent manner. It was previously reported that GM3 inhibits EGF stimulated cell growth in KB cells. Cells in the presence of 50 nmol/ ml GM3 (1ng/ ml EGF) showed a 65 % inhibition of mitogenesis[12] Whereas HK1-ceramide showed a comparable effect at an approximatly 8 fold lower concentration. In conclusion, HK1 ceramide has a similar inhibiting effect on EGF mediated tyrosine phosphorylation and EGF dependent mitogenesis as GM3 however, at lower concentration.

4.2 A novel polyclonal antibody directed against the lactone form of ganglioside GM3: Analyses of its potential as tumor marker for melanomas.

Cutaneous melanoma accounts for about 1 % of malignant tumors. Although melanoma only represents 3 % of malignant skin tumors, it is responsible of 65 % of skin cancer deaths. Its incidence is rapidly rising[91] The depth of invasion is the main prognostic factor of cutaneous melanoma. It is quantified according to methods by Clark or by Breslow.[92] Breslow measures the tumor‘s thickness in millimeters; different tumor thickness categories can be defined and an inverse correlation between thickness and survival was established. Level of invasion I is characterized by the localization of the tumor in the epidermis. In further stages of invasion (II - V), the tumor cells invade in papillary dermis, reticular dermis and subcutis[91] The goal of this study was to investigate the expression pattern of gangliosides on melanoma cells with the new polyclonal HK1-antibody. The HK1-antibody was raised against HK1-ceramide and shows immunoreactivity against GM3-lactone and GM3. To this point, an antibody selectivity for GM3-lactone/ GM3 is unknown. Here it could be shown by using the polyclonal HK1-antibody that the expression pattern of GM3-lactone and GM3 are very similar in different types of malignant melanoma (SSM, LMM, ALM) with only slight degree of variation. Melanoma cells within these lesions express GM3-lactone or GM3 at the dermal-epidermal junction as well as within atypical nests of the upper dermis. Lower dermal parts of the tumor show either a very weak staining or a complete loss of expression. These results clearly indicate a correlation with the ganglioside expression of neoplastically transformed melanocytes where a positive HK1-antibody staining was found (level of invasion I)

and negative stainings with lower dermal parts (level of invasion II-V). Further results support this hypothesis. The melanophages were found as packed cells with strong staining granules. This leads to the suggestion that gangliosides are shedded, a mechanism that was already observed by others. High amounts of GD3 in melanoma ascites fluid support this hypthesis, that GM3 and GD3 were shedded from proliferating melanoma cells.[93] Gangliosides, especially GM3 and most likely GM3-lactone have an inhibitory effect on EGF dependent tyrosine phosphorylation and therefore on modulation of cell growth and an immunomodulatory influence.[93] In dysplastic melanocytic nevi only melanocytes aggregated in the epidermal compartment showed a positive staining of HK1-antibody. The intradermal lying nests of melanocytes were negative and atypical nests of malignant melanoma within a congenital melanocytic nevus proved a strong immunoreactivity for HK1-antibody, whereas the surrounding melanocytic cells were negative. The melanocytes in the basal layer of normal skin displayed no expression of gangliosides. The study shows that staining with HK1-antibody allows to differentiate between normal skin, transformed melanocytes in level of invasion I and higher levels of invasion.

In summary, GM3 and GM3-lactone might be of crucial importance to tumor progression of malignant melanomas and dysplastic melanocatic nevi. Further investigations will be helpful in clearing up the detailed mechanism. The novel HK1-antibody might be used as an indicator for a tumor marker for malignant melanomas and dysplastic melanocytic nevi in early stages.

4.3. Evaluation of the *seco*-CBI-derivative AF86.1 for its potential use in antibody directed enzyme prodrug therapy

Preliminary clinical trials of ADEPT have been very encouraging, but they have also illustrated the problems of its clinical application, where the research should focus on over the next years.[22] One major problem is a low ratio between the activity of precurser and activated drug: Most known ADEPT-systems have only a ratio of 20 – 200, whereas this AF86.1 ADEPT-system shows an ΔSD_{50} of 1600. Penicillin-G Amidase, an E. coli enzyme has been shown to activate the phenylacetamido derivatives of doxirubicin and melphalan.[94,95] For the melphalan compound a 20-fold difference in SD_{50} value was demonstrated between drug and prodrug *in vitro*.[94] Other enzymes used are Carbopeptidase A and B. Bovine pancreatic carboxypeptidase A and porcine pancreatic carboxypeptidase B can remove alanine residues from a-peptidyl methotrexate derivatives [97] , producing the active methotrexate molecule. This molecule, which is 200-fold more active than its precurser, is an anticancer drug with a broad spectrum of activity. Conjugates of these enzymes with mABs (monoclonal antibodies) have shown some cytotoxicity in an ADEPT system, in the L1210 leukemia cells and the UCLA-P3 lung adenocarcinoma cell line.[33] In this study it has been shown that AF86.1 was non-toxic to normal organs and blood parameters of SCID mice. This indicates that the prodrug is not converted by enzymes expressed by the SCID-mice. These results are necessarily prerequisites for an effective ADEPT system. To evaluate the potency of AF86.1 treatment *in vivo*, subcutaneous tumors of the human lung tumor cell line A549 and the pancreatic ductal adenocarcinoma cell line PancTu1 in SCID-mice were generated. This subcutaneous tumor model had two advantages: 1) To this point the antibody-enzyme-conjugate (AEC) production was not finished and both, antibody and enzyme could have been injected separately into the exposed tumors

without surgical operation. 2) The mode of prodrug application and prodrug concentration could have been assessed without further parameters like unsuitable AEC concentrations. The results are very striking. AF86.1 treated A549 tumors showed marked necrosis and more than 80 % of tumor cells stopped to proliferate after only one cycle of treatment. The main problem of ADEPT is the immunogenicity of the AEC, that limits the application of ADEPT to a few chemotherapy cycles only.[22] In this study it could be shown that the ratio between activity of precurser and activated drug is extremely high *in vivo*. The next steps will be the preparation of an active AEC and proof of principle of this ADEPT system in the orthotopic SCID-mouse model. This ADEPT system holds the potential of an effective, non-toxic treatment of cancer *in vitro* and *in vivo*.

4.4. Evaluation of the antitumor and antimetastatic effect of different MMP inhibitors on human pancreatic adenocarcinomas in the orthotopic SCID-mouse model.

To test antioncogenic agents for the treatment of human malignancies, *in vivo* models have been developed in immunocompromised animals.[69-77] For the evaluation of different MMP inhibitors an orthotopic model for human ductal adenocarcinoma of the pancreas in SCID mice was established which resemble the human counterpart. Using the human ductal adenocarcinoma cell line PancTu 1, tumor cells were implanted in the SCID mouse pancreas, which produced a poorly differentiated adenocarcinoma that invaded the surrounding organs and metastasized to other sites in the abdomen and to the lung. Since inhibition of MMPs, presumably the key enzymes in the metastatic process could play a crucial role in an antimetastatic therapy, this orthotopic cancer model was used to test the efficacy of

different MMP inhibitors to reduce tumor growth and progression in human pancreatic ductal adenocarcinoma. The results of the studies showed that AG3340 and the novel MMP inhibitor Ro28-2653 markedly inhibited tumor growth and dissemination and induced necrosis, fibrotic tissue and differentiation of a poorly differentiated ductal adenocarcinoma of the pancreas. AG3340 resulted in an inhibition of 81 % and Ro28-2653 (45 mg/kg bw) in an inhibition of 67 % in local tumor growth when compared to controls. Therefore, it cannot be ruled out that the inhibitory effect on tumor progression is in part a reflection of the striking inhibitory effect of AG3340 and Ro28-2653 on tumor growth. The degree of growth inhibition is comparable with results from studies in subcutaneously implanted malignant glioma tumor model U87, in which AG3340 led to a decrease in tumor size by 78 % compared to controls.[66] Orally given AG3340 at a concentration of 200 mg/ kg and 50 mg/ kg twice a day resulted in an inhibition of tumor growth of 60.3 % and 39.4 %, respectively, and in an induction of tumor necrosis in a chemoresistant human non-small cell lung cancer tumor.[67]

The novel MMP inhibitor Ro28-2653 was investigated in the pancreatic carcinoma model in SCID mice and compared to the effect of AG3340 on tumor progression. In order to to evaluate the optimal concentration, the effect of different concentrations of Ro28-2653 on tumor progression was analyzed. Treatment, orally once a day for 21 days, was started one week after orthotopic implantation of the human pancreatic ductal carcinoma cell line PancTu 1. Controls, receiving vehicle only, showed similar results as the controls of the AG3340 study. Treatment with Ro28-2653 was well tolerated and reduced the primary tumor volume significantly in a dose dependent manner to 33 % of control (45 mg/ kg bw), 41 % of control (22.5 mg/ kg bw) and 57 % of control (11 mg/ kg bw). Invasion was not observed in 67 % of Ro28-2653 treated

mice and metastases were reduced markedly. No additional micrometastases were observed in lung and liver in the Ro28-2653 treated groups when compared to control animals. The conclusion is that Ro28-2653 is highly effective in inhibiting pancreatic carcinoma growth and progression in an orthotopic cancer model. The efficacy of AG3340 and Ro28-2653 to inhibit tumor growth were comparable. AG3340 showed a slight better inhibitiory effect on local tumor growth (81% vs. 67%), however Ro28-2653 was used for further investigations cause of the splenomegalie side effect in AG3340 treated mice. MMP inhibitors have classically been thought to show antitumor effect only by blocking tumor invasion and metastasis by merely degrading extracellular structural compartments. The mechanism of AG3340 and Ro28-2653 as primarily noncytotoxic MMP inhibitors on the marked inhibition on tumor growth *in vivo* is not well understood, in fact a direct antiproliferative effect of AG3340 and other MMP inhibitors *in vitro*, in cell culture experiments, could not be demonstrated.[67] It is discussed, that the inhibitor may have an indirect effect on tumor growth by disrupting signaling and attachment functions of the cellular matrix, on which host and carcinoma cells depend for survival, e. g. by inhibiting liberation of bioactive fragments of extracellular matrix, release of sequestered growth factors and of angiogenesis mediators and shedding of cell surface receptors and ligands.[1,66,98]Therefore, the marked growth inhibitory effect of AG3340 and Ro28-2653 is only observed *in vivo*. One might also speculate that the formation of central necrosis and fibrotic tissue in the AG 3340 MMP inhibitor treated tumors in this study could partly be the result of an effect of MMP inhibitors on angiogenesis. Since MMPs appear to be involved in the formation of new vessels in tumors by mediating remodelling of the extracellular matrix that must accompany new capillary formation [53], inhibition of this process could also contribute to the prominent growth inhibitory

effect of this drug. The mechanisms that let to an improved differentiation of the tumor tissue by AG3340 are currently not understood. These findings point to the expanding appreciation for the multifunctional and complex roles of MMPs and their inhibitors in tumor progression.

Therapy was started in this cancer model during early neoplastic progression, seven days after transplantation. In a previous study, autopsy of the tumor bearing mice at various time points demonstrated that the orthotopic transplantation of PancTu 1 cells resulted at day 8 in small pancreatic tumors with tumor volumes < 12 mm^3, locally grown within the pancreas without any signs of tumor spread. Intraabdominal metastases were observed only at a late time point, after three weeks (Alves et al., accepted with revision). The results in this model extend the observations by others on the inhibitory effect of AG3340 on tumor growth by showing that intraperitoneal administration of AG3340 and also orally administration of Ro28-2653 resulted in a marked inhibition or even prevention of tumor invasion and metastasis of PancTu 1 cells to the lung. The efficacy of AG3340 on tumor progression could be due to the fact that AG3340 acts by inhibiting MMPs, with a selectivity for MMP-2 and MMP-9, MMP-3, MMP-13 and MT1-MMP, and Ro28-2653 by inhibiting key MMPs, with a selectivity for.MMP-2, MMP-9 and MT-MMP, consequently both inhibit the breakdown of extracellular matrix reducing or even preventing invasion and metastasis. The ability of AG3340 to inhibit gelatinases, MMP-2 and MMP-9, *in vitro* was confirmed by zymography.[66] The presence and the activity of MMP-2 and MMP-9 in xenografts of PancTu 1 cells developed in SCID-mice have been demonstrated by zymography (data not shown) and immunohistochemistry (Alves et al., accepted with revision). Of all MMPs, MMP-2 is described to be most involved in the progression of pancreatic

cancer as well as to correlate with an aggressive phenotype.[52,99] In an orthotopic pancreatic tumor model of HPAC cells inhibition of MMP2 by batimastat seems to be most important in prolonging survival in nude mice.[100]

In order to initiate a study with Ro 28-2653 in combination with a chemotherapeutic drug, the inhibitory effect of different concentrations of the chemotherapeutic agent gemcitabine on tumor growth and progression was evaluated in the orthotopic SCID mouse model. Treatment of gemcitabine, intraperiotenally, every 48 h for 21 days, was started one week after orthotopic implantation of the human pancreatic ductal carcinoma cell line PancTu 1. Controls, receiving vehicle only, showed similar tumor growth and tumor spread as control animals from previous studies. Treatment with gemcitabine was well tolerated with the exception of the group of animals receiving high doses of gemcitabine (6.6 mg/ kg bw); 3/5 showed a splenomegaly. Gemcitabine reduced the primary tumor volume significantly in a dose dependent manner to 2.5 % of control (6.6 mg/ kg bw), 6 % of control (2.2 mg/ kg bw) and 27 % of control (0.9 mg/ kg bw) with induction of necrosis and fibrotic tissue in the pancreatic tumor. Invasion was not observed in all gemcitabine treated mice and metastases were reduced markedly. Gemcitabine is already used in the clinic in the therapy for patients with pancreatic cancer. In conclusion, gemcitabine is also highly effective in inhibiting pancreatic carcinoma growth and progression in the orthotopic cancer model. The efficacy in inhibiting tumor growth of gemcitabine in this model is higher compared to AG3340 or Ro28-2653. But the effect of gemcitabine as antitumor drug has its limitation. Only 10 % of patients respond to gemcitabine. Long term therapy is not possible due to tumor drug resistance and toxicity.[101] For the combination study Ro28-2653 (45 mg/ kg bw) and gemcitabine (2.2 mg/ kg bw) were

given. Controls, receiving vehicle only, resembled control animals of previous studies. Treatment schedules with Ro28-2653 or gemcitabine alone as well as the combination therapy were well tolerated and reduced the primary tumor volume significantly to 35 % of control (Ro28-2653), 16 % of control (gemcitabine) and 6 % of control (Ro28-2653 and gemcitabine in combination) with induction of necrosis within the tumor in the group receiving the combination therapy of Ro28-2653 and gemcitabine. Therefore, the estimation of tumor volumes in the Ro28-2653 and gemcitabine treated mice by caliper measurement underestimated the actual percent inhibition of growth because both viable and necrotic tumor areas were included. The application of gemcitabine was more efficient in reducing the tumor volume in comparison to the treatment with Ro28-2653 alone. Invasion was not observed in all mice receiving gemcitabine alone, Ro28-2653/ gemcitabine in combination and in 53 % of Ro28-2653 treated mice. Metastases were reduced markedly in the animals receiving gemcitabine alone or Ro28-2653/ gemcitabine in combination. In the Ro28-2653 treated groups no additional micrometastases were observed in lung and liver when compared to control animals. In conclusion, the combination therapy with the MMP inhibitor Ro28-2653 and the chemotherapeuticum gemcitabine is more effective in inhibiting pancreatic carcinoma growth and progression in the orthotopic cancer model as Ro28-2653 or gemcitabine alone. To eradicate the remaining tumor cells, MMP inhibitors have already been combined with surgical intervention after therapy or with cytotoxic agents. The latter have already been shown to potentiate the antitumor activity of the broad spectrum MMP inhibitor batimastat in ovarian cancer [102] and pancreatic cancer [103] as well as of AG3340, which has been combined with carboplatin and paclitaxel in a human non-small cell lung cancer tumor model.[67] A phase I study of marimastat in combination with doxorubicin and cyclophosphamide

was reported in patients with metastatic breast cancer.[104]. The survival study was designed in analogy to the combination study. Ro28-2653 and gemcitabine were given as single drugs or in combination. In one group the combination therapy was started at late stage disease, 21 days after orthotopic implantation of the tumor cells. In controls, receiving vehicle only, and in all treated animals at end stage disease the poorly differentiated ductal adenocarcinoma invaded into adjacent organs and metastasized to different sites in the abdomen. At autopsy, the sizes and number of metastases especially in the mesentery were reduced in animals that have received gemcitabine alone or the combination therapy with Ro28-2653 or gemcitabine. Treatment with Ro28-2653 or gemcitabine alone as well as the combination therapy were well tolerated and prolonged the survival of the tumor bearing animals to further 13 days (Ro28-2653), 26 days (gemcitabine), 33 days (Ro28-2653 and gemcitabine in combination) and 18 days (Ro28-2653 and gemcitabine in combination, late begin of therapy). In conclusion, the combination therapy with the MMP inhibitor Ro28-2653 and the chemotherapeuticum gemcitabine is more effective in prolonging survival of animals with pancreatic carcinoma in an orthotopic cancer model than treatment with Ro28-2653 or gemcitabine alone. Since most of the pancreatic tumors are diagnosed at a very late stage of the disease, further studies should be conducted, starting treatment after invasion of the local tumor has already occurred. Results have already been presented for a Phase III clinical trial with marimastat. Patients with advanced pancreatic cancer were randomised to receive either 5, 10 or 25 mg b.i.d. marimastat or gemcitabine given by the standard i.v. schedule (100 patients per arm). The primary endpoint of the trial was overall survival with time to disease progression and quality of life as secondary endpoints. The results showed the survival of patients receiving gemcitabine to be superior, by log-rank analysis, to that

of patients receiving two lower doses of marimastat. However, the survival of patients receiving the highest dose of marimastat was not significantly different from the survival of the gemcitabine patients. Although the survival of marimastat patients was lower than that of gemcitabine patients over the initial five months of the study (median 125 *vs*. 167 days, respectively), the survival curves thereafter converged and survival was equivalent in terms of the proportion of patients alive at one year (20 *vs.* 19 %, respectively).[105] The MMP inhibitors certainly represent a potent way to elucidate and cure tissue remodelling-related diseases. In malignancy, therapeutic use of more selective MMP inhibitors such as AG3340 and Ro28-2653 could present many advantages: 1) Lower incidence of side effects. MMP expression is only upregulated at the tumor site. This should determine a selectivity of action to the site of disease. 2) No drug resistance. MMPs release mainly depends on stromal cells (fibroblasts, macrophages and immune cells), which are not genetically stable and 3) additive action with chemotherapy, as already demonstrated by preclinical and clinical studies.[106] In the past, partial regression induced with chemotherapy, radiation therapy or surgery has not consistently translated into prolonged survival. The possible inhibition of MMPs by MMP inhibitors is likely to be in combination with other cytoreductive or cytostatic agents in desease controling regiments. The optimal use of MMP inhibitors is yet to be identified. It may be in combination therapy or in sequence after cytotoxic agents, as well as in adjuvantive therapy.[104] Future clinical trials will be necessary to analyze the best application form and target deaseases of these novel agents.

5. Summary

5.1. Regulation of EGF receptor activity by HK1-ceramide, a stable synthesized analogue of the ganglioside GM3-lactone.

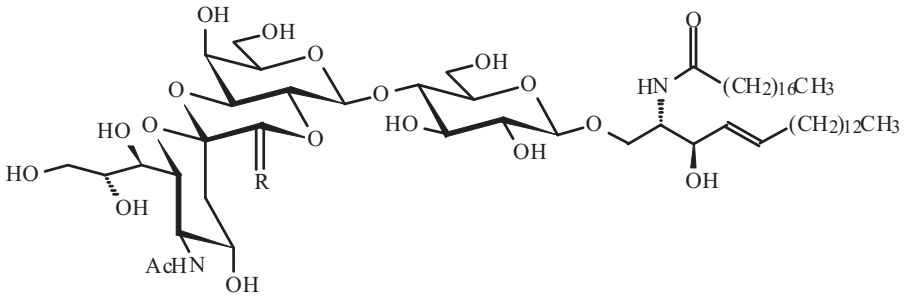

Figure 32: Structure of GM3-lactone and HK1-ceramide. GM3-lactone **1**: R = O. HK1-ceramid **2**: R = H_2

It could be demonstrated that the GM3 lactone analogue HK1-ceramide (**2**, figure 32,) has, in similarity to GM3, an inhibitory effect on EGF dependent tyrosine phosphorylation and therefore on modulation of cell growth. Specific inhibition on EGF dependent tyrosine phosphorylation by HK1-ceramide in A431 cells is achieved at low concentration of 25 μM in a small range of concentration, whereas GM3 showed a dose dependent effect and a similar inhibition at a much higher concentration of 500 μM (20 fold). The underlying mechanisms of the eggect of HK1-ceramide is not well understood. With changes in the pH < 7 GM3 had no variable effect on EGF dependent receptor phosphorylation and it is not likely that a lactonization of GM3 is responsible for the effect of GM3 on receptor activation observed in A431 cells. In similarity to GM3, HK1-ceramide seems to have no influence on the binding of EGF to the cell surface receptor. Furthermore, growth of KB cells was inhibited by HK1-ceramide in a dose dependent manner. HK1-ceramide

showed a similar inhibitory effect on mitogenesis compared as GM3 at approximatly 8 fold lower concentration. HK1-ceramide and GM3 might be an interesting tool to study EGF receptor signal transduction.

5.2. A novel polyclonal antibody directed against the lactone form of ganglioside GM3: Analyses of its potential as tumor marker for melanomas.

In this study it has been shown by using the polyclonal antibody HK1 that the expression pattern of GM3-lactone and GM3 in different types of malignant melanoma (SSM, LMM, ALM) are very similar with only slight degree of variation. Melanoma cells within these lesions express GM3-lactone or GM3 at the dermal-epidermal junction as well as within atypical nests of the upper dermis. Lower dermal parts of the tumor show either a very weak staining or a complete loss of expression. A correlation with the ganglioside pattern in neoplastically transformed melanocytes was found: a positive HK1-antibody staining was demonstrated in melanomas showing level of invasion I and negative stainings in lower dermal parts for level of invasion II-V. Melanophages were found as packed cells with strong staining granules. This leads to the acceptance of a ganglioside shedding mechanism. In dysplastic melanocytic nevi only a positive HK1-antibody staining of melanocytes aggregated in the epidermal compartment was found. The intradermal lying nests of melanocytes were negative and atypical nests of malignant melanoma cells within a congenital melanocytic nevus showed a strong positive effect, whereas the surrounding melanocytic cells were negative The melanocytes in the basal layer of normal skin showed no expression of gangliosides. Immunhistochemical staining of HK1-antibody allows to differentiate between normal skin, transformed melanocytes in level of invasion I and higher levels. Therefore, the novel HK1-antibody might be

useful as an indicator of a tumor marker for malignant melanomas and dysplastic melanocytic nevi in early stages.

5.3. Evaluation of the *seco*-CBI-derivative AF86.1 for its potential use in antibody directed enzyme prodrug therapy.

The seco-CBI-prodrug AF86.1 is not toxic to normal organs and blood parameters of SCID mice in concentration of 20 µg/ kg and higher. This indicates that the prodrug is not converted by enzymes expressed in the SCID-mice. In order to evaluate the potency of AF86.1 treatment *in vivo*, subcutaneous tumors of A549 and PancTu1 cells were generated in SCID-mice. AF86.1 treated A549 tumors showed marked necrosis and more than 80 % of tumor cells stopped proliferation activity after only one treatment cycle. It could be shown *in vivo* that the difference of toxicity between the prodrug and corresponding drug is very high *in vivo*. The ADEPT system using the prodrug AF86.1 holds the potential of an effective, non-toxic treatment of cancer and the present animal studies are very promising for treatment of solid tumors.

5.4. Evaluation of the antitumor and antimetastatic effect of different matrix metalloproteinase inhibitors on human pancreatic ductal adenocacinoma in the orthotopic SCID-mouse model.

It was demonstrated that the potency of MMP inhibitors on pancreatic tumor progression can efficiently be tested in an *in vivo* human pancreatic ductal adenocarcinoma model where cooperation between tumor and stromal cells occurs. Transplanting the tumor cells orthotopically in their original microenvironment in the pancreas results in invasion and dissemination of tumors with distant metastases to the lung which makes this model ideal to evaluate the initially aimed effect of MMP

inhibitors to reduce tumor progression. It was shown here for the first time that treatment with the MMP inhibitors AG3340 and Ro28-2653 as single agent and in combination with the chemotherapeutic agent gemcitabine during early neoplastic progression are highly effective in inhibiting pancreatic carcinoma growth, invasion and metastasis in the orthotopic SCID mouse model. Particularly MMP inhibitor Ro28-2653 in combination with gemcitabine should be considered for further clinical trials.

6. References

[1] G. Bergers, L. M. Coussens, *Curr. Opin. Genetics Dev.* **2000**,*10,*120-127.

[2] Y. C. Lee, R. T. Lee, *Acc. Chem. Rev.* **1995**, *28*, 321.

[3] H. F. Oettgen, *Gangliosides and Cancer* 1st ed., VCH, Weinheim, **1989**.

[4] S. Zhang, C. C. Cordon, H. S. Zhang, V. E. Reuter, S. Adluri, W. B. Hamilton, K. O. Lloyd, P. O. Livingston, *Int. J. Cancer*, **1997**, *61*, 42-49.

[5] P. O. Livingston, R. Ragupathi, S. Zhang, K. O. Lloyd, *Cancer Immunol. Immunother.* **1997**,1.

[6] I. Kawashima, M. Kotani, H. Ozawa, M. Suzuki, T. Tai, *Int. J. Cancer* **1994**, *58*, 263-268.

[7] G. A. Nores, T. Dohi, M. Taniguchi, S. Hakomori, *J. Immunol.,* **1987**, *139(9)*, 3171-3176.

[8] E. A. Tekieva, E. V. Diatlovitskaia, *Biokhimiia* **1993**, *58(10),* 1641-1644.

[9] T. Sato, M. Ishii, F. Ohtake, K. Nagata, T. Terabayashi, Y. Kawanishi, Y. Okahata, *Glycoconj. J.* **1999**, *16(3),* 223-227.

[10] J. Zhu, Y. T. Li, S. C. Li, R. B. Cole, *Glycobilogy* **1999**, 9(10), 985-993.

[11] L. F. Tietze, H. Keim, *Angew. Chem.***1997**, *109*, 1704; (1997) *Angew. Chem. Int. Ed. Engl.***1997**, *36*, 1615.

[12] E. G. Bremer, J. Schlessinger, J.,S. Hakomori, *Biol. Chem.***1986**, *261***,** 2434-2440.

[13] T. Mattar, K. Kochhar, R. Bartlett, E. G. Bremer, A. Finnegan, *FEBS Lett.* **1993**, *334(2)*, 161-164.

[14] E. G. Bremer, *Glycoshingolipids as effectors of growth and differentiation*. In D. Hoekstra, (ed.) *Cell Lipids*. *Current Topics in Membranes*, **1994**, *40*, Academic Press, Orlando, 387-411.

[15] A. Rebbaa, J. Hurh, H. Yamamoto, D. S. Kersey, E. G. Bremer, E. G. *Glycobiol.* **1996**, *6,* 399-406.

[16] J. M. Carubia, R. K. Yu, L. J. Macala, J. M. Kirkwood, J. M. Varga, *Biochem. Biophys. Res. Commun.* **1984**, *120*, 500-504.

[17] H. F. Oettgen, *Gangliosides and Cancer* 1st ed., M. H. Ravindranath, T. Tsuchida, R. F. Irie, *Diversity of ganglioside expression in human melanoma,* VCH, Weinheim, **1989**.

[18] L. A. Liotta, *Cancer Res.* **1986**, *46*, 1.

[19] B. Holzmann, J. P. Johnson, P. Kaudewitz, G. Riethmüller, *J. Exp. Med.* **1985**, *164*, 366.

[20] J. M. Lehmann, B. Holzmann, E. W. Breitbart, P. Schmiegelow, G. Riethmüller, J. P. Johnson, *Cancer Res.* **1987**, *47*, 841.

[21] H. F. Oettgen, *Gangliosides and Cancer* 1st ed., F. Schriever, R. D. Dennis, B. Pallmann, G. Riethmüller, J. P. Johnson, *A GM3 epitope expressed in tumor infiltrating macrophages is generated in phagocytizing monocytes in vitro,* VCH, Weinheim, **1989**.

[22] K. N. Syrigos, A. A. Epenetos, *Anticancer Res.* **1999**, *19*, 605-614.

[23] M. E. Whisson, T. A. Connors, *Nature* **1965**, *206*, 689-91.

[24] T. A. Connors, P. B. Farmer, A. B. Foster, A. M. Gilsenan, M. Jarman, M. J. Tisdale, *Biochem. Pharmacol.* **1973**, *22*, 1971-1980.

[25) T. A. Connors, A. B. Foster, A. M. Gilsenan, M. Jarman, M. J. Tisdale, *Bioch. Pharmacol.* **1972**, 1309-1316.

[26] G. W. Philpott, R. J. Bower, C. W. Parker, *Surgery* **1973**, *74*, 51-58.

[27] G. W. Philpott, W. T. Shearer, R. J. Bower, C. W. Parker, *J. Immunol.* **1973**, *111*, 921-929.

[28] K. D. Bagshawe, *Br. J. Cancer* **1987**, *56*, 531-532.

[29] K. D. Bagshawe, C. J. Springer, F. Searle, P. Antoniw, S. K. Sharma, R. G. Melton, R. F. Sherwood, *Br. J. Cancer* **1988**, *58*, 700-703.

[30] P. D. Senter, M. G. Saulnier, G. J. Schreiber, D. L. Hirschberg, J. P. Brown, I. Hellström, K. E. Hellström, *Proc. Natl. Acad. Sci. USA* **1988**, *85*, 4842-4846.

[31] P. D. Senter, G. J. Schreiber, D. L. Hirschberg, S A. Ashe, K. E. Hellsröm, I. Hellström, *Cancer Res.* **1989**, *49*, 5789-5792.

[32] R. H. Begent, *Biochim. Biophys.* Acta **1985**, *780*, 151-166.

[33] E. Haenseler, A. Esswein, K. S. Vitols, Y. Montejano, B. M. Mueller, R. A. Reisfeld, F. M. Huennekens, *Biochemistry* **1980**, *31*, 891-897.

[34] E. Tagliabue, G. Porro, P. Barbanti, G. Della Torre, S. Menard, F. Rilke, *Hybridoma* **1986**, *5*, 107-115.

[35] S. Y. Chan, G. I. Evan, A. Ritson, J. Watson, P. Wraight, K. Sikora, *Br. J. Cancer* **1986**, *54*, 767-769.

[36] J. W. Park, K. Hong, P. Carter, H. Asgari, L. Y. Guo, G. A. Keller, C. Wirth, R. Shelaby, C. Kotts, W. I. Wood, *Proc. Natl. Acad. Sci. UAS* **1995**, *92*, 1327-1331.

[37] L. M. Cobb, J. A. Humphrey, A. Harrison, *Br. J. Cancer* **1987**, *55*, 53-55.

[38] V. Moshakis, R. A. McIlhinney, A. M. Neville, *Br. J.* Cancer **1981**, *44*, 663-669.

[39] V. Moshakis, R. A. McIlhinney, D. Raghaven, A. M. Neville, *Br. J. Cancer* **1981**, *44*, 91-99.

[40] Y. Boucher, L. T. Baxter, R. K. Jain, *Cancer Res.* **1990**, *50*, 4478-4484.

[41] L. J. Hanka, A. Dietz, S. A. Gerpheide, L. Kuentzel, D. G. Martin, *J. Antibiot.* 1978, 31, 1211-1217; D. G. Martin, C. Biles, S. A. Gerpheide, L. J. Hanka, W. C. Krueger, J. P. McGovren, S. A. Mizsak, G. L. Neil, J. C. Stewart, J. Visser, *J. Antibiot.* **1981**, *34*, 1119-1125.

[42] L. H. Hurley, C.-S. Lee, J. P. McGovren, M. A. Warpehoski, M. A. Mitchell, R. C. Kelly, P. A. Aristoff, *Biochemistry* **1988**, *27*, 3886-3892; L. H. Hurley, M. A. Warpehoski, C.-S. Lee, J. P. McGovren, T. A. Scahill, R. C. Kelly, M. A. Mitchell, N. A. Wienienski, I. Gebhard, P. D. Joohnson, V. S. Bradford, *J. Am. Chem. Soc.* **1990**, *112*, 4633-4649.

[43] D. L. Boger, D. L. Herzog, B. Bollinger, D. S. Johnson, H. Cai, J. Goldberg, P. Turnbull, *J. Am. Chem. Soc.* **1997**, *119*, 4977-4986; D. L. Boger, B. Bollinger, D. L. Hertzog, D. S. Johnson, H. Cai, P. Mésini, R. M. Garbaccio, Q. Jin, P. A. Kitos, *J. Am. Chem. Soc.* **1997**, *119*, 4987-4998.

[44] D. L. Boger, R. S. Coleman, B. J. Invergo, S. M. Sakya, T. Ishizaki, S. A. Munk, H. Zarrinmayeh, P. A. Kitos, S. C. Thompson, *J. Am. Chem. Soc.* **1990**, *112*, 4623-4632; D. L. Boger, D. S. Johnson, W. Yun, C. M. Tarby, *Bioorg. Med. Chem.* **1994**, *2*, 115-135.

[45] J. P. McGovren, G. L. Clarke, E. A. Pratt, T. F. Dekoning, *J. Antibiot.* **1984**, *37*, 63-70.

[46] A. Fecher, Dissertation, Göttingen 2000.

[47] E.P. DiMagno, *Ann. Oncol.* **1999**, *10*, 140-142.

[48] U. Borchers, Diplomarbeit, Göttingen **1998**.

[49] O. Brummer, S. Athar, L. Riethdorf, T. Lönning, H. Herbst, *Virchows Arch.* **1999**, *435*, 566-573.

[50] S.R. Bramhall, J.P. Neoptolemos, G.W. Stamp, N.R. Lemoine, *J. Pathol.* **1997**, *182*, 347-355.

[51] T. Imamura, G. Ohshio, M. Mise, T. Harada, H. Suwa, N. Okada, Z. Wang, S. Yoshitomi, T. Tanaka, H. Sato, S. Arii, M. Seiki, M. Imamura, *J. Cancer Res. Clin. Oncol.* **1998**, *124*, 65-72.

[52] V. Ellenrieder, B. Alber, U. Lacher, S.F. Hendler, A. Menke, W. Boeck, M. Wagner, M. Wilda, H. Friess, M. Buchler, G. Adler, T.M. Gress, *Int. J. Cancer* **2000**, *85*, 14-20.

[53] T. Itoh, M. Tanioka, H. Yoshida, T. Yohsioka, H. Nishimoto, S. Itohara, *Cancer Res.* **1998**, *58*, 1048-1051.

[54] F. Grams, M. Crimmin, L. Hinnes, *Biochemistry* **1995**, *34*, 14012-14020.

[55] P. D. Brown, *Exp. Opin. Invest. Drugs* **2000**, *9(9)*, 2167-2177.

[56] B. Davies, P.D. Brown, N. East, M.J. Crimmin, F.R. Balkwill, *Cancer Res.* **1993**, *53*, 2087-2091.

[57] R.G.S. Chirivi, A. Garofalo, M.J. Crimmin, L.J. Bawden, A. Stoppacciaro, P.D. Brown, R. Giavazzi, *Int. J. Cancer* **1994**, *58*, 460-464.

[58] X. Wang, X. Fu, P.D. Brown, M.J. Crimmin, R.M. Hoffman, *Cancer Res.* **1994**, *54*, 4726-4728.

[59] G. Taraboletti, A. Garofalo, D. Belotti, T. Drudis, P. Borsotti, E. Scanziani, P.D. Brown, R. Giavazzi, *J. Natl. Cancer Inst.* **1995**, *87*, 293-298.

[60] J.A. Low, M.D. Johnson, E.A. Bone, R.B. Dickson, *Clin. Cancer Res.* **1996**, *2*, 1207-1214.

[61] G. Bergers, K. Javaherian, K.M. Lo, J. Folkman, D. Hanahan, *Science* **1999**, *284*, 808-812.

[62] E.E. Zervos, J.G. Norman, W.R. Gower, M.G. Franz, A.S. Rosemurgy, *J. Surg. Res.* **1997**, *69*, 367-371.

[63] L. Jones, P. Ganeh, M. Humphreys, J.P. Neoptolemos, *Ann. N. Y. Acad. Sci.* **1999**, *880*, 288-307.

[64] O. Santos, C.D. McDermott, R.G. Daniels, K. Appelt, *Clin. Exp. Metastasis* **1997**, *15*, 499-508.

[65] D.R. Shalinsky, J. Brekken, H. Zhou, C.D. McDermott, P. Forsyth, D. Edwards, S. Margosiak, S. Bender, G. Truitt, A. Wood, N.M. Variki, K. Appelt, *Ann. NY Acad. Sci.* **1999**, *878*, 236-270.

[66] A. Price, Q. Shi, D. Morris, M.E. Wilcox, P.M.A. Brasher, N.B. Rewcastle, D. Shalinsky, H. Zou, K. Appelt, R.N. Johnston, V.W. Yong, D. Edwards, P. Forsyth, *Clin. Cancer Res.* **1999**, *5*, 845-854.

[67] D.R. Shalinsky, J. Brekken, H. Zou, L.A. Bloom, C.D. McDermott, S. Zook, N.M. Varki, K. Appelt, *Clin. Cancer Res.* **1999**, *5*, 1905-1917.

[68] N.J. Nelson, *J. Natl. Cancer Inst.* **1998**, *90*, 960-963.

[69] J. Fogh, T. Orfeo, J. Tiso, F.E. Sharkey, J.M. Fogh, W.P. Daniels, *Exp. Cell Biol.* **1980**, *48*, 229-239.

[70] M.P. Vezeridis, G.M. Doremus, L.M. Tibbetts, G. Tzanakakis, B.T. Jackson, *J. Surg. Oncol.* **1989**, *40*, 261-265.

[71] X. Fu, F. Guadagni, R.M. Hoffman, *Proc. Natl. Acad. Sci. USA* **1992**, *89*, 5645-5649.

[72]. T. Furukawa,T. Kubota, M. Watanabe, M. Kitajima, R.M. Hoffman, *Cancer Res.* **1993**, *53*, 3070-3072.

[73] D.V. Gold, R. Alisauskas, R.M. Sharkey, *Cancer Res.* **1995**, *55*, 1105-1110.

[74] Z. An, X. Wang, T. Kubota, A.R. Moossa, R.M. Hoffman, *Anticancer Res.* **1996**, *16*, 627-631.

[75] C.J. Bruns, H. Shiohara, M.T. Harbison, D.W. Davis, G. Nelkin, J.J. Killion, D.J. McConkey, Z. Dong, I.J. Fidler, *Cancer Res.* **2000**, *60*, 2-7.

[76] B.M. Mueller, R.A. Reisfeld, *Cancer Metastasis Rev.* **1991**, *10*, 193-200.

[77] E. Gallo-Hendrikx, J. Copps, D. Percy, B.A. Croy, A.G. Wildeman, *Oncogene* **1994**, *9*, 2983-2990.

[78] T. Tomoo, T. Kondo, H. Abe, *Carbohydr Res (Netherlands)*, **1996**, *284(2)*, 207-222.

[79] Drexler HG, Dierks W, MacLeod RAF, Quentmeier H, Steube K, Uphoff CC *(eds): DSMZ Catalogue of Human and Animal Cell Lines*, Seventh Edition, Braunschweig, **1999**.

[80] T. Kawamoto, J. D. Sato, A. Le, J. Polikoff, G. H. Sato, J. Mendelsohn, *Proc. Natl. Acad. Sci. U.S.A.***1983**, *80*, 1337-1341.

[81] A. C. King, P. Cuatracasas, *J. Biol. Chem*. **1982**, *257*, 3053-3060.

[82] H. Kalthoff, W. Schmiegel, C. Roeder, D. Kasche, A. Schmidt, G. Lauer, H.-G. Thiele, G. Honold, K. Pantel, G. Riethmüller, E. Scherer, J. Maurer, H. Maacke, W. Deppert, *Oncogene* **1993**, *8*, 289-298.

[83] G. Scatchard, *Ann. N.Y. Acad. Sci.* **1949***, 51*, 660-672.

[84] G.C. Bosma, M. Fried, R.P. Custer, A. Carroll, D.M. Gibson, M.J. Bosma, *J. Exp. Med.* **1988**, *167*, 1016-1033.

[85] S.L. Bender, *Structure-based design of MMP inhibitors: discovery and development of AG3340. 214th National Meeting of the American Chemical Society, Las Vegas, N.V.,* **1997**.

[86] I. Jannink, P.J. van Diest, J.P. Baak, Hum. *Pathol.* **1995**, *26*, 1086-1092.

[87] F.E. Satterthwaite, *Biometri Bull.* **1946**, *2*, 110-114.

[88] H. F. Oettgen, *Gangliosides and Cancer* 1st ed., Y. Harada, M. Sakatsume, M. Taniguchi, *Role of soluble GM3 melanoma antigene in anti-tumor immune responses of mice,* VCH, Weinheim, **1989**.

[89] H. F. Oettgen, *Gangliosides and Cancer* 1st ed., T. Dohi, G. A. Nores, H. Oguchi, H. Inufusa, S. Hakomori, *GM3 lactone as an immunogen associated with melanoma: effect of immunization with GM3 lactone on melanoma growth in vivo,* VCH, Weinheim, **1989**.

[90] N. Hanai, G. A. Nores, C. MacLeod, C.-R. Torres-Mendez, S-i. Hakomori, *J. Biol. Chem.* **1986**, *263*, 10915-10921.

[91] J. P. Droz, E. Cvitkovic, J. P. Armand, S. Khoury, *Handbook of chemotherapy in clinical oncology*, F.I.I.S., USA, **1987**.

[92] C. M. Balch, *Ann. Surg.* **1978**, *118*, 732-742.

[93] H. F. Oettgen, *Gangliosides and Cancer* 1st ed., J. Portoukalian, *Immunoregulatory activity of gangliosides shed by melanoma tumors,* VCH, Weinheim, **1989**.

[94] D. E. Kerr, P. D. Senter, W. V. Burnett, D. L. Hirschberg, I. Hellström, K. E. Hellström, *Cancer Immunol. Immunoether* **1990**, *31*, 202-206.

[95] G. S. Bignami, P. D. Senter, P. G. Grothaus, K. J. Fischer, T. Humphreys, P. M. Wallace, *Cancer Res.* **1992**, *52*, 5759-5764.

[96] V. M. Vrudhuls, P. D. Senter, K. J. Fischer, P. M. Wallace, *J. Med. Chem.* **1993**, *36*, 919-923.

[97] U. Kuefner, U. Lohrmann, Y. D. Montejano, K. S. Vitols, F. M. Huennekens, *Biochemistry* **1989**, *28*, 2288-2297.

[98] A.F. Chambers, L.M. Matrisian, *J. Natl. Cancer Inst.* **1997**, *89*, 1260-1270.

[99] T. Koshiba, R. Hosotani, M. Wada, Y Miyamoto, K. Fujimoto, J.U. Lee, R. Doi, S. Arii, M. Imamura, *Cancer* **1998**, *82*, 642-650.

[100] E.E. Zervos, A.E. Shafii, A.S. Rosemurgy, *J. Surg. Res.* **1999**, *81*, 65-68.

[101] *Kongress ÖGHO-Tagung, Mai 2000, Wien, Hämatologie/Onkologie,***2000**, *3*, 42.

[102] R. Giavazzi, A. Garofalo, C. Ferri, V. Lucchini, E.A. Bone, S. Chiari, P.D. Brown, M.I. Nicoletti, G. Taraboletti, *Clin. Cancer Res.* **1998**, *4*, 985-992.

[103] M. Haq, A. Shafii, E.E. Zervos, A.S. Rosemurgy, *Cancer Res.* **2000**, *60*, 3207-3211.

[104] E. I. Heath, L. B. Grochow, *Drugs* **2000**, *59(5)*, 1044-1054.

[105] A. Rosemurgy, R. Buckels, R. Charnley, *Proc. Am. Soc. Clin. Oncol.* **1999**, *18, Abstract 1005*, 261a.

[106] R. Scatena, *Exp. Opin. Invest. Drugs* **2000**, *9(9)*, 2159-2165.

[107] I. Svennerholm, *J. Neurochem.* **1963**, *10*, 613-623.

[108] F. Searle, C. S. Partridge, A. Kardana, A. J. Greon, R. G. Buckley, R. H. Bogent, G. A. Rawlins, *Int. J. Cancer* **1984**, *33*, 429-434.

[109] F. Searle, C. Bier, R. G. Buckley, S. Newman, R. B. Pedley, K. D. Bagshawe, R. G. Melton, S. M. Alwan, R. F. Sherwood, *Br. J. Cancer* **1986**, *53*, 377-384.

[110] R. G. Melton, F. Searle, R. F. Sherwood, , K. D. Bagshawe, J. A. Boden, *Br. J. Cancer* **1990**, *61*, 420-424.

[111] K. D. Bagshawe, S. K. Sharma, C. J. Springer, P. Antoniw, *Tumour target* **1995**, *1*, 17-19.

7. Abbreviations and Acronymes

A431	Ovarial epidermoid carcinoma cell line
A549	Human bronchial carcinoma cell line
ADEPT	Antibody Directed Enzyme Produg Therapy
AEC	Aminoethylcarbazole
AEC	Antibody-enzyme conjugate
AF86. 1	*rac*-{2-Chloro-4-[5' –((1*H*-indole-2" –carbonyl)-amino)-1*H*-indole-2'- carbonyl]-1,2,3,4-tetrahydro-benzo[*f*]chinolin-6-yl}-β-D-galactopyranoside
AG3340	3(S)-2,2-dimethyl-4-[4-pyridine-4-yloxy)-benzenesulfonyl]-thimorpholine-3-carboxylic acid hydroxyamide
BB-94	Batimastat
BCA	Bicichonine acid
CMC	Carboxymethylcellulosis
CPI	Cyclopropapyrroloindole
DMA	Dimethylacetamide
DMEM	Dulbecco`s modified Eagle`s medium
DMSO	Dimethylsulfoxide
ECM	Extracellular matrix
EGF	Epidermal growth factor
^{125}I-EGF	3-[^{125}-I]iodotyrosyl) EGF
EGF-R	Epidermal growth factor receptor
EGTA	[Ethylenebis(oxyethylenenitrilo)]tetraacetic acid
ELISA	Enzyme-linked-immunosorbentassay
EMA	Epithelial membrane antigen
ERK	Extracellular signal regulated protein kinase
Erk 1	Extracellular signal regulated protein kinase 1
Erk 2	Extracellular signal regulated protein kinase 2
FCS	Fetal calf serum
GD2	Ganglioside, is abbreviated according to the nomenclature of Svennerholm[107]
GD3	Ganglioside, is abbreviated according to the nomenclature of Svennerholm[107]

GM2	Ganglioside, is abbreviated according to the nomenclature of Svennerholm[107] : GM3 Ganglioside, is abbreviated according to the nomenclature of Svennerholm[107]
Grb2	Adapter protein
H&E	Hematoxylin and eosin
HEPES	4-(2-hydroxyethyl)-1-piperazine-ethanesulfonic acid
HK1-ceramide	(2S,3R,4E)-3-Hydroxy-2-(octadecanamido)octadec-4-enyl-4-O-[3-O-(5- acetamido-1,3,5-trideoxy-D-glycero-α-D-galacto-2-nonulopyranosyloyl-1“→2’-pyranosyl)-β-D-galactopyranosyl]-β-D-glucopyranoside
HK2-ceramide	(2S,3R,4E)-3-Hydroxy-2-(octadecanamido)octadec-4-enyl-4-O-[3-O-(5-acetamido-1,3,5-trideoxy-D-glycero-β-D-galacto-2-nonulopyranosyloyl-1“→2’-pyranosyl)-β-D-galactopyranosyl]-β-D-glucopyranoside
KB	Human oral epidermoid carcinoma cell line
KD	Kilo Dalton
KI67	MIB-1
MAbs	Monoclonal antibodies
MAP kinase	Mitogen activated protein kinase
MEK	MAP kinase/ ERK kinase
MMPs	Matrix metalloproteinases
MMP-1	Collagenase-1
MMP-2	Gelatinase-A
MMP-3	Stromelysin-1
MMP-9	Gelatinase-B
MMP-13	Collagenase-3
MT-MMPs	Membrane type MMPs
PAGE	Polyacrylamide gel electrophoresis
PBS	Phosphate-buffered saline
PEG400	Polyethylenglycole
PDE	Pyrrolodihydroindole
PMSF	Phenylmethylsulfonyl fluoride
pY	Phosphotyrosine

PancTu1	Human pancreatic ductal adenocarcinoma cell line
SCID	Severe combined immuno deficiency
SD	Single dose
SH	Src homology
TIMPs	Tissue inhibitors of metalloproteinases

8. Acknowledgments

Special thanks to Dr. F. Alves for the help and encouragement in the laboratory, from her I learnt the basic experimental techniques for the SCID-mouse-experiments. I thank her for her friendship and her constantly interest for this work including the numerous suggestions and discussions.

I thank all my colleagues and former colleagues for providing a motivating work atmosphere.

The motivation and support from my friends and family made me accomplish this work.

This work was supported by grants from the Deutsche Forschungsgemeinschaft and the Roche Diagnostics GmbH.

CURRICULUM VITAE

Personal Information

Name, First Name	Borchers, Ulrich
Date of Birth	30.08.1971
Place of Birth	Hamburg, Germany
Material Status	Married
Nationality	German

Education

08.1978- 07.1982	Primary School, Volksdorf-Hamburg
21.06.1991	Abitur (German equivalent to A-levels)
08.1991- 09.1992	Cival service
from 04.1993	Studies of chemistry,Georg-August-University of Göttingen, Germany
from 12.1996	Examination works, Medical Institute, University of Göttingen, Germany (Department of Hematology and Oncology under the guidance of Prof. Dr. Dr. h.c. L. F. Tietze and Dr. F.Alves Titel of work: Biologische Charakterisierung von Analoga des GM3-Gangliosid-Lactons als tumorassoziierten Antigens.
22.02.1998	Examination
from 02.1998	Work at the Institute of Organic Chemistry and starting of the dissertation under the guidance of Prof. Dr. Dr. h.c. L. F. Tietze.